IMPACT OF CLIMATE CHANGE ON THERMAL BEHAVIOUR OF PAVEMENT STRUCTURES IN ONTARIO

Abdul Basit

A THESIS SUBMITTED TO THE FACULTY OF GRADUATE STUDIES IN PARTIAL FULFILLMENT OF THE REQUIREMENTS FOR THE DEGREE OF MASTER OF APPLIED SCIENCE

GRADUATE PROGRAM IN CIVIL ENGINEERING

YORK UNIVERSITY

TORONTO, ONTARIO

MAY 2022

Abstract

In recent years, numerous studies have highlighted that the climate across the world is changing rapidly due to increased Green House Gas (GHG) emissions. The Intergovernmental Panel on Climate Change (IPCC) has reported that ambient temperatures across Canada are rising twice than the rest of the world. In light of climate change, it is vital to adapt our best practices in pavement material selection and road weight restrictions to avoid potential disruption. Traditionally, asphalt binder selection based on the Superior Performing Asphalt Pavements (Superpave) Performance Grade Asphalt Concrete (PGAC) system relies on historic climatic conditions in relation to the expected in-service temperature range of the flexible pavement. Moreover, in Canada, the Spring Load Restriction (SLR) periods are imposed on the basis of subsurface temperature data obtained from Road Weather Information System (RWIS) and Spring Load Adjustment (SLA) stations in conjunction with visual observations. In view of climate change, it is crucial to investigate the extent to which pavement surface and subsurface temperatures will be affected by ambient conditions in the future. This is to assess the relative impact on appropriate PGAC selection and appropriate SLR recommendations for more durable and resilient pavement structures. In this study, regression models were developed to determine the relationships between asphalt pavement surface temperature and ambient weather data from various weather stations within the Ontario Ministry of Transportation's RWIS. Moreover, this study also involves the investigation of climate change effect on SLR periods using future climate projections. Regression models were developed to determine the relationships between freeze/thaw depths and climate indices using data from existing SLA and RWIS stations within Ontario. Firstly, the relative impact of climate change on pavement surface and subsurface temperature extremes were estimated for different Representative Concentration Pathways (RCPs)

using the regression models. After that, appropriate PGAC selection and SLR recommendations to meet projected pavement temperatures were assessed. It was anticipated that in the future, climate change could potentially cause changes to asphalt binder grades and changes in SLR periods across the Province of Ontario depending on the severity of the projected warming due to climate change.

Acknowledgements

I am grateful to my supervisors, Dr. Rashid Bashir and Dr. Matthew A. Perras, for supporting my work over the years and guiding me along the path that led to this thesis. I am appreciative for all of the advice and scientific support they have given me. They had been helpful throughout all of the challenges I've had while writing my thesis, especially during the life-changing pandemic. I am grateful to my committee member, Dr. Mohammad Shafiee, for his continued support with this research. I'd want to offer my heartfelt gratitude to Ms. Sindy Mahal and Mr. Kunjan for their invaluable assistance and support. My heartfelt gratitude goes to Mr. James Brouwer from MTO and Dr. Diar Hassan, from Wood plc. This research would not have been possible without their help.

Table of Contents

List of Figures

List of Tables

1. Introduction

It is now globally accepted that the climate is changing, and both surface air and sea surface temperatures are increasing (IPCC, 2013). The globe has witnessed a dramatic change in climate and Canada is a prime example of a country where global warming has changed the climate from past norms, which has an influence on the built infrastructure. Climate change is increasing infrastructure damage and service interruptions across Canada, which is already facing significant repair and maintenance expenditures (Ness et al., 2021). Air temperature is increasing with climate change and results in changes in pavement surface temperatures. The increase in pavement surface temperatures in many instances can be greater than the design temperature of the asphalt used in pavement construction. The operation of roads is impacted because climate change makes the typical air temperature different than the design temperature of the asphalt. In instances where the pavement surface temperature is different than the design temperature, the asphalt does not behave as intended, resulting in increased damage. Furthermore, changes in air temperatures changes the thawing period of ice in the pavement layers, leading to changes in Spring Load Restriction (SLR) periods. These restriction periods, if not determined accurately, result in damage of low volume pavements i.e., pavements which experience less than 1000 vehicles per day and thus are built with minimal sub-base. Many climate change impacts are irreversible and will affect transportation infrastructure. This makes it necessary for the road pavements to be replaced with more resilient materials and incorporation of accurate SLR periods. The road network in Canada is among one of the largest in the world with the province of Ontario alone, having about 116,000 kms of local roads (Statistics Canada, 2018) and 40,000 kms of highways. This has a net book asset value of $26.7 billion (FAO, 2019). Therefore, Ontario, Canada, is one of the most suitable places to investigate the impacts of climate change on pavements.

1.1. Background

In 1987, the Strategic Highway Research Program (SHRP) began creating the Superior Performing Asphalt Pavements method (Superpave), a novel approach for specifying asphalt materials (McGennis et al., 1995). The performance-based specification for selecting Performance Graded Asphalt Cements (PGACs) defines binders based on historical climatic conditions in relation to the adaptive pavements' predicted in-service temperature scale (McGennis et al., 1995). To develop this approach, data from over 6000 meteorological stations across Canada and the United States were used to build pavement temperature models (Fletcher et al., 2016), which are referred to as Long Term Pavement Performance (LTPP) models. These models are commonly used to calculate pavement temperatures and select appropriate PGACs for pavement surface layer. By 2001, the province of Ontario had fully embraced this binder standard (Goodman et al., 2002).

A web-based tool has been created to assist pavement professionals in determining PGAC for any given site in the United States and Canada. The most recent version of this programme is LTPPBind V3.1. This was created in 2005, by Pavement Systems LLC, for the Federal Highway Administration (FHWA) in the Unites States (Mohseni et al., 2005). This tool allows the user to use National Aeronautics and Space Administration’s (NASA) Modern-Era Retrospective Analysis for Research and Application (MERRA) climate data, LTPP climate data. The user also has an option to input their own climate data. This application aids in the selection of PGAC based on user-defined traffic statistics and operating speed by employing the most recent LTPP models. To minimise early degradation of flexible pavements and extend their service life, it is vital to select a suitable asphalt binder grade for each road construction or road repair project.

The environment has a significant impact on the materials used in pavement construction. Surface temperatures rise as air temperatures rises and this influences the strength and stiffness of the asphalt. The PGAC selection is based on a design temperature which is selected based on the historical climate. With rising temperatures due to climate change, it is crucial that the effect of climate change be considered in asphalt binder selection techniques. Consideration of climate change will ensure the sustainability of pavement during its design life and avoid additional maintenance costs.

1.1.1 Ontario's Road Network and Monitoring

The transportation system of Canada is one of the world's largest systems with all the four primary modes of transportation (i.e., roadways, railways, airways, and sea/marine ways) playing vital roles in the movement of people and products. The road network system of Canada includes more than one million kms length of two-lane equivalent public roads (Statistics Canada, 2018). For Ontario, in addition to the local roads and highways mentioned previously, there are around 2,756 bridges (Ontario Ministry of Northern Development and Mines, 2012). Figure 1.1 represents the road network in Ontario, which is characteristically very dense in Southern Ontario and progressively less dense further north. As it can be seen in Figure 1.1, mostly the province is located on no permafrost zone however, in the up north, many locations lie on the discontinuous and continuous permafrost zones. Permafrost zones or areas are the ones where the ground temperatures remain below 0 °C for two or more years. Whereas, in no permafrost areas, the ground temperatures rise above 0 °C as well. In this study, the models for determining surface temperatures and SLR periods were developed and tested using climatic, surface and sub surface data from no permafrost locations and are therefore limited to no permafrost locations of the province.

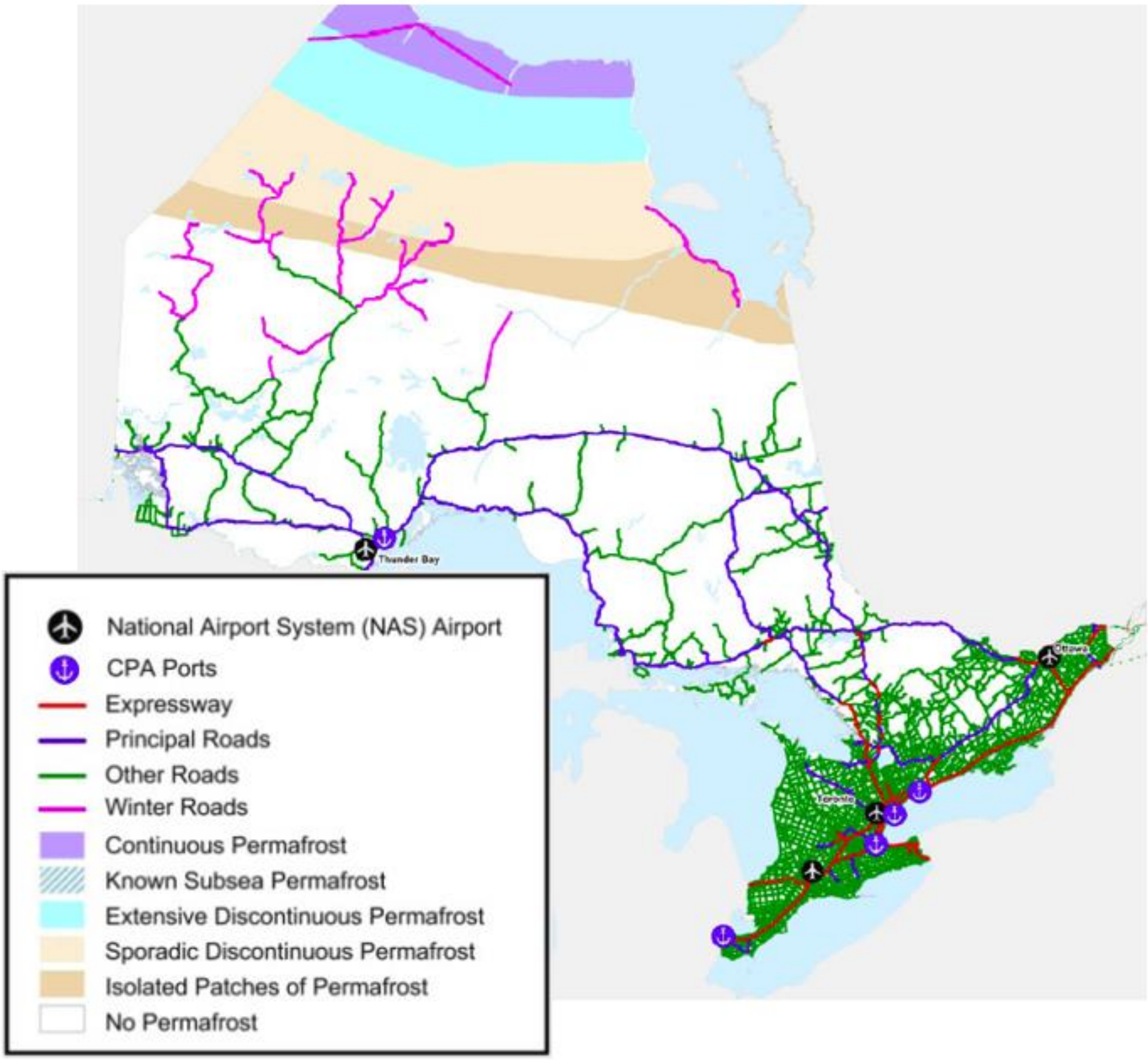

Figure 1.1 Road Infrastructure in Ontario. (Source: Woudsma et al., 2017)

It has been reported that more than 11 million road vehicle registrations were recorded in Ontario in 2013 with 237,000 heavy vehicles (Statistics Canada, 2015a). The province of Ontario, on average, accounts for 39 percent of the overall national Gross Domestic Product (GDP) and its economy is heavily reliant on road surface transportation (Statistics Canada, 2016). Furthermore, it has been reported that trucking contributed the most in Ontario's trade with United States in

2015 (Transport Canada, adapted from Statistics Canada, International Trade database). There are more than 3,000 kms of winter roads which connect remote locations with the provincial highways in Northern and Central Ontario. These roads are constructed and maintained by local municipalities and provide only seasonal access.

1.1.2 Low Volume Pavement Structure

The roads which experience less than 1000 vehicles per day can be categorized as low volume roads (Ningyuan et al., 2006). These roads are built to access remote locations and are mostly used by the transportation industry, thus subjected to infrequent but intensive loadings. These roads comprised around 20% or 3,715 center-line km of the whole roadway network in Ontario. Due to low traffic, these roads are built with minimal sub-base. Typical structural details of low volume roads in Ontario are provided below and are illustrated in Figure 1.2 (Ningyuan et al., 2006).

- Typical Structure 1: 40mm hot mix HL4 Surface + 40mm hot mix HL4 Binder +150mm Granular A Base + 650mm Granular B Sub-base;
- Typical Structure 2: 50mm hot mix HL4 Surface + 150mm Granular A Base + 700mm Granular B Sub-base;
- Typical Structure 3: Surface Treatment + 100mm Granular A Base + 700mm Granular B Sub-base.

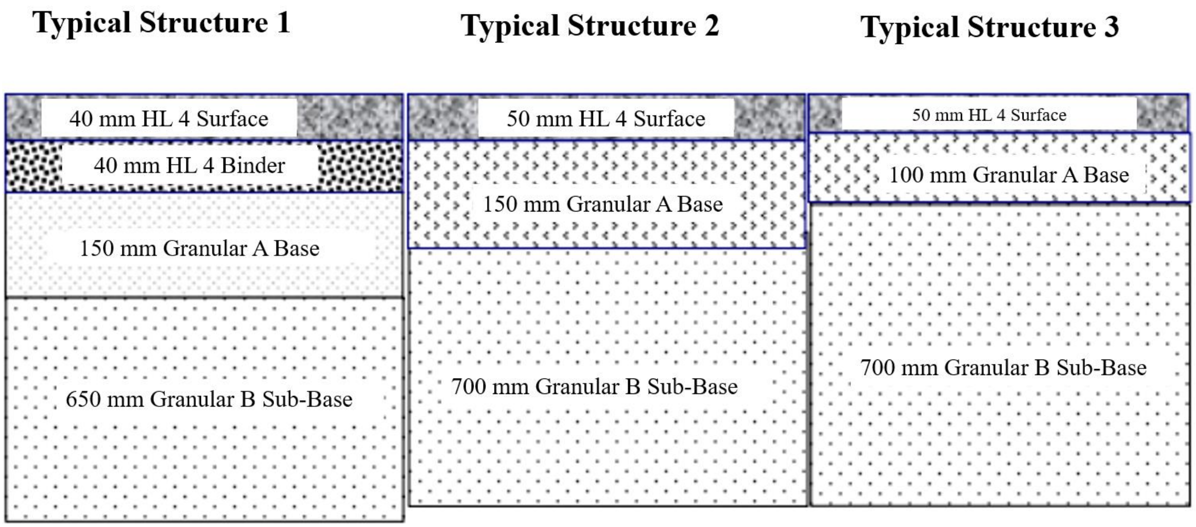

Figure 1.2 Typical Low Volume Pavement Structures used in Ontario. HL 4 is a type of Hot Mix Asphalt Mixtures which is used as a Surface and Binder Course in Ontario. (Source: Ningyuan et al., 2006)

In these roads, Hot Mix Asphalt (HMA) or surface treatment is used in the surface layers, granular material is used in the base and sub-base layers and sometimes hot mix binder is used between surface and base layers. The subgrade layer differs by region and is made up of local materials ranging from organic waste to bedrock (Baiz et al., 2007). In these locations where the traffic volume is low, the roads are usually constructed on natural foundations with minimal sub-base. Most of the Ontario's low-volume roadways are constructed with thin bituminous pavement surface layers, classifying them as flexible pavement structures. In flexible pavements, the traffic loads are transmitted from the surface to the subsequent pavement layers in such a way that the whole pavement shows deflections without cracking (TAC, 1997). Most of these roads are built to accommodate year-round traffic, but they are not designed to withstand frost effects and are thus prone to early degradation (Baiz et al., 2007).

The Ministry of Transportation Ontario (MTO) owns and operates many Spring Load Adjustment (SLA) and Road Weather Information System (RWIS) stations to monitor the road network. The SLA stations measure and collect soil temperature data at depths ranging from 5 cm to 255 cm, whereas the RWIS stations collect this information for 40 cm and 150 cm depths. However, both types of stations record other information as well, such as air and surface temperatures, relative humidity, wind speed, and precipitation data. The data obtained from these stations is utilized in many ways such as the design and repair of roads, winter maintenance of pavement structures, determination of SLR periods, and for research, and development.

It is also anticipated that climate change may impact SLR periods. The second part of this research investigates the implications of climate change on SLRs in Ontario, Canada. Roads with less than 1000 cars per day are classified as low volume roads within the framework of pavement design (Ningyuan et al., 2006). These roads are constructed to provide access to isolated and remote places and are mostly utilised by the transportation sector. Therefore, these roads see intermittent traffic, but that traffic consists of mostly high weight vehicles. These low-volume roads account for around 20% of Ontario's total highway network (Ningyuan et al., 2006), and are often constructed with a minimum sub-base and surface treatment on a natural foundation. When the air temperature drops below the freezing point, it causes frost penetration in the pavement system thus creating a water-rich frost zone in the pavement layers. During the spring thaw periods, when the air temperature starts to increase, the water-rich frost zone starts to thaw (Salour et al., 2013). The thawing in the pavement layers initiates from top down, due to increased air temperatures, and from the bottom up, due to the geothermal flux caused by the geothermal gradient (Chapin et al., 2012). In these thawing periods, the surface temperatures greater than 0 °C in conjunction with the warming of bottom of pavement structure due to geothermal flux generates two 0 °C temperature interface boundaries, with one at the bottom and one at the top of frozen layer (Chapin et al., 2010). These conditions result in the energy transfer into the frozen layer thereby thawing the frozen layer and reducing its thickness (Chapin et al., 2010). This results in the moisture being trapped between the frozen layer below and relatively impermeable pavement surface course above (Chapin et al., 2010), thus temporarily increases the water content in the unbound pavement layers (Salour et al., 2013). In these conditions, there is little or no drainage of the accumulated moisture/water. Excess pore pressure and water saturation conditions under heavy traffic loads can lead to loss of shear strength and internal friction in the unbound layers, degradation of pavement materials and loss of underlying support (Janoo, 2002). Once the moisture content inside the pavement system returns to pre thawing level, the pavement structure regains its true strength. During these times of weakness, authorities apply a SLR to the truck traffic. On the one hand, the SLR extends the life of the pavement structure, but on the other, they reduce the load capacity of the trucks and result in economic loss. Truck payload restrictions result in a higher number of journeys and, as a result, increased fuel consumption. As a result, properly determining the SLR application and removal dates is critical. The MTO utilizes the actively adjusting SLR dates approach whereas, most of the regional municipalities make use of pre-scheduled dates for SLR. Since, in most of the cases, these pre-scheduled dates are not revised for years, therefore there is fair chance that SLR in those regions remain in effect even when these restrictions are no longer required. When the SLR is correctly implemented and removed, it results in little pavement damage from truck traffic and minimizes economic hardship for the trucking business during these times (Chapin et al., 2012).

1.1.3 Asphalt Binder Selection

Asphalt cement is a viscoelastic material having temperature-dependent physical characteristics, and properties. A binder's performance is primarily concerned with two areas of poor performance: rutting and low temperature cracking. The PG asphalt binders are chosen based on the year's high and low pavement temperature extremes, as well as a predetermined level of reliability. At high and low temperatures, this offers maximal resistance to rutting or pavement deformation, as well as thermal cracking. Rutting happens when the pavement temperature is high, which is defined as the average 7-day maximum pavement temperature, whereas low temperature cracking happens when the pavement temperature is low, which is defined as the average 1-day lowest pavement temperature. As a result, the asphalt binder PG is divided into two parts: high and low pavement service temperatures, as shown Figure 1.3

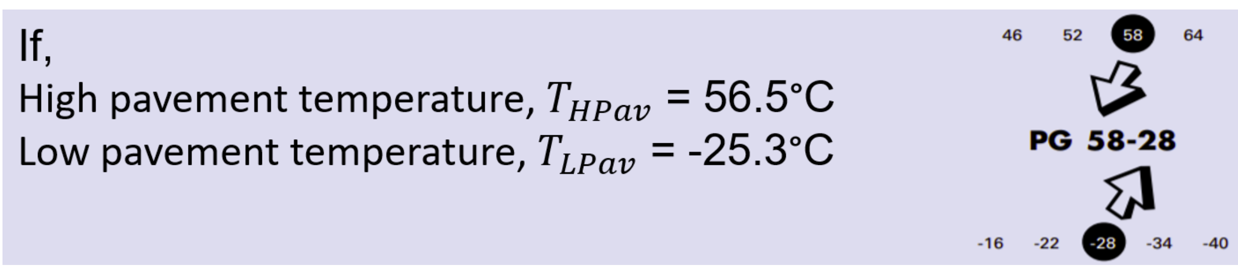

Figure 1.3 Asphalt Binder Selection (modified from Corun, R., 2006)

1.1.4 Spring Load Restrictions

Pavements in cold climates are those that get exposed and impacted by frost, ice, and snow over extended periods. Many of these roads are low volume roads and are built with minimal sub-base as described earlier. During the winter, these pavements are subjected to negative temperatures for long enough to cause frost penetration in the layers of pavement and sub-grade soil. Water gathers in the pavement structure throughout the winter, forming ice lenses. During the thawing phase, moisture rises in the unbound pavement layers, resulting in structural stiffness loss and a reduction in load bearing capability. During the spring-thaw season, several road agencies and municipalities across Canada and the United States impose SLRs to mitigate the damage to low-volume roadways. The SLRs should ideally begin when the thawing reaches a depth that causes considerable pavement structural deterioration or when the pavement structure loses most of its strength. Whereas the removal of SLR should take place after complete thawing of the pavement structure. This gives proper time to pavement structure for restoration of natural drainage conditions and regain the designed bearing capacity.

1.2. Problem Statement

The asphalt binder is a viscoelastic temperature dependent material and its selection for pavement construction is heavily influenced by the environmental factors. If atmospheric temperatures rise, so do the pavement surface temperatures, necessitating research into improved asphalt binder selection procedures that consider expected climate changes. A recent study has shown that warmer temperatures cause pavement structures to degrade quicker, necessitating earlier or more rehabilitation (Chen et al., 2021). Therefore, it is critical to choose an appropriate asphalt binder grade for any given project to avoid early degradation of flexible pavements. To assess the relative effect of climate change on suitable PG for more robust pavement design, it is vital to examine how projected atmospheric conditions may impact pavement surface temperatures.

The Ministry of Transportation Ontario (MTO) owns a number of SLA and RWIS stations spread all over the province. As mentioned before, these stations have several sensors embedded in the road which measure and collect climatic, surface, and subsurface data. The subsurface temperatures at different depths, obtained from these stations, are utilized to impose SLR periods across the province. All the analytical models developed so far were either developed for specific climates and/or require site specific calibration. Most of them were developed using very limited climate data and have not been updated with more recent information and data. Therefore, it is very crucial to develop a network level model which can predict SLR periods using air temperatures. Moreover, the outlook of SLR periods across Ontario, Canada may also be predicted for changing climate using climate change projections.

1.3. Research Objectives

The objectives of this study were to develop a network level model which can predict SLR periods using air temperatures, and to quantify the effects of climate change on asphalt PG and SLR across Ontario, Canada. To achieve these objectives, the following steps were considered:

- To collect the historical and projected climate data for determining asphalt PG and SLR across Ontario.
- To review and analyse the historical and projected climate data, within the context of rising temperatures.
- To collect and analyse the data from different RWIS and SLA stations to develop and validate regression models.

Figure 1.4 presents the summary of the strategy adopted in this research. In this study, the data set used for models' development, and the details of models' validation processes are also presented. Furthermore, the effects of long-term climate change on asphalt PG and SLR are quantified and discussed for four different future time periods i.e., short term (2021-2040), mid century (2041-2060), third quarter (2061-2080) and end century (2081-2100). The long-term climate change refers to change in mean temperatures over a number of years say decades whereas the year-to-year climate variability refers to deviation of mean annual temperature from average of temperatures over a number of years. The models developed in this study majorly depend on air temperatures. The change in air temperatures will change the results. In this study, the results were generated to capture long-term climate change effects. The results of this study suggested that the developed models can capture the long-term changes, based on which it is believed that these models should be capable of capturing year to year variations of similar magnitude. As more measurements become available, the capability of models, in terms of capturing the year-to-year variation, can be improved. The findings of this study are expected to provide invaluable information for pavement designers and policy makers within the context of climate change.

1.4. Organization Of Thesis

This thesis is divided into six chapters.

- Chapter 1 presents the introduction of this research followed by a detailed background in which the road network of Ontario and its monitoring is discussed. This chapter also provides a brief introduction to the asphalt binder selection and spring load restrictions. This chapter concludes with the problem statement and objectives of this research.
- Chapter 2 highlights the potential impacts on the Ontario's road network within the context of climate change. This chapter provides information about the mechanical behaviour and changes in the material properties of asphalt under varying climatic influences. The effect of climatic parameters on deterioration of the asphalt pavements are also briefly discussed. This chapter also provides a brief overview of several models, developed to date for predicting the asphalt pavement's temperatures and SLR periods.
- Chapter 3 presents a detailed overview of all the data sources that are considered and used in this research effort. Moreover, this chapter also provides pertinent details on data analysis and the development of regression models.

- Chapter 4 demonstrates the effects of climate change on asphalt binder selection across the province of Ontario. This chapter provides the details regarding the development of Ontario specific models for the determination of asphalt PG binders. Furthermore, a quantitative analysis of change in asphalt PG grade, using the developed models and existing LTPP models, by the end-century is also presented in this chapter.
- Chapter 5 presents the impacts of climate change on SLR periods across Ontario. The details of the development of Ontario-specific models, for determining the SLR periods, are also provided in this chapter. Moreover, this chapter also includes a quantitative analysis of change in SLR periods by the end of the century. The quantitative analysis is carried out using existing and models developed as part of this research.
- Chapter 6 demonstrates the conclusions, recommendations, and limitations of this study.

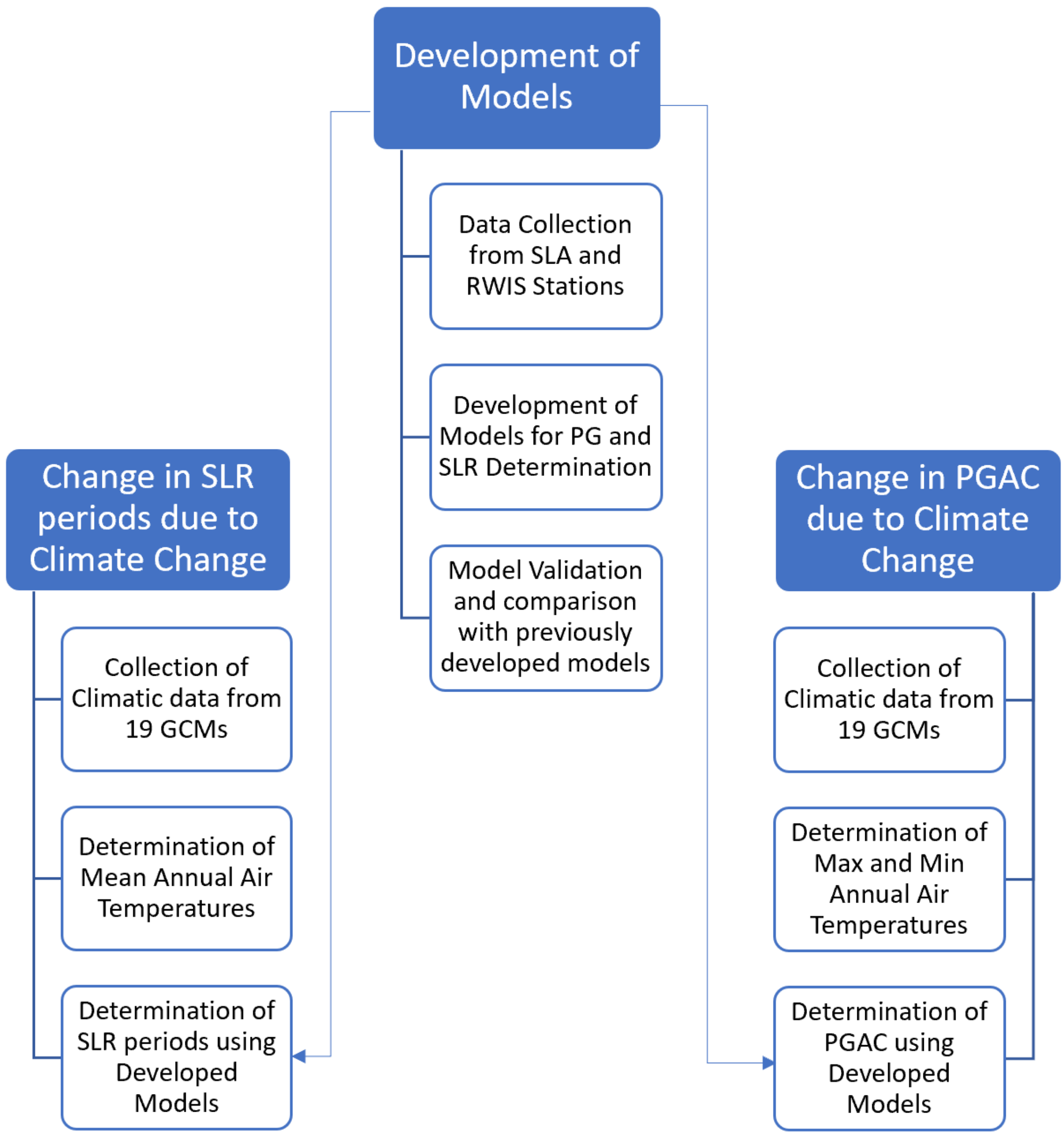

Figure 1.4 Summary of Research Strategy

2. Climate Change and the Impact on Ontario's Road Network – A Literature Review

2.1. Climate Change

The increase in air temperatures due to climate change, causes the surface temperatures to rise and thus will affect the behaviour of pavement. Hartmann et al (2013), highlighted that the global mean surface temperatures have increased by 0.85 degree Celsius during the 1880 to 2012 period and termed the 1980 to 2010 decades as the warmest since 1850. Moreover, 2020 has been found to be one of the three warmest years in the recent past, with around 1.2-degree Celsius increase in the global mean temperatures, as compared to the 1850-1900 baseline (WMO, 2020). During the last century, almost each part of the world has experienced climate change. The change was not uniform globally due to different heat absorption rates and climatic variability in different regions (Hartman et al., 2013). The magnitude of rising temperatures has been greater in the high northern latitudes (Bush et al., 2019) and because Canada is partly located in high northern latitudes, it has witnessed relatively higher warming rates than the rest of the world (Bush et al., 2019).

The ambient temperatures in Canada are said to be increasing twice as quickly as the rest of the world (Bush et al., 2019). Between 1948 and 2016, the annual mean air temperature across Canada increased by an average of 1.7 degrees Celsius (Bush et al., 2019), whereas it increased by around 1.5 degrees Celsius in Ontario between 1948 and 2008 (Gough et al., 2016). According to reports, Green House Gasses (GHG) emissions in Ontario, Canada, increased by 10 mega tonnes in 2018 compared to 2017 (National Inventory Report Canada, 2018). With such emission rates, mean annual air temperatures in Ontario are likely to rise by 3 to 8 degrees Celsius over the next century, thus leading to increased surface temperature of pavement on roads across the province.

The design and service life of pavements are heavily influenced by the climate. Figure 2.1 shows different factors affecting the road performance (Haas, 2004). This figure highlights the interaction of weather and climate factors with different variables involved in pavement construction and rehabilitation. The most important issue in evaluating the performance of pavements is their resistance to deformation and cracking under varying climates (Sun et al., 2019). It is anticipated that a hotter and more variable climate will put more strain on Canada's roads, reducing their reliability and level of service (Ness et al., 2021). With the rapidly changing climate, the probability of thermal distress may increase which is the most noticeable distress in asphalt concrete pavements (Dong et al., 2018). Moreover, changing climate and warmer temperatures may cause early failure of pavements, thus necessitating more rehabilitation procedures (Y. Qiao et al., 2015, Wang et al., 2021). The increasing temperatures can possibly surpass the maximum temperature threshold that asphalt binders are intended for, thus leading to their inefficiency which will cause rutting and early deterioration of pavement (Ness et al., 2021).

The water balance of permafrost zones will also be influenced by climate change, resulting in more rainfall, and decreasing snowfall quantities (Ming-ko Woo, 1990), leading to permafrost degradation (Batenipour et al., 2009). Climate change will increase the number of freeze and thaw cycles (Haas et al., 2004), hastening road damage (Haas et al., 1997, Mills et al., 2009, Erik et al., 1997, Shafiee et al., 2021). The increasing air temperatures effects the time require by the thawing front to reach the sub-base of pavement structure which impacts the SLR period. It is therefore critical to examine the effects of climate a change in PG selection and SLR periods to build safer and long-lasting roadways.

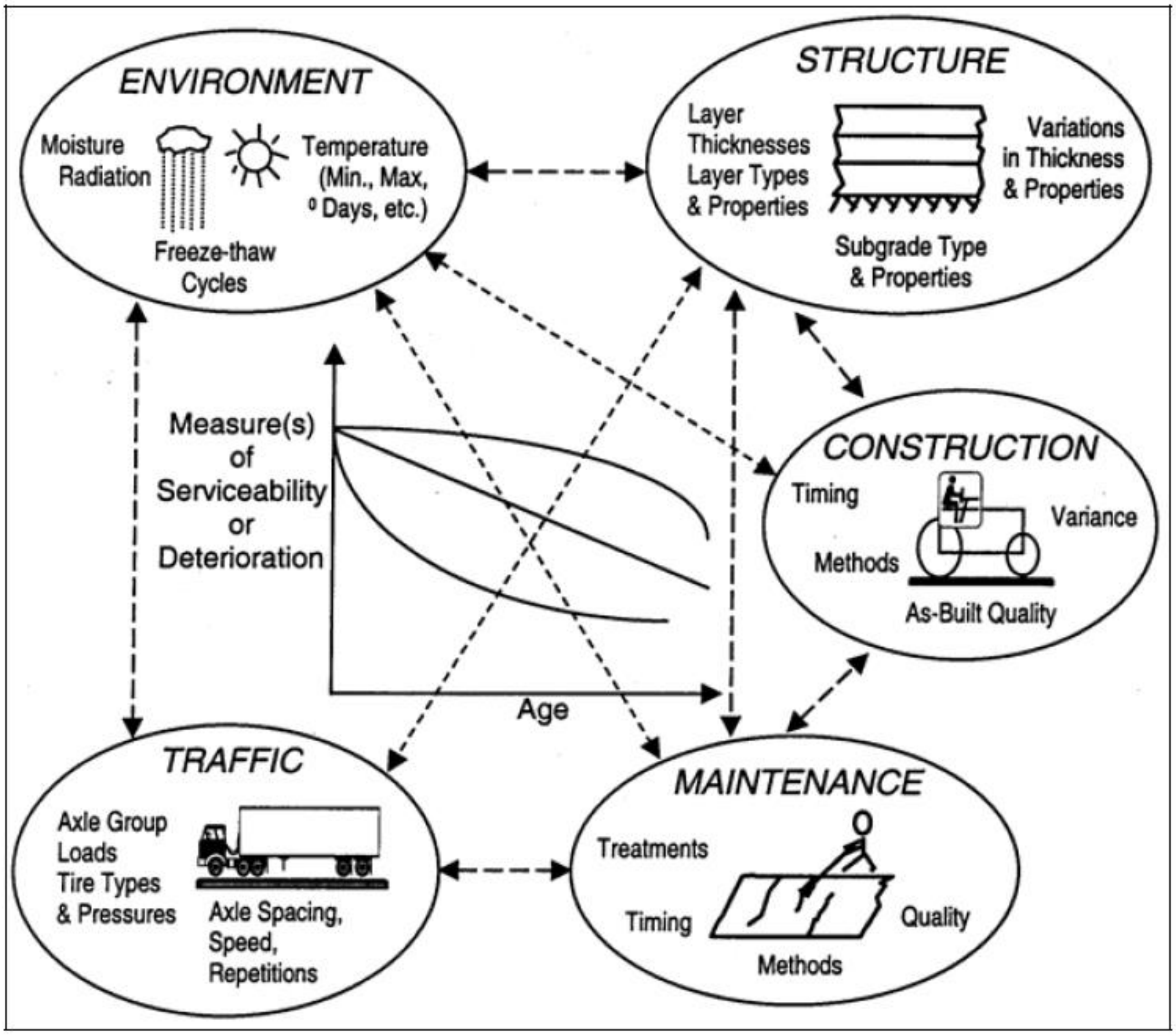

Figure 2.1 Factors affecting road performance (Haas, 2004)

2.2. Mechanical Behaviour of Asphalt under Varying Climatic Influences

2.2.1. Damage to Asphalt During Seasonal Changes

During seasonal changes, the thermal stresses on pavement structures vary and impact its performance and can lead to deterioration. Among different stresses, thermal cracking can result and will impact the pavement's structural performance. Thermal cracking may be divided into two categories. The first is low-temperature transverse cracking, which occurs when cracks run roughly parallel to the pavement centerline and are spaced evenly throughout the length of the road (Shenoy, 2002). Thermal fatigue cracking is the second kind, which is caused by the aging of pavement material as well as accumulated residual stresses from a significant number of thermal loading cycles. Different factors such as material homogeneity, ductility of asphalt concrete, frictional constraint between the layers, and cooling rate all play a role in thermal cracking (Shen and Kirkner, 2001). As the temperature drops and the pavement compresses, frictional constraint, and tensile stress increase until the tension surpasses the pavement's tensile strength, causing cracking (Raad et al., 1998; Sebaaly et al., 2002). Epps (2000) found that low temperature cracking occurs more frequently at temperatures below -7 °C whereas, temperature fatigue cracking is most typically caused by an accumulation of daily thermal cycles between -7 °C and 21 °C. Extreme maximum pavement temperature can also increase age-hardening (Mills et al., 2007). The age-hardening occurs primarily due to the oxidation of asphalt, which enhances the asphalt viscosity and thus increases the stiffness of the mixture (Airey, 2003). Higher temperatures may cause premature age-hardening and brittleness in the pavement, making it more susceptible to low-temperature cracking.

The most important climate-related mechanisms that can affect pavement degradation in Canada are frost heave and thaw weakening (Mills et al., 2007). Frost heave occurs when pore water freezes and/or ice lenses form in the underlying layers, causing a raise in the pavement surface (TAC, 1997). Heaving is particularly common in poorly constructed roads with fine-grained sub-grades that are in areas with frequent freeze-thaw cycles and significant precipitation (Haas et al., 2004;). Low-volume roads in frost-prone locations are especially vulnerable (Tighe et al., 2001; Kestler, 2003). According to Dore' (1995), cracking under frost conditions is a two-phase process.

The first step is initiation, during which the pavement resists the strains caused by frost heave. Crack propagation is the second phase, which occurs as soon as the first crack develops. Surface roughness, which may be determined from the longitudinal profiles of pavement sections, reflects heaving-related damage (Fradette et al., 2005). Most frost-related damage occurs during the thawing phase (Mills et al., 2007, Chapin et al., 2010). The phase in which the pavement has increased strength, on the other hand, occurs when the pavement structure is entirely frozen and somewhat free of moisture.

Rutting is a type of pavement distress in which permanent deformations accumulate to form a surface depression in the wheel path of pavements caused by the passing of vehicles. This deformation occurs at high temperatures when the asphalt binder becomes softer or less stiff. It is mainly caused by using unsuitable asphalt grades and/or asphalt mix, inadequate pavement thickness and insufficient compaction. This type of distress decreases the ride quality and safety of pavements. Due to rutting, water gets trapped in the depressions which causes cracking in the pavements thus leading to pavement deterioration. Long-term degradation patterns may be determined in part by the timing and sequence of environmental variables. According to Mishalani and Kumar (2005), warmer and cooler weather over the first few years following initial construction has been observed to have a favourable influence on long-term rutting due to the less hardened pavement in the early stages of its life. Furthermore, after construction, the rutting to design sensitivity increases as the early warm temperature rises and the early cold temperature falls. It means that assuming a stable long-term average temperature, the bigger the year-to-year temperature variability, the more likely it is that a design with higher safety factor or reliability will be more favourable.

2.3. Performance Graded Asphalt Cements

Asphalt is a black, sticky, viscoelastic liquid form of petroleum which is used as a binder material in pavements. It is also utilized in sealing and waterproofing. Since it exhibits both, viscous and elastic behaviour, it can dissipate the energy added in the form of deformation and heat, or it can store the added energy. It follows the principle of time-temperature superposition. Therefore, its stiffness increases at a faster loading rate or at low temperatures, whereas its stiffness decreases at a slower loading rate or at high temperatures.

The Performance Grade (PG) is a classification system for asphalt binders used in pavement construction. This system classifies the binders based on their performance at various temperatures. This system was developed in the 1987 under the Strategic Highway Research Program (SHRP) and was termed as Superpave. This performance-based grading system uses on site conditions under which the asphalt binder is expected to perform. These conditions include historical air and pavement temperatures, design Equivalent Single Axle Load (ESAL), and type of road. The PG asphalt binders are specified based on the best performance which is 15 to 20 years of service under traffic with minimal maintenance.

The asphalt cement is a temperature dependent viscoelastic material, and its physical properties change with the change in temperature. The performance of a binder mainly addresses two areas of poor performance i.e., rutting at high temperature, and low temperature cracking. The PG asphalt binders are selected based on high and low pavement temperature extremes in a year with a specified reliability level. This ensures maximum resistance to rutting or pavement deformation and thermal cracking at high and low temperatures, respectively. The rutting occurs at high pavement temperatures which are defined as average 7-day maximum pavement temperature whereas, low temperature cracking occurs at low pavement temperatures which are defined as average 1-day minimum pavement temperature. Thus, the asphalt binder PG consists of two portions i.e., high, and low pavement service temperature. For example, PG 52-28, as shown in Figure 2.2, the PG represents performance graded binder, 52 shows the desirable high temperature physical properties up to 52 °C and -28 indicates the desirable low temperature physical properties up to -28 °C. The Superpave system defines binder grades at 6 °C intervals. For example, for any location, if the average 7-day maximum pavement temperature is 48.5 °C and 1-day minimum pavement temperature is -24 °C, then the binder grade for that location will be 52-28 before traffic and road type adjustments. Figure 2.2 also shows typical range of asphalt PG values. In Canada, suppliers also provide these binder grades at 3 °C intervals.

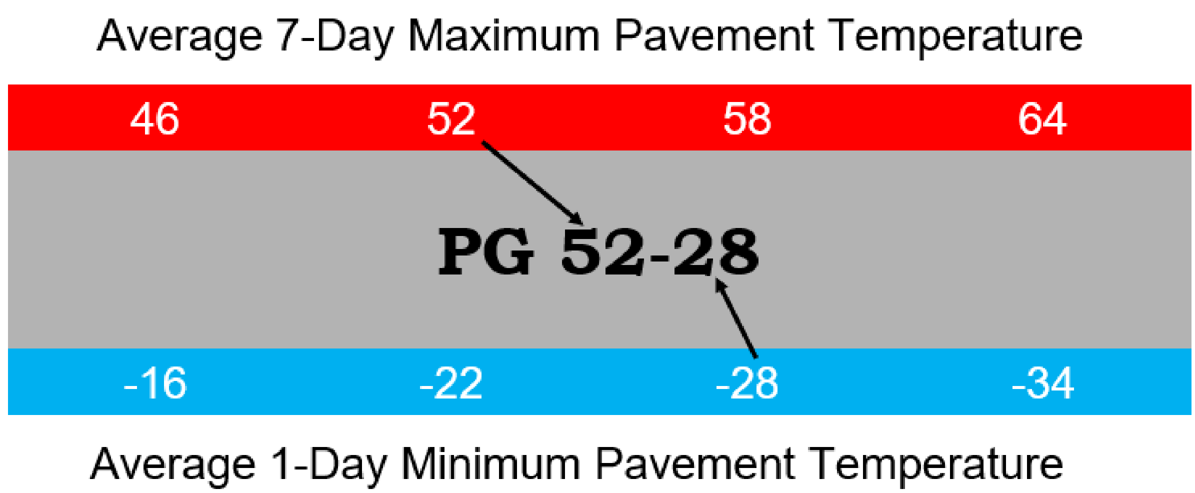

Figure 2.2 Typical Superpave binder grades used in pavement construction

The American Association of State Highway and Transportation Officials (AASHTO) has defined standards and specifications for selecting asphalt binder PGs. The AASHTO M 320 and AASHTO M 332 are the latest and most widely used specifications for selecting asphalt PGs

(Gundla et al., 2020). The AASHTO M 320 PG binder grades cover a wide range of climatic conditions, from PG 46 to PG 82 for hot temperatures and -10 to -40 for cold temperatures. The high pavement design temperatures are determined using the number of degree days over 10°C, whereas the minimum pavement design temperatures are based on minimum air temperatures. The limiting factors of this specification are based on the asphalt binder's rheological characteristics, which were evaluated at various temperatures and ageing circumstances. At the prescribed test temperatures, the stress strain relationships in the binder are determined at extremely low stress and strains using Bending Beam Rheometer (BBR) and Dynamic Shear Rheometer (DSR) tests. In this specification, grade bumping is used to address traffic speed and loading factors as shown in Table 2.1.

Table 2.1 AASHTO M 320 High-Temperature Grade Bumping Criteria

Design ESALs (Million)	**Adjustment to the High-Temperature Binder Grade**		
	Rate of Traffic Loading		
	Standard	**Slow**	**Standing**
< 0.3	-	-	-
0.3 to < 3	-	1	2
3 to < 10	-	1	2
10 to < 30	-	1	2
>= 30	1	1	2

The Multiple Stress Creep Recovery (MSCR) tests are used to grade asphalt binders in accordance with the AASHTO M 332 specification. The asphalt grades are defined based on degree days above 10 °C for maximum pavement design temperature, minimum pavement design temperature and traffic loading. In this specification, the stress strain relationship in the binder is determined at high stress and strains levels as well to better simulate what happens in a real pavement. The grade bumping specification defined in the AASHTO M 332 is different than that of AASHTO M 320 and is based on the Non-Recoverable Creep Compliance (J_{nr}) value as shown in the Table 2.2.

Table 2.2 AASHTO M 332 High-Temperature Grade Bumping Criteria

New PG Grade Designation	**MSCR J_{nr}**	**Design Traffic Level**
PG 64S-XX	Less than or equal to 4.5	Standard < 3 million ESALs
PG 64H-XX	Less than or equal to 2.0	Heavy > 3 million ESALs
PG 64V-XX	Less than or equal to 1.0	Very Heavy > 10 million ESALs
PG 64E-XX	Less than or equal to 0.5	Extreme > 30 million ESALs

The material reaction in the MSCR test differs considerably than that of DSR testing when loading is applied. As mentioned before, the high temperature parameter is determined under extremely low strain in the AASHTO M 320 specification. It can be one of the reasons why the high temperature parameter of this specification does not adequately reflect the resistance to rutting in the case of polymer modified binders (Cascione, 2018). The polymer network does not adequately engaged at the low levels of stress and strain found in dynamic shear modulus testing. Currently, the polymer is solely measured as a filler that stiffens the asphalt in the AASHTO M 320 PG specification. In the MSCR test, the binder is subjected to higher amounts of stress and strain, more closely resembling what occurs in a real pavement. In this way, the reaction of the asphalt binder encapsulates not only the stiffening effects of the polymer, but also the delayed elastic effects. Such tests are used to understand the laboratory behaviour to design the pavement, however, monitoring of the actual road conditions is necessary to predict the behaviour in-situ and to determine changes in the service life of the existing pavement structure.

2.4. Monitoring and Predicting Asphalt Behaviour

2.4.1. Seasonal Monitoring Program (SMP)

The LTPP-SMP program was initiated by the SHRP in the 1990s to collect pavement response data at several sites in the United States and Canada. The purpose of this program is to utilize the data, collected from the SMP sites, to analyze critical conditions in pavement design, and to develop and validate different models involved in pavement design. Under this program, 7500 stations have been installed and operated to create and maintain temperature database and pavement response data. A typical SMP station uses different instruments such as a temperature probe, rain gauge, thermistor probe, and pavement surface temperature sensors to collect pavement response data. A datalogger is used to collect and save the data from the instrumentation for further use.

2.4.2. SHRP Studies

The estimation of design pavement temperatures is the first stage while selecting the SHRP PG binder grades. In 1987, SHRP started developing models for pavement surface temperature predictions under the Superpave program. Solaimanian and Bolzan (1993), developed a model to predict high pavement temperatures under this program. It was first identified by this program that low pavement temperatures and air temperatures are equal. However, this approach was superseded by low pavement temperature prediction model, which was proposed by Robertson (1995). Since the data availability for validating Superpave specifications was very limited, therefore the SHRP initiated the Long-Term Pavement Performance (LTPP) Seasonal Monitoring Program (SMP) program. Under this program, a temperature database consisting of around 7500 stations in United states and Canada were developed. The data obtained from this database was then utilized for the development of LTPP pavement prediction and PG determination models.

2.4.3. Solaimanian et al., 1993

In 1993, Solaimanian and Kennedy proposed this simple and quick method for the determination of maximum pavement temperatures. It is one the earliest models developed under the SHRP program. This method utilized maximum air temperatures and hourly solar radiation for surface temperature calculation. It was developed on the principle of surface energy balance thus achieving the temperature equilibrium. In the model development, reasonable assumptions were also considered related to thermal properties of asphalt concrete. This study also proposed that the minimum pavement temperature can be assumed equal to minimum air temperature. This study concluded that solar radiation is an important parameter while determining maximum pavement temperatures. For this, latitude of the site was considered in this model. It was also evaluated that, at higher latitudes, the difference between maximum air and pavement temperatures is expected to decrease. Furthermore, maximum air temperatures and maximum pavement temperatures have a linear relationship (Solaimanian et al., 1993).

2.4.4. Robertson 1995 and 1997

Deme (1995) discovered that surface temperatures are higher than air temperatures, which were previously considered equal. Robertson (1995) proposed a model for the determination of low pavement temperatures using air temperatures. This model was a modification of the algorithm which was developed by Deme (1995). The equation developed for the determination of surface temperatures is as follows:

$$T_{surf} = 0.859T_{air} + 1.7 \qquad 2.1$$

Where T_{air} is the 1-day minimum air temperature in °C and T_{surf} is the minimum surface temperature. Robertson and Christison (1995) suggested the inclusion of reliability by evaluating the above equation. It was done by replacing the T_{air} term with $(T_{air} - n\sigma)$. The final equation is as follows:

$$T_{surf} = 0.859(T_{air} - n\sigma) + 1.7 \qquad 2.2$$

Where σ is the standard deviation and n is the standard normal distribution value which is 2.055 at 98% reliability. This model was further refined by Robertson in 1997 in which the standard deviation of actual pavement temperatures was considered. In doing so, two reliabilities, one for air and second for pavement temperatures, were considered for the determination of the pavement surface temperatures. The equation developed after this modification is provided below:

$$T_{surf} = 0.794(T_{air} - n\sigma) + 1.5n \qquad 2.3$$

In this equation, the 1.5 value was assumed for standard deviation of actual pavement temperatures. The inclusion of two reliabilities decreased the risk of the model underestimating the pavement surface temperature.

2.4.5. Lukanen et al., 1998

The LTPP SMP program, initiated by SHRP, constructed a number of weather stations in the United States and Canada to create a temperature database. This data was utilized by Lukanen et al., (1998) to develop better models, as compared to previously developed models, for the determination of pavement temperatures. These models utilized air temperatures and latitudes to determine pavement temperatures at 20 mm depth. The equations developed by Lukanen et al., 1998 are as follows:

$$Td_{max} = 0.52 + 6.225\phi - 0.15\phi^2 + 0.0011\phi^3$$

$$+0.28Ta_{max} - 8.37LN(d + 40) \qquad 2.4$$

$$Td_{min} = -0.14 - 1.7\phi + 0.06\phi^2 - 0.0007\phi^3$$

$$+0.69Ta_{min} + 4.12LN(d + 100) \qquad 2.5$$

Where Td_{max} is the high pavement design temperature in °C, Ta_{max} is the high air temperature in °C, d is depth in pavement in mm (20mm), ϕ is latitude in degrees, Td_{min} is the minimum pavement design temperature in °C, and Ta_{min} is the low air temperature in °C.

2.4.6. Bosscher et al., 1998

In the same year, Bosscher et al. also developed models for the determination of pavement temperatures at surface (6.4 mm depth) and at any desired depth. The researchers developed different equations for different temperature ranges. For minimum pavement temperatures, two different equations were proposed i.e., when air temperature is below 0 °C and -5 °C. Whereas, for high pavement temperatures, different equations for air temperature higher than 10 °C and below 10 °C were developed. Equations for minimum pavement temperature are provided below:

- When the air temperature is below 0 °C

$$T_{Pav\ @\ 6.4mm\ (\mathrm{min})} = 6.83 + 1.014T_{Air\ min} \quad 2.6$$

- When the air temperature is below -5 °C

$$T_{Pav\ @\ 6.4mm\ (\mathrm{min})} = 0.3768 + 0.687T_{Air\ min} \quad 2.7$$

- Minimum pavement temperature at any desired depth

$$T_{d\ min} = T_{Pav\ @\ 6.4\ mm\ (\mathrm{min})} - \left(0.00123T_{Pav\ @\ 6.4\ mm\ (\mathrm{min})}(d - 6.4)\right)$$

$$+0.0146(d - 6.4) \quad 2.8$$

Where $T_{d\ min}$ is the minimum pavement temperature at any desired depth in °C, $T_{Pav\ @\ 6.4\ mm\ (\mathrm{min})}$ is the minimum pavement at 6.4 mm in °C and d is the depth from surface in mm. For the determination of maximum pavement temperature, the following equations were developed:

- When the air temperature is above 10 °C

$$T_{Pav\ @\ 6.4mm\ (\mathrm{max})} = -0.519 + 0.820\ T_{Air\ max} + 0.00335\ Solar \quad 2.9$$

- When the air temperature is below 10 °C

$$T_{Pav\ @\ 6.4mm\ (\mathrm{max})} = 2.811 + 1.087\ T_{Air\ max} + 0.00246\ Solar \quad 2.10$$

- Maximum pavement temperature at any desired depth

$$T_{d(\mathrm{max})} = T_{Pav@6.4mm\ (max)} - 2.68 * 10^{-3}(d - 6.4)\ T_{Pav@6.4mm\ (\mathrm{max})}$$

$$+4.25 * 10^{-4}(d - 6.4)^2 \qquad 2.11$$

Where $T_{Pav\ @\ 6.4mm\ (\max)}$ is the maximum pavement temperature at 6.4 mm depth in °C, $T_{Air\ max}$ is the maximum air temperature in °C and $Solar$ is the total daily solar radiation intensity in Whr/m^2. The researchers concluded the solar radiation as a critical parameter while determining maximum pavement temperatures and recommended that while measuring air temperatures, solar radiation intensity should also be measured (Bosscher et al., 1998).

2.4.7. Mohseni et al., 1998

In this study, the database for pavement temperatures was developed by utilizing the LTPP-SMP data. This data was then utilized for the development of high and low pavement temperature models. These models were developed to improve the SHRP asphalt PG grade selection procedure in the Superpave program. For the models' development, daily air and pavement temperature data were used. To determine the highest pavement temperature, average 7-day high air temperature were considered. It was observed by Mohseni et al. (1998) that rutting happened during extended heat waves. Using of 1-day maximum temperature was considered non-conservative and therefore a 7-day average was considered. In these models, an error term was introduced to account for variabilities in determining the pavement temperatures (Mohseni et al., 1998). Two types of variabilities i.e., mean air temperature and estimated pavement temperature were considered while determining the design pavement temperatures. For the air temperature variability, the standard deviation of the mean air temperature (high and low) was used whereas, for the pavement temperature variability, the Root Mean Square Error (RMSE) of the model was considered. The error term was coupled with the reliability factor to have results at any desired reliability. In terms of asphalt PG selection, reliability is defined as "the probability (in percentage) in a single year that the actual low pavement temperatures will not decrease, and the actual high pavement temperatures will not increase the corresponding design temperatures" (Brown et al., 2009). The error term was subtracted from the low pavement temperature equation and added to the high pavement temperature equation to obtain higher reliability. The regression models obtained by corelating low and high pavement temperatures with air temperatures and latitudes are provided below:

$$Tp_{min} = -1.56 + 0.72\, Ta_{min} - 0.004\, Lat^2 +$$

$$6.26\, Log(H + 25) - Z\, (4.4 + 0.52\sigma_{Tair\, min}{}^2)^{1/2} \qquad 2.12$$

$$Tp_{max} = 54.32 + 0.78\, Ta_{max} - 0.0025\, Lat^2 -$$

$$15.14\, Log(H + 25) + Z\, (9 + 0.61\sigma_{Tair\, max}{}^2)^{1/2} \qquad 2.13$$

Where $T_{P\,max}$ is the highest mean 7-day pavement temperature in °C, $T_{air\,max}$ is the highest mean 7-day air temperature in °C, $\sigma_{Tair\,max}$ is the standard deviation of highest mean 7-day air temperature in °C, $T_{P\,min}$ is the lowest pavement temperature in °C, $T_{air\,min}$ is the lowest air temperature in °C, $\sigma_{Tair\,min}$ is the standard deviation of lowest air temperature in °C, Lat is the latitude in degrees, H is the depth in mm and Z is the standard normal distribution value i.e., 2.055 for 98% reliability. It was concluded that both models should be updated as more SMP data become available.

2.4.8. Mohseni et al., 2005

Mohseni et al., 2005 proposed improved methodology for the determination of high temperature PG grade for asphalt binders. In this research, improved transfer function for average 7-day high pavement temperatures, and a rutting damage model was developed using the SMP data. For the development of improved high-temperature transfer function, an Integrated Climatic Model (ICM) was comprehensively utilized. To get a more accurate and refined picture of high temperatures in a pavement, the hourly climatic data was utilized in the model development. A performance based, rut damage model was then developed utilizing the hourly climatic data and previously developed models for rut predictions and Hot Mix Asphalt (HMA) stiffness. The newly developed performance-based procedure was able to account for extended hot periods, which was not considered in the original procedure.

A new high pavement temperature model like SHRP was developed using the hourly data obtained from the temperature database. To achieve more accuracy, this model was developed to estimate pavement temperatures at a depth of 20 mm below surface. The following is the new high pavement temperature model based on an average 7-day high temperature.

$$Tp_{max} = 32.7 + 0.837\, Ta_{max} - 0.0029\, Lat^2 + Z\left(\delta_{air}^2 + \delta_{Model}{}^2\right)^{1/2} \qquad 2.14$$

Where $T_{P\,max}$ is the highest mean 7-day pavement temperature in °C, $T_{air\,max}$ is the highest mean 7-day air temperature in °C, δ_{air} is the standard deviation of highest mean 7-day air temperature in °C, δ_{Model} is the standard error of model i.e., 2.1 in °C, Lat is the latitude in degrees, H is the depth in mm and Z is the standard normal distribution value i.e., 2.055 for 98% reliability. As mentioned before, it was determined that the 7-day average temperature approach could not account for the extended heat waves.

For the development of performance based, rut damage model, different parameters such as traffic speed, ESAL, latitude and longitude of site along with the estimated high and low pavement temperatures were utilized. The climatic data from around 186 sites throughout the United Sates was used. This method used the degree days approach instead of the traditional average 7-day temperatures to account for extended hot periods in a climate. The determination of high temperature PG grade is a step-by-step procedure. The first step is the estimation of damage-based PG which requires degree-days and a target rut depth with 50% reliability as input. The equation developed for determining damage-based PG is given below:

$$PGd = 48.2 + 14\,DD - 0.96\,DD^2 - 2\,RD \qquad 2.15$$

Where PGd is the estimated damage-based PG in °C, DD is the average yearly degree-days of air temperature over 10 °C (x1000 °C-days) and RD is the target rut depth (5-13 mm). The degree-day is defined as the summation of daily high air temperatures over a span of one year whenever the daily air temperature is more than 10 °C. An average value of degree-days over an observation period is used. The damage-based PG is the high pavement temperature and the subsequent binder grade in 6 °C increment is the base grade. The PGd calculated from the above equation demonstrates the high pavement surface temperature at 50% reliability under normal conditions i.e., less than 3 million ESAL of traffic load and fast traffic speed. The second step involves the estimation of the coefficient of variation of the base temperature. It is to adjust the base temperature for reliability. The equation developed for the estimation of this coefficient is provided below:

$$CVPG = 0.000034\,(Lat - 20)^2 RD^2 \qquad 2.16$$

The PGd transfer function was developed using the yearly degree days with a base of 10 °C over a 20-year period. To account for more rutting damage in the early years after construction, it was critical to adjust the PG transfer function for yearly variation. The coefficient of variation estimated from the above equation is utilized to determine asphalt PG at any desired reliability. It can be estimated using the following equation:

$$PGrel = PGd + Z\ PGd * \left(\frac{CVPG}{100}\right) \quad 2.17$$

Where $PGrel$ is the PG at any desired reliability in °C, Z is the standard normal distribution value from the Standard probability table and $CVPG$ is the yearly PG coefficient of variation in %. As mentioned before, the equation developed for PGd determination could only account for normal conditions i.e., less than 3 million ESAL of traffic load and fast traffic speed. Therefore, to account for slow traffic speed and greater than 3 million ESAL of traffic load, the PGd equation should be adjusted for traffic loading and speed. This study proposed grade bumping criteria to adjust traffic loading and speed. Since the grade bumping was proposed only for fast and slow speed, therefore Advanced Asphalt Technologies (AAT), 2011 proposed a more refined criteria for speed and traffic loading adjustment. In this, very slow speed was also incorporated. Table 2.3 and Table 2.4 shows the LTPP and AAT criteria for traffic load and traffic speed adjustment.

Table 2.3 Damage Based PG Grade Bumping for Traffic Loading and Speed. Mohseni et al., 2005

		Traffic Loading ESAL, Millions			
Speed	**Base Grade**	**< 3**	**3-10**	**10-30**	**> 30**
Fast	52	0	10.3	16.8	19.3
	58	0	8.7	14.5	16.8
	64	0	7.4	12.7	14.9
	70	0	6.1	10.8	12.9
Slow	52	3.1	13	19.2	21.6

	58	2.9	11.2	16.8	19
	64	2.7	9.8	14.9	17
	70	2.5	8.4	12.9	14.9

Table 2.4 Damage Based PG Grade Bumping for Traffic Loading and Speed. NCHRP 673

Design Traffic (ESALs)	**Grade Adjustment for Average Vehicle Speed in kph (mph)**		
	Very Slow	**Slow**	**Fast**
	< 25 (< 15)	**25 to < 70 (15 to < 45)**	**>= 70 (>= 45)**
< 0.3	-	-	-
0.3 to < 3	12	6	-
3 to < 10	18*	13	6
10 to < 30	22*	16*	10
>= 30	-	21*	15*

* Consider use of polymer modified binder. If a polymer modified binder is used, high temperature grade may be reduced one grade (6 °C), provided rut resistance is verified using suitable performance testing.

To select a high temperature asphalt PG at any desired depth, equation 2.14 can be used (Mohseni et al., 2005). Using this equation, high pavement temperature at surface and at any desired depth is estimated. The difference between these temperatures is then calculated which is termed as temperature correction factor for depth. This correction factor is then added to $PGrel$ to select high temperature PG, before applying the traffic correction.

2.4.9. LTPPBind

LTPPBind is an online tool which is widely being used by the designers and transportation engineering personnel to accurately select the most appropriate asphalt binder PG for pavement construction at a specific site. The latest version of this tool is LTPPBind V3.1. It was developed by Pavement Systems, LLC for the Federal Highway Administration (FHWA) (Mohseni et al., 2005). This tool allows the user to use National Aeronautics and Space Administration's (NASA) Modern-Era Retrospective Analysis for Research and Application (MERRA) climatic data, LTPP climatic data, and user provided data for the determination of asphalt PG binder. The LTPP climatic data is obtained from the database of around 7500 weather stations installed and operated in the United States and Canada. The databases which are utilized to obtain data are Surface Land Daily and Canadian Daily Climatic Data. Data includes ID name, latitude, longitude, elevation of a weather station and climatic data such as high and low air temperatures, evaporation, precipitation, snowfall, snow depth, 24-hour wind movement and maximum and minimum soil temperatures as provided by each weather station. The LTPPBind V3.1 uses the five nearest weather stations to assess the environmental parameters while examining the binder grade for a given area. The average of the environmental characteristics for the five locations is used to propose a binder grade.

The LTPPBIND V3.1 uses meteorological data that includes maximum and minimum daily air temperatures (Mohseni et al., 2005). To estimate the low pavement temperature, the Mohseni et al., 1998 model is utilized as provided in equation 2.12. As mentioned before, this model was developed by the regression analysis of LTPP SMP data. This model estimates low pavement temperatures using low air temperatures, latitude, and depth (Mohseni et al., 1998). Whereas, for high pavement temperature, this tool uses the latest LTPP performance-based rut damage model and the procedure as described above in section 2.3.5.6 (Mohseni et al., 2005).

This tool also offers the user to input their own data. While using this approach to determine asphalt PG binder, the user must input the values for certain parameters such as target rut depth, asphalt layer depth, base high temperature PG, traffic loading cumulative ESAL, traffic speed. Utilizing the input information, the tool suggests the asphalt PG under AASHTO M 323-13 and AASHTO M 332-14 standards. Figure 2.3 and Figure 2.4 shows the screenshots of LTPPBind online tool while selecting a location and suggested asphalt PG using the manual data input approach.

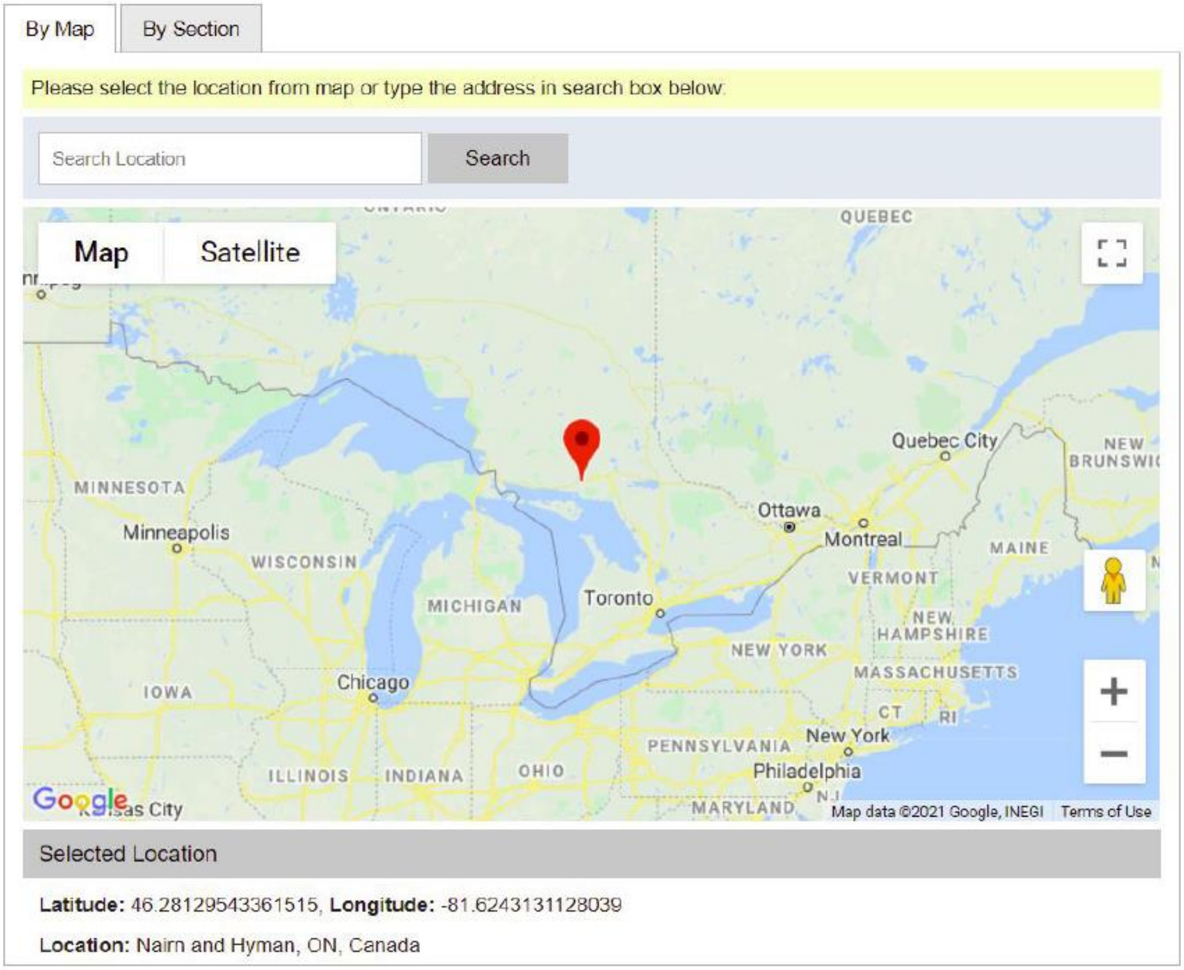

Figure 2.3 Screenshot of LTPPBind Online on Location Selection

AASHTO M323-13 Performance-Graded Asphalt Binder		
PG Temperature	High	Low
Performance Grade Temperature at 50% Reliability	44.9	-27.7
Performance Grade Temperature at 98% Reliability	47.9	-34.7
Adjustment for Traffic (AASHTO M323-13)	0.0	
Adjustment for Depth	-3.9	1.6
Adjusted Performance Grade Temperature	44.0	-33.1
Selected PG Grade	**52**	**-34**
PG Grade	**M323, PG 52-34**	

AASHTO M 332-14 Performance-Grade Asphalt Binder using Multiple Stress Creep Recovery (MSCR) Test		
PG Temperature	High	Low
Performance Grade Temperature at 50% Reliability	44.9	-27.7
Performance Grade Temperature at 98% Reliability	47.9	-34.7
Designation for traffic loading	S	
Selected PG Grade	**46**	**-34**
PG Grade	**M332, PG 46S-34**	

Temperature Report	
Lowest Yearly Air Temperature, °C:	-36.59
Low Air Temp Standard Deviation, °C:	3.69
Yearly Degree-Days > 10 Deg. °C:	1767.71
High Air Temperature of high 7 days:	28.47
Standard Dev. of the high 7 days:	1.98
Low Pavement Temperature 50%:	-33.10
Low Pavement Temperature 98%:	-40.20
High Avg Pavement Temperature of 7 Days 50%:	50.26
High Avg Pavement Temperature of 7 Days 98%:	54.43

Figure 2.4 Screenshot of LTPPBind Online showing Suggested Asphalt PG

2.4.10. Other Studies

Barber (1957) computed pavement temperatures using climatic data, which was one of the first studies to employ analytical methods to forecast pavement temperatures. Climate elements, such as geographical and meteorological data, are the fundamental aspects of this pavement temperature modelling effort. After that, many different researchers across the globe developed different analytical models for the prediction of pavement temperatures. In this section, some of the analytical models developed in North America are summarized in Table 2.5.

Table 2.5 Pavement Temperature Prediction Models

Ref, Year	**Influencing Factors**	**Summary and Findings**
Barber (1957)	• Air Temperature • Pavement Temperature • Wind • Solar Radiation • Precipitation • Coefficient of Thermal Properties	• One of the first analytical model to predict pavement temperatures. • The results of the model were validated on asphalt pavements having a thickness of 63.5 mm. • The estimated results were compared with the actual pavement temperatures and was concluded that the model showed around 3 to 5 °C of maximum temperature error. • The developed model could predict maximum as well as minimum temperature of pavements
Higher and Wall (1984)	• Asphalt pavement's thermal conduction under various specific densities	• A recycling process was incorporated in which the heat was applied to the asphalt pavement using an external heat source.

		• The spread of heat conduction in the limestone’s surface and base course was significantly different.
Liang and Niu (1998)	• Air Temperature • Pavement’s Surface Temperature	• A three-layer system was utilized in the determination of analytical solution with a simplified boundary condition involving only the heat transfer between air and the pavement surface. • The researchers concluded that the distribution of temperature could be non-linear within the depth of pavement structure.
Park et al. (2001)	• Surface Temperature • Depth • Coefficient associated with time	• The model was verified for a range of surface temperatures between -28.4 °C to 53.7 °C and depth between 14 to 27.7 cm.
Diefenderfer et al. (2003)	• Maximum/Minimum air Temperature • Day of the Year • Depth below surface	• Two different models for determining maximum and minimum pavement temperatures were developed. • These models were validated using data from the SMP sites in the United States and can be used for the four seasons and for different climate zones.

2.5. Application and Removal of Load Restrictions in the Spring

The freezing and thawing in soils are overall complicated processes. With the soil temperature approaching the freezing point, the water present in the soil begins to freeze which leads to frost heave. This frost heave causes a loss of strength in the pavement structure during the thawing season (Andersland and Ladanyi, 2004). The required circumstances for producing alternating bands of soil and ice result from a combination of unstable heat transport near the ground surface from fluctuations in air temperatures, as well as crystal ice nucleation and growth. During the freezing season, the creation of ice bands and the segregation of ice leads to an increase in the volume of the soil/water system (Andersland and Ladanyi, 2004), which is the key process involved in frost heaving.

During the winter season, when the temperature drops below freezing, the pore water in the pavement structures start to convert to ice lenses (Salour et al., 2013). The frozen layer grows deeper into the pavement structure until it reaches a point when the freezing slows down and formation of ice lenses halts due to reduced heat flow (Salour et al., 2013). This results in the formation of water-rich frost zone in the structure (Salour et al., 2013). This frozen layer borders by an unfrozen layer below (Chapin et al., 2010).

During the spring thaw periods, when the air temperature starts to increase, the water-rich frost zone starts to thaw and the water present in the form of ice lenses transforms back into the liquid state (Salour et al., 2013). The thawing in the pavement layers initiates from top down, due to increased air temperatures, and from the bottom up, due to the geothermal flux caused by the geothermal gradient (Chapin et al., 2012). In these thawing periods, the surface temperatures greater than 0 °C in conjunction with the warming of bottom of pavement structure due to geothermal flux generates two 0 °C temperature interface boundaries, with one at the bottom and one at the top of frozen layer (Chapin et al., 2010). These conditions result in the energy transfer into the frozen layer thereby thawing the frozen layer and reducing its thickness (Chapin et al., 2010). This results in the moisture being trapped between the frozen layer below and relatively impermeable pavement surface course above (Chapin et al., 2010), thus temporarily increases the water content in the unbound pavement layers (Salour et al., 2013). In these conditions, there is little or no drainage of the accumulated moisture/water. The change in moisture content not only effects the stress states through pore-water pressures but also the soil structure due to damage of the particles' cementation bonds (Lekarp, Isacsson, & Dawson, 2000). Excess pore pressure and water saturation conditions under heavy traffic loads can lead to loss of shear strength and internal friction in the unbound layers, degradation of pavement materials and loss of underlying support (Janoo, 2002). The entrapped water reduces the strength of subgrade and sub-base thus reduces the material's bearing capacity to support overlying pavement structure (Van Deusen, 1998). Once the moisture content inside the pavement system returns to pre thawing level, the pavement structure regains its true strength (Chapin et al., 2010).

It has been observed that the average annual surface temperatures do not vary consistently with the corresponding average annual air temperatures (Andersland and Ladanyi, 2004). The difference between air and surface temperatures is caused by several factors, including net solar radiation, snow cover, vegetation, subsurface drainage, and ground thermal properties. The surface temperatures can be estimated from the air temperatures using the n-factor approach (Chapin, 2010). The n-factor is a multiplier which is used to correct the air freezing and thawing indices (Dore et al., 2008). It is an empirically developed approach and defines the n-factor as follows (Dore et al., 2008):

$$n_f = \frac{FI_s}{FI_a} \tag{2.18}$$

$$n_t = \frac{TI_s}{TI_a} \tag{2.19}$$

Where n_f, n_t are the freezing and thawing n-factors, FI_s, FI_a are the surface and air freezing indices, and TI_s, TI_a are the surface and air thawing indices, respectively. Different n-factors, for both freezing and thawing seasons, have been proposed and can be utilized for the determination of surface temperatures. A freezing index is the running summation of negative mean daily temperatures, whereas a thawing index is the running summation of positive mean daily temperatures over a specified period. The freezing and thawing air and surface indices are defined as follows:

$$FI_a = \sum_0^t -MDAT_- \tag{2.20}$$

$$TI_a = \sum_0^t MDAT_+ \tag{2.21}$$

$$FI_s = \sum_0^t -MDST_- \tag{2.22}$$

$$TI_s = \sum_0^t MDST_+ \tag{2.23}$$

Where T_+ and T_- are temperatures above and below 0 °C, respectively, $MDAT$ and $MDST$ are mean daily air and surface temperatures, respectively, and t is the time period considered. The degree-day notion is used by the temperature indices to characterise the intensity of air and surface temperature fluctuations. Different n-factors, for both freezing and thawing seasons, have been proposed and can be utilized for the determination of surface temperatures.

During the spring-thaw weakening season, several road agencies and municipalities across Canada and the United States impose SLRs to mitigate the damage to low-volume roadways. SLRs should ideally begin when thawing front migration reaches a depth that causes considerable pavement structural deterioration. Different studies such as Kestler et al., 1999, and Hein and Cole, 2002, suggest that as soon as thawing starts in the pavement, the SLR should be implemented. However, other researchers recommend that the thawing front should reach a specific depth in order to decrease the pavement stiffness significantly. Using this approach, Van Deusen, 1998 investigated the influence of air temperature on frost and thaw depths and concluded that, when the thawing front reaches the base layer of the pavement, it causes significant decrease in the stiffness of aggregate base layer. In another study, Ovik et al., 2000, performed a number of Falling Weight Deflectometer (FWD) tests at the Minnesota road test site. The results showed significant increase in the pavement deflections when the thawing front reached a depth between 300 mm to 600 mm. The thickness of the asphalt concrete layer, according to Rutherford, 1989, has a substantial impact on pavement strength. In the same research, it was concluded that the thin pavements drastically loose their stiffness during the base thawing, but thicker pavements did not demonstrate the same behaviour until substantial sub-grade thawing has occurred. Moreover, the effect of thawing followed by refreezing, which is frequent throughout most thawing seasons, is also a key concern in the implementation of SLRs.

The removal of these restrictions is also a complicated process and should be done with great care. The removal of SLR should take place after complete thawing of the pavement structure (Andersland and Ladanyi, 2004). This gives proper time to pavement structure for the restoration of natural drainage conditions. A study was carried out in which, after analyzing the results of several pavement deflections tests, suggested that the time necessary to accomplish complete thawing of the pavement structure can be less than or even half of the time the pavement is structurally weak (Cole, 2002). Furthermore, in another study, the results estimated from Falling Weigh Deflectometer (FWD) tests suggested that the strength of pavement is not entirely recovered until around 7 days following full thawing of the pavement structure (Berg, 2010). This does not mean that a standard addition or multiplication of the thawing time is needed to capture the weakened time of the pavement structure. In this study, the approach used for determining the application and removal of SLR is the same as utilized by the MTO i.e., the most significant loss of pavement strength occurs when the thaw starts in the base, and the least significant loss occurs when the thaw reached a depth of around 1 meter. The MTO uses a thawing depth of 1.5 to 1.65 meters which ensures the required drainage of water from the pavement layers.

2.6. Methods of Determining Spring Load Restrictions

In the North America, particularly in Canada and the United States, DOTs and municipalities have been using different approaches to implement and remove SLRs. These include the use of prescheduled calendar dates, engineering judgement, pavement deflection testing, measuring of temperature at different depths and empirical models.

Methods such as engineering judgement and pavement deflection testing need a lag time of around 3 to 4 days between the detection of pavement deflections and the implementation of SLR. The transportation sector requires this lag time to give enough notice to companies so that they can make suitable arrangements. During this lag time, since SLR is not implemented, the pavement structure is prone to severe damage under normal or full loads. The approach of using prescheduled dates, for SLR implementation and removal, efficiently removes the lag period's difficulties. However, because limits may be in place while the pavement structure is totally thawed or its strength is fully recovered, this strategy can drastically extend the duration that SLRs are imposed on a highway. This can cause the transportation industry to face higher expenses over a longer period of time. In the event of an abnormally warm spell in late winter, they may be placed too late, causing harm to the highway. As the climate continues to change, establishing acceptable prescheduled times on a year-to-year basis becomes more challenging.

The method of measuring actual temperatures at different depths of a pavement structure ensures greater accuracy but requires high costs in installation and maintenance of temperature sensors. Moreover, during the time of pavement repairs, sensors can get damaged and no longer operate until they are fixed. During this time, no temperature data is being recorded thus could potentially lead to inaccurate SLR periods. Several empirical models have been developed for implementation and removal of SLR. These methods utilize variations in the air temperatures to predict freezing/thawing indices and depths within the pavement structures. Most of these empirical models require pavement deflection data to predict results.

2.6.1. Empirical Approaches

Mahoney et al., 1987

Mahoney et al., 1987 suggested an empirical method for the determination of the SLR periods by calculating Cumulative Thawing Index (CTI) and Cumulative Freezing Index (CFI) using a fixed reference temperature and daily average air temperatures. The proposed relationship can be expressed as follows:

CTI = $\sum(T_{avg} - T_r)$ 2.24

Where, T_{avg} is the average daily temperature and T_r is the reference temperature which is basically an average air temperature when the pavement surface temperature fluctuates around 0^oC. Usually, the T_r value decreases gradually as the season changes, from early winter to late winter or early spring, which accounts for the increased solar radiation experienced by the pavement in that season. This decreased value of T_r suggests that the pavement thawing occurs at lower air temperatures during this season. However, this method uses a fixed value of -1.67^oC for T_r for the determination of CTI. This method recommends that the SLRs should be applied when the CTI value reaches 15^oC and must be applied when the CTI reaches 28^oC for thick pavements. While calculating the CTI, its value should be reset to zero in case it obtains a negative value (Mahoney et al., 1987). This method suggests that the SLR should be removed when the value of CTI becomes equal to the 30% of the value of CFI (Mahoney et al., 1987). Where CFI can be determined by taking sum of temperatures below 0 ^oC.

Corté et al., 1995

This empirical method was developed by Corté et al. in 1995 which calculates the freezing index transmitted through the pavement structure for the determination of SLR periods. The transmitted freezing index can be calculated as follows:

$$FI_t = \left(\frac{\sqrt{FI_s} - b_e h}{1+ah}\right)^2 \tag{2.25}$$

Where, FI_t is the freezing index transmitted at the surface of the sub-grade soil, FI_s is the freezing index at the surface of the pavement, h is the total pavement thickness in cm and a, b_e are the coefficients based on the nature of pavement materials (Guy Doré, 2009). If the pavement structure is made up of a single material, then b_e is equal to b and if the pavement structure is made up of several layers of material, then b_e can be calculated as follows:

$$b_e = \frac{\sum_{i=1}^{n} b_i h_i}{\sum_{i=1}^{n} h_i} \quad 2.26$$

Where, b_i is the coefficient for materials in layer *i* and h_i is the thickness of layer *i* in cm. A typical value used for a is 0.008 and for *b* is, 0.06 for asphalt concrete or 0.10 for granular material (Guy Doré, 2009). In this method, the frost penetration into the sub-grade can be calculated by using the modified Stefan equation which can be expressed as follows:

$$X_{ss} = \sqrt{\frac{2\left(k_f - (SP * L)\right)}{L_s} * FI_t} \quad 2.27$$

Where X_{ss} is the frost depth in m, k_f is the thermal conductivity of frozen soil in W/m.^{o}C, L is the latent heat of fusion of water in MJ/m^3, L_s is the latent heat of fusion of freezing soil and SP is the segregation potential of freezing soil in m^2/s.^{o}C. This method requires a lot of input parameters for the determination of the SLR periods which makes it difficult to use.

Minnesota Department of Transportation, 2004

This is an empirical method which was developed in 2004 by the Minnesota Department of Transportation (Mn/DOT) and was derived from the concepts investigated by the Washington Department of Transportation (Ovik et al., 2000). This method uses the reference temperatures and measured air temperatures to calculate daily FI and TI values. According to the Mn/DOT, FI is “the positive cumulative deviation between a reference freezing temperature and the mean daily air temperature for successive days” (Ovik et al., 2000) while TI is “the positive cumulative deviation between the mean daily air temperature and a reference thawing temperature for successive days” (Ovik et al., 2000). The reference temperature in this method is a floating value which is used to convert the air temperatures into corresponding surface temperatures. The value of this reference temperature is taken as -1.5°C which begins on 1st February, and it decreases by 0.5°C every week until it reaches to a value of -9.5 °C during 24th – 30th May (Mn/DOT, 2004). The values of TI and FI are then used to determine the cumulative thawing index as shown in the following equations (Mn/DOT, 2004):

$$CTI = \sum_{i=1}^{n}(Daily\ Thawing\ Index - 0.5 * Daily\ Freezing\ Index) \tag{2.28}$$

- Case A: when $\left(\frac{T_{max}+T_{min}}{2} - T_{reference}\right) > 0°C$ (The pavement structure is thawing)

  Then, $Daily\ Thawing\ Index = \left(\frac{T_{max}+T_{min}}{2} - T_{reference}\right)$

  and $Daily\ Freezing\ Index = 0°C$

- Case B: when $\left(\frac{T_{max}+T_{min}}{2} - T_{reference}\right) < 0°C$

  And $CTI_{n-1} \leq 0.5$ x $\left(0°C - \frac{T_{max}+T_{min}}{2}\right)$, (Significant thawing has not yet occurred)

  Then, $Daily\ Thawing\ Index = 0°C$ and $Daily\ Freezing\ Index = 0°C$

- Case C: When $\left(\frac{T_{max}+T_{min}}{2} - T_{reference}\right) < 0°C$

  And $CTI_{n-1} > 0.5$ x $\left(0°C - \frac{T_{max}+T_{min}}{2}\right)$, (Pavement structure is refreezing)

  Then, $Daily\ Thawing\ Index = 0°C$ and $Daily\ Freezing\ Index = \left(0°C - \frac{T_{max}+T_{min}}{2}\right)$

where CTI is the cumulative thawing index calculated over a period from 1 to n days in °C -days, CTI resets to zero on January 1st, T_{max} is the maximum daily air temperature in °C, T_{min} is the minimum daily air temperatures in °C and T_{ref} is the reference air temperature in °C. As mentioned before, the reference temperatures are utilized to adjust for the temperature difference between the air and asphalt temperatures (Mn/DOT, 2004). While determining the CTI, the 0.5

factor is applied to the *FI* which accounts for the partial phase change of water and therefore known as the refreeze factor.

This method suggests that the SLRs should be implemented when a 3-day forecasted temperature period gives a CTI greater than 14^{o}C-days. There is no specific value of CTI, suggested by this method, which corresponds to the removal of SLRs however, some variables such as cumulative spring precipitation, accumulated fall precipitation measured during the preceding year and CTI are used to provide a better judgement for the SLR removal. Generally, it is recommended that SLRs should remain in place for a minimum of 4 weeks and a maximum of 8 weeks. This method requires the only input of air temperature values which makes it quick and easy to apply. However, it is an empirical approach and doesn't account for site specific conditions such as subsurface properties.

Baiz et al., 2007

This is a semi-empirical method which uses air temperatures and pavement surface temperatures to calculate freeze and thaw indices (Baiz et al., 2007). Freezing index is the degree days whenever the temperature falls below 0^{o}C and remains negative while thawing index is the degree days whenever the temperature rises above 0^{o}C and remain positive. In this method, the thawing indices are based on the determination of reference temperature which is a site-specific constant which shows the temperature lag between the air temperature and pavement surface temperature. Reference temperatures can be determined from the intercept of best fit line of air temperatures and corresponding pavement surface temperatures. Mathematical expressions for the calculation of reference temperature are provided below (Baiz et al., 2007):

$$T_{Air} = \sum_{i=1}^{N} T_{ai} \tag{2.29}$$

$$T_{Srf} = \sum_{i=1}^{N} T_{si} \tag{2.30}$$

$$T_{ref} = T_{Air} - T_{Srf} * \frac{\sum(T_{si} - T_{Sfc}) * (T_{ai} - T_{Air})}{\sum(T_{si} - T_{Sfc})^2} \tag{2.31}$$

Where, T_{ref} is the reference temperature in ^{o}C, T_{si} is the surface temperature value in ^{o}C at site on day i and T_{ai} is the air temperature value in ^{o}C at site on day i. The reference temperature is determined on monthly basis and N is the number of days of the month. Here i is the number of days after the day indexed as day i = 0 and the day on which air temperature first falls below 0^{o}C. The freezing and thawing indices can be calculated using the following relations (Baiz et al., 2007):

$$\begin{cases} FI_0 = -T_0 \\ FI_{i+1} = FI_i - T_{i+1} \\ FI_i < 0 \rightarrow FI_i \equiv 0 \end{cases} \tag{2.32}$$

$$\begin{cases} TI_0 = -T_{ref} \\ TI_{i+1} = TI_{i+1} - TI_i \\ TI_i < 0 \rightarrow TI_i \equiv 0 \end{cases} \tag{2.33}$$

Where, TI_0 and FI_0 is the thawing index and freezing index value on day i = 0 in ^{o}C, and TI_i and FI_i is the thawing and freezing index value on day i in ^{o}C. Using TI, FI and calibration coefficients, the frost and thaw depths can be calculated using the following equations (Baiz et al., 2007):

$$0 \le i \le i_o \rightarrow \begin{cases} FD_i = a + b\sqrt{FI_i} + c\sqrt{TI_i} \\ TD_i = d + e\sqrt{FI_i} + f\sqrt{TI_i} \end{cases} \quad 2.34$$

$$i \ge i_o \rightarrow \begin{cases} FD_i = g + h\sqrt{FI_i} + i\sqrt{TI_i} \\ TD_i = j + k\sqrt{FI_i} + l\sqrt{TI_i} \end{cases} \quad 2.35$$

Where TD_i and FD_i are the thaw and frost depths on day i which are from the surface of the pavement in negative cm, and *a, b, c, d, e, f, g, h, i, j, k, l* are the calibration coefficients which can be calculated with a best fit regression analysis of the TI, FI and corresponding measured site specific frost and thaw depths. This method suggests that the SLR should be implemented on day i_0 and should be removed when the pavement structure thawed completely (Baiz et al., 2007). An algorithm is usually developed which indicates complete thawing of pavement structure.

Using this method, the frost and thaw depths can be predicted using measured air, pavement surface temperatures and measured frost & thaw depths however, it needs a database of reference temperatures and algorithm coefficients based on numerous sites which is a limitation to this method.

Bradley et al., 2012

The Manitoba Department of Infrastructure and Transportation (MIT) developed an empirical model to determine the SLR periods using air temperatures, surface temperatures, moisture data and FWD deflection measurements (Bradley et al., 2012). Before 2012, the MIT used to have a fixed date policy for the implementation and removal of SLRs. These restrictions typically stayed in effect for ten weeks in Manitoba. This observation motivated the MIT to improve its SLR implementation and removal policy, and thus CTI was monitored for several locations in Manitoba. It was then suggested by the MIT that the SLRs should be implemented whenever the

CTI value reaches 15^{o}C-days at any of these locations after the fixed start dates (Bradley et al., 2012). The relationship used by MIT for the determination of CTI is expressed as follows:

$$CTI = \sum Daily\ Thawing\ Index = \sum[T_{REF} + (T_{Max} + T_{Min})/2] \qquad 2.36$$

- If $(T_{Max} + T_{Min})/2 < 0$, then the Daily Thawing Index = $[T_{REF} + (T_{Max} + T_{Min})/4]$
- If $CTI < 0$, CTI is reset to 0

Where T_{Max} and T_{Min} are the maximum and minimum daily air temperatures, and T_{REF} is the reference temperature. The value of T_{REF} is taken as 1.7 ^{o}C starting from March 1 and it keep on increasing on daily basis by a value of 0.06^{o}C until May 31 and it resets to zero afterwards (Bradley et al., 2012).

For the development of this model, the MIT installed several thermistor stations, from 2007 to 2008 in both southern and northern regions of Manitoba, to measure pavement surface temperatures and moisture content. The historical and current climate data was taken from nearby Environment Canada weather stations for the calculation of CTI and CFI values (Bradley et al., 2012).

From the thermistor and moisture content sensors readings, it was observed that the thawing started when the temperature first reached 0^{o}C and/or when there's the first rise in the moisture content level in the granular base. Using the thermistor readings from several datasets, the average of CTI was determined when first thaw occurred in the granular base. This value came out to be equal to 15^{o}C which corresponded well with existing MIT SLR implementation threshold value when freezing conditions persisted past the fixed starting dates (Bradley et al., 2012).

The SLR removal threshold was determined by conducting Falling Weight Deflectometer (FWD) surveys by the MIT. From the results of FWD surveys, three criterions were defined for the removal of SLRs i.e. (1) when the CTI value reaches 350^{o}C-days, (2) no later than eight weeks after the application date and (3) 31 May (Bradley et al., 2012) as under these conditions, the entrapped excess water drained out of the system and/or the pavement showed only minor deflections which didn't affected the pavement structure (Bradley et al., 2012).

Chapin et al., (2013) and Pernia et al., (2014) Research

Chapin et al. (2013) and Pernia et al. (2014) proposed a model corelating frost and thaw depths with indices. For determining freezing and thawing indices, they proposed the utilization of MnDOT equations and reference temperatures. The CFI and CTI were then used to estimate frost and thaw depths using an empirical model which was created through regression analysis. The calibration coefficients for the prediction model were determined by plotting the measured frost or thaw depth against the day's matching CFI or CTI value. Chapin et al. (2013) and Pernia et al. (2014) compared the R-squared values of a linear and polynomial trend functions and found that the polynomial model produced higher R-squared value for their research sites. As a result, their prediction model is based on a second-order quadratic equation which is given below:

$$y = ax^2 + bx + c \qquad 2.37$$

Where, y is the frost or thaw depth, x is CFI or CTI and a, b, c are the regression coefficients.

2.6.2. Numerical Modelling Approaches

Thermal Modelling with Temp/W

The thermal numerical modelling using the finite element method can be employed to determine the SLR period at a given site. In this type of analysis, a numerical model is used to simulate freezing and thawing processes (TEMP/W, 2014). TEMP/W, a module of Geostudio developed by Geoslope Int., is a finite element software which is used to study the thermal behavior of soil or pavements under different environmental conditions and provide the temperature profile of the soil to any specified depth of interest. Moreover, TEMP/W can be coupled with SEEP/W to study the effect of moisture movement on the thermal behavior of soils (TEMP/W, 2014).

SLR periods can be determined using a coupled TEMP/W and SEEP/W analysis which provides the thermal variation in the subsurface in the presence of water. This thermal profile. along the depth, leads to the determination of frost and thaw depths, from which SLR application and removal dates can be estimated. The process of developing a numerical model in TEMP/W starts with defining the project in which different physical constants, such as latent heat of water and phase change temperature, are provided and different parameters such as analysis type, convergence criteria, initial temperature profile and time steps are defined. TEMP/W allows the user to provide any suitable value for phase change temperature while incorporating the salinity effect. After that, a geometry is defined which can be either 1-D, 2-D or 3D based on the consideration of the physical domain. This geometry can be divided into any specified numbers of nodes and elements and great care is required while doing this as it plays an important role in the model convergence. In the next step, materials and their properties are assigned to the geometry using the functions in one of the five material models (TEMP/W, 2014) which include Simplified Thermal, Full Thermal and Coupled Convective Thermal processes. While determining the frost and thaw depths, it is better to use the Full Thermal Material model as it gives more accurate results than the other two (J. Chapin, 2010). Boundary conditions are also applied to the model which includes the upper and the lower thermal boundary conditions. TEMP/W allows the user to choose from any of the four different sets of boundary conditions such as Temperature, Heat Rate, Heat Flux, and Convective Surface, which can be constant or variable in time. In addition, TEMP/W also has the flexibility of applying system dependent boundary conditions such as thermosyphon, n-factor and surface energy balance, which uses functions of different parameters like air temperature, wind speed, solar radiation etc.

Generally, the ground or surface temperatures can be estimated using the n-factor approach which uses an empirically determined coefficient called the n-factor (TEMP/W, 2014). This approach is preferred due to its simplicity as it requires only a few input parameters. The n-factor is basically a ratio of surface freezing or thawing index to the air freezing or thawing index. It is represented by the following equations.

$$n_f = \frac{I_{sf}}{I_{af}},\ n_t = \frac{I_{st}}{I_{at}}, \qquad 2.38$$

While defining the boundary condition at the surface, a modifier along with the temperature function can be used which describes the variation of n-factor as a function of ground temperature. The ground temperature at every new time step is thus calculated using the following equation (TEMP/W, 2014).

$$T_{ground} = (n - factor)\left(T_{air} - T_{phase}\right) + T_{phase} \qquad 2.39$$

TEMP/W assumes the value of n-factor to be equal to 1 whenever no modifier function is defined (TEMP/W, 2014). The numerical model simulation with appropriate geometry, material properties, upper and lower thermal boundary conditions provide with an estimate of temperature profile from surface to the bottom of the model using indicating the frost and thaw depths and hence SLR periods can be determined.

Numerical modelling has various advantages such that several scenarios can be simulated in a very short period, variation of temperature can be obtained for any location through out the cross section of the model and results can be obtained with reasonable accuracy, depending on the proper definition of thermal properties of various materials and appropriate boundary conditions.

However, it has some disadvantages such as it requires a lot of input information and modeling experience. Additionally, when uncoupled with a flow and stress strain models cannot take into account for porewater pressure and volume changes in the subsurface and their effect on temperature profiles.

New Hampshire Department of Transportation, 2006

This method was developed in 2006 and is used by the New Hampshire Department of Transportation (NH/DOT) for the determination of SLR periods. This method estimates the FI and TI values from surface temperatures, air temperatures and sinusoidal air temperature amplitude (Eaton et al., 2009). The process begins by assuming a trial value of air temperature amplitude in the Sanger (1963) equation which is expressed as follows:

$$|FI| = \left(\frac{365}{\pi}\right)\left[\sqrt{(A^2 - V^2} - V_o \cos^{-1}\left(\frac{V_o}{A}\right)\right] \qquad 2.40$$

- If V_o is positive, $0 < \cos^{-1}(\frac{V_o}{A}) < \frac{\pi}{2}$
- If V_o is negative, $\pi/2 < \cos^{-1}(\frac{V_o}{A}) < \pi$ and $\cos^{-1}(\frac{V_o}{A})$ is in radians

Where, $|FI|$ is the absolute value of the freezing index in ^{o}C-days, V_o is the mean annual air temperature in ^{o}C and A is the amplitude of sinusoidal variation in ^{o}C. For the determination of amplitude of sinusoidal variation, the value of amplitude is kept on variation until the calculated FI becomes equal to the absolute FI value determined from mean monthly air temperatures (Eaton et al., 2009). In order to determine the pavement surface FI and TI values, the freeze and thaw n-factors values are multiplied by the air freeze & thaw indices, and this process is repeated again and again until the calculated values became equal to the value of air freezing index multiplied by the n-factor value of the freezing season (Eaton et al., 2009). It is done by using the sanger's (1963) relationship which was developed from the properties of the annual sinusoidal temperature variation. It is expressed as follows:

$$n_t TI + n_f FI = 365 v_o \tag{2.41}$$

Where, FI is the freezing index, TI is the thawing index, n_t is the thawing n-factor and n_f is the freezing n-factor. The daily air and pavement surface temperature values can be determined by inputting the mean annual temperature and amplitude in the annual sinusoidal temperature variation equation developed by Sanger in 1963. This equation is expressed as follows:

$$T_D = MAT + A * \sin\left[\left(2 * \frac{\pi}{365}\right) * (Day - Lag)\right] \tag{2.42}$$

Where, T_D is the temperature on Day in ^{o}C, MAT is the mean annual temperature in ^{o}C, A is amplitude in ^{o}C, Day is the number of days after December 31 and Lag is the time lag in days. This method generally runs from February 15 to May 30 therefore, the difference between air temperatures and pavement surface temperatures between this period is used in the determination of SLR. The steps involved in calculating SLR periods for this method are similar to the ones used in the Mn/DOT method. The only difference is in the value of reference temperature which is taken as 0^{o}C (Eaton et al., 2009).

By using these relationships, the Enhanced Integrated Climatic Model (EICM) was developed which is being used by the NH/DOT. This model is a finite element based, coupled heat and mass flow program which uses various parameters, such as air temperature, precipitation, wind speed and estimated sunshine, to define the upper boundary conditions and a fixed temperature which is equal to the average annual temperature at a depth of 9.1m as the bottom boundary condition. In order to define the pavement structure properties, material properties such as grain size and Atterberg limits are used. Using this model, the frost and thaw depths can be determined which further leads to the SLRs application and removal dates (Berg, Personal Communication, 2010). This method can be used for any pavement structure under any climatic conditions however, it requires numerous input parameters which makes it very difficult to use.

2.6.3. Alternative Approach

British Columbia Department of Transportation, 2008

The research from British Columbia Department of Transportation (2008) suggests a unique approach in order to utilize thaw weakened pavement structures. Instead of applying SLRs, the stresses are brought to a lower value on the pavement by increasing the tire surface area which is not harmful for the weakened pavement structures. The province of British Columbia along with the Forest Engineers Research Institute of Canada (FERIC) have studied the effects of vehicles equipped with Tire Pressure Control Systems (TPCS) on weakened pavement structures in order to determine the feasibility of resuming full load hauling (Mabood et al., 2008). This study concluded that fully loaded logging trucks, which were equipped with TPCS, were able to use the thaw weakened roads three to five weeks prior to the SLR without causing considerable pavement cracking or rutting (Mabood et al., 2008). This is since the TPCS increases the surface area of the tire thus causing very little or no damage to the thaw weakened pavement structure. However, this is only for such vehicles which are equipped with appropriate tire deflation mechanisms. The TPCS would be an expensive investment for trucking companies, but that an incentive program could offset the cost.

2.7. Summary

In this chapter, the potential impacts of climate change, that might influence the road network in Ontario, were highlighted. In this regard, different areas such as mechanical behaviour and changes in the material properties of asphalt under varying climatic influences, which lead to damage of the asphalt pavement, were discussed. Furthermore, a brief overview of various models, which have been developed so far, for predicting asphalt pavement's temperatures and SLR periods, were also presented in the later part. The next chapter presents the details related to data collection and analysis, which were used in the models developed in this study, for determining asphalt PG and SLR periods across Ontario.

3. Data Collection and Analysis

This chapter describes different sources of data and procedures involved in the data analysis for this research. Data sources such as RWIS, SLA, OCDP and Environment and Climate Change Canada were utilized to collect the climatic data. The climatic data obtained from RWIS and SLA stations were analysed and used in the development and validation of regression models for determining asphalt PG and SLR periods. The future climate data estimated by 19 different GCMs from (name of the modeling group here) was employed to assess changes in asphalt PG and SLR across Ontario up to the year 2100.

3.1. Ontario's Road Weather Information System

Different road agencies and authorities are employing RWIS stations to collect accurate and adequate weather information for design and maintenance of roadways. The Ministry of Transportation of Ontario (MTO) oversees and administers the province's highway system. To better manage and administer the highway network, MTO has divided the province into five administrative regions. These regions are Western, Central, Eastern, Northeastern and Northwestern, as shown in Figure 3.1. The ministry owns and operates more than 165 RWIS stations across the province. These RWIS stations are spread throughout all the five administrative regions, as shown in Figure 3.2. The data obtained from these stations plays a vital role in carrying out winter maintenance activities across the province (Buchanan, 2005). The MTO is a member in the AURORA initiative, which is a worldwide collaboration of public organisations that conducts cooperative research in the use of RWIS stations.

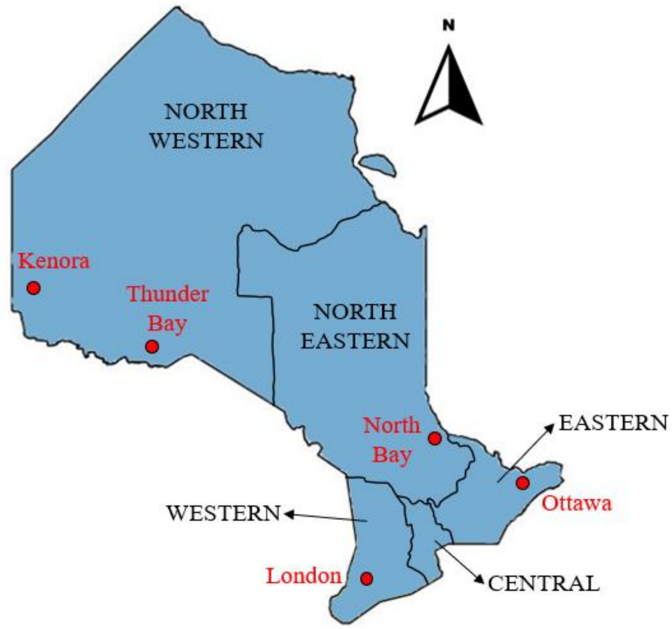

Figure 3.1 The Ministry of Transportation of Ontario's five highway network Administrative Regions.

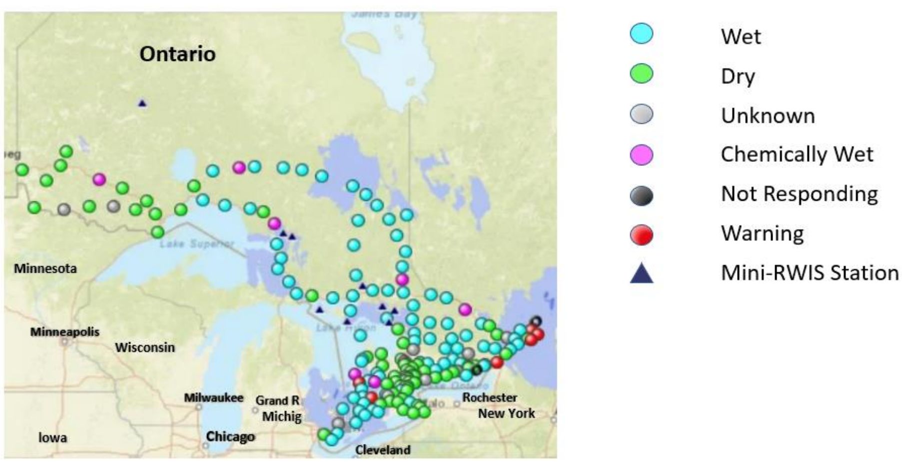

Figure 3.2 Locations and Conditions of RWIS Stations across Ontario (Source: https://weather.amec.com)

Over the last few decades, different equipment and techniques for winter maintenance activities have been developed. Visual examination was once the most popular method of detecting and predicting the quantity of snow on the surface of the road. The RWIS stations have been utilised in Europe since the 1980s, and they are gaining popularity in North America (Crevier and Delage, 2001). An RWIS station is a combination of different sensors, such as pavement and meteorological sensors, and a monitoring and prediction system which uses historical data, real-time data, and computer programs to anticipate unfavorable pavement conditions for winter maintenance (Minsk, 1998). This system can collect the real-time data every 20 minutes and uploads it to a web portal. The data is then utilized to make predictions and archive them (AMEC, 2007). Figure 3.3 shows a typical RWIS station.

Figure 3.3 A Typical RWIS station (Source: Campbell Scientific Canada)

The pavement sensors not only measure the pavement's surface temperature but also evaluate and record road surface conditions (Bernstein et al., 2004). The road sensors make use of the multi spectral measurement technology to determine the road surface condition such as ice, snow, water thickness on the surface. The sensors then transmit the measured readings to the data logger. Apart from pavement design, the RWIS data may also be used to anticipate when moisture is expected to freeze on the pavement surface, which aids in the effective deployment of staff for winter maintenance (Karlsson, 2001). Typical meteorological sensors and a pavement sensor are presented in Figure 3.4 and Figure 3.5, respectively.

Figure 3.4 Typical Meteorological Sensors Installed on RWIS Stations (Source:

www.gis.esri.com)

Figure 3.5 Typical Pavement Temperature Sensor used in RWIS stations (Source:

https://hsierra.com/products/rwis/)

3.1.1. Weather Parameters Recorded by an RWIS Station

An RWIS station, installed in Ontario, measures, and collects data for several different weather parameters. These include air temperatures, relative humidity, maximum gust wind speed, average wind speed, average wind direction, dew point temperature, air pressure, precipitation state and visibility. The specific measurement parameters for each sensor are listed below;

- The temperature of air is measured in degrees Celsius at a height of around 1.5 metres above ground.
- Relative humidity can be defined as a ratio of partial pressure of water vapor to the saturated pressure of water vapor at a given temperature in an air-water system. It is expressed in percentage. A value of 100% implies that the air is saturated, and it cannot take up any more moisture. Whereas 0% indicates no moisture in the air.
- Maximum gust wind speed represents the maximum speed of wind in km/h during an interval. The interval or the data frequency can be defined by the user. The data used in this study had intervals ranging from 15 minutes to 8 hours. The average wind speed is measured in km/h for each recording interval. The average wind direction is measured in degrees from North for each recording interval.
- The dew point refers to a temperature at which air becomes saturated under a constant atmospheric pressure. It is measured in degrees Celsius. If the pavement's surface temperature drops such that it reaches the dew point temperature, then there will be moisture on the surface of the pavement.
- Air pressure is defined as the force per unit area. In this case, the force is exerted by the air column above a particular location. It is recorded in kPa.

- The precipitation state indicates either its raining or snowing and their intensities such as lightly, moderately, or heavily. It is sensed and determined by using rainfall gauge with built-in microprocessor. The microprocessor calculates the average intensity by dividing the measured rainfall or snow depth with the duration of storm.
- Visibility refers to the maximum distance at which an object can be seen by a naked eye. It is expressed in km. The visibility sensors are used to sense and determine the visibility. These sensors are comprised of a light emitter, a light receiver, and a microprocessor controller. The emitter generates light pulses, while the receiver detects light intensity pulses from air particle scattering. All data acquired by a measuring microcontroller is converted into a meteorological visibility distance by a particular mathematical model algorithm.

3.1.2. Pavement Parameters Recorded by an RWIS Station

The sensors installed on the surface and within the layers of pavement record different variables such as surface temperature, subsurface temperature and surface condition.

- The surface temperature represents the temperature of the surface of pavement in degrees Celsius.
- The subsurface temperature refers to the pavement temperature at 40 cm from the surface. RWIS stations installed after 2016 also measure subsurface temperature at 150 cm from the surface of pavement.
- The surface condition parameter describes whether the surface of the pavement is wet, chemically wet, dry, slushy, damp, wet above freezing, wet below freezing. This parameter also helps in determining whether a snow or ice watch, black ice warning or snow warning is advisable or not.

- The freezing point of any liquid is a temperature at which its state of matter changes from liquid to solid. It is recorded in degrees Celsius. This parameter helps in determining the quantity of the road salt and deciding whether more salt is required, to melt the ice or snow, or not.

3.1.3. RWIS Data Collection and Analysis

The data was collected from 149 RWIS stations for the period between 2012 and 2019. From these 149 stations, 40 stations are located in Northeastern, 22 in the Northwestern, 32 in the Eastern, 23 in the Central and 32 stations were installed in the Western administrative regions. These stations were then filtered and shortlisted based on the availability of the data. During the data analysis, it was observed that the surface temperature observations, for several stations, were missing for some periods. In some cases, this period was 2 to 4 months whereas in most of the cases, it was 3 to 4 weeks. The stations with more than 2 continuous weeks of missing data were not considered. Furthermore, only 3 to 4 stations were considered for a particular location where several stations' data showed the same trend. The missing data from these RWIS stations can be attributed to many different factors such as broken apparatus, cut off signal between sensors and the data logger, missing temperature sensors. During the rehabilitation and maintenance work of roadways, when the shaving and repaving of the layers is being carried out, some of the sensors, especially the surface temperature sensor, easily gets damaged and/or disconnected. The missing data was estimated for the stations having less than 2 continuous weeks of missing data. Where one day of temperature data was missing, the average of previous and next day temperature data was estimated to fill the missing day's data. For two days of missing data, the temperature data from the previous day and next day was utilized to fill the missing two days of data. For three to fourteen days of missing data, the average of temperature data for a particular date from other years was used as an estimate. For example, if the temperature data from 5th to 10th March 2012 is missing, then the average of other available years was calculated to fill the data for each missing day.

The RWIS station data collection interval is 20 minutes. As mentioned before, the weather sensors, which are installed on a 10 m high tower, provide data including air temperature, relative humidity, wind speed and direction, dew point, pressure, wind gust and precipitation state. Whereas, the pavement sensors record surface and subsurface temperatures, surface condition and freezing point information. From all these parameters, only air, surface and subsurface temperatures were considered. From 149 stations, after detailed analysis, data from 36 RWIS stations were utilized in the pavement surface temperature models. The approximate locations of selected RWIS stations are presented in Figure 3.6 whereas Table 3.1 shows their IDs, Longitudes and Latitudes. To get an idea of the trend of the data, maximum and minimum air and surface temperatures were plotted against latitudes as shown in Figure 3.7 and Figure 3.8, respectively. Since the maximum 7-day average temperature is used for the determination of high temperature asphalt PG, therefore this parameter was estimated from the available data to represent the maximum air and surface temperatures. From Figure 3.7, it was observed that the annual maximum 7-day average surface temperatures showed a lot of variations across the considered time, as compared to the maximum 7-day air temperatures, for most of the locations. It was also observed from Figure 3.7 that both the maximum 7-day air and surface temperatures slightly decreased with the increase in latitudes. From Figure 3.8, it was observed that both the annual minimum air and surface temperatures decreased significantly with the increase in latitudes.

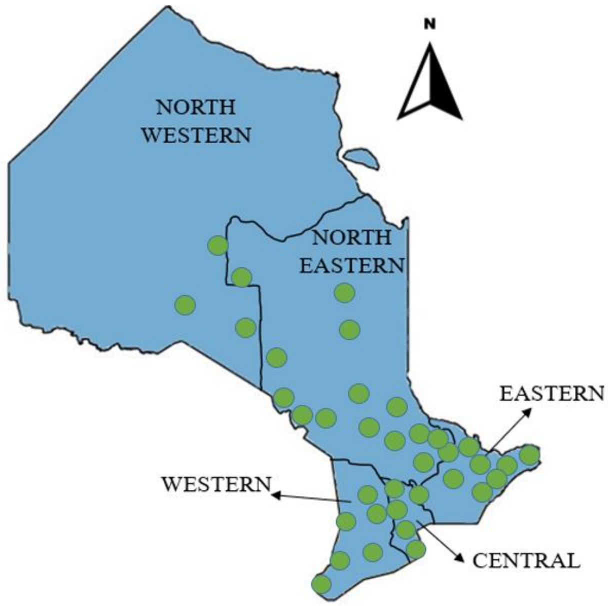

Figure 3.6 Approximate locations of selected RWIS stations across all five administrative regions of Ontario.

Table 3.1 Selected RWIS stations across all five administrative regions of Ontario.

Station ID	**Latitude**	**Longitude**	**Station ID**	**Latitude**	**Longitude**
SW35	42.067	82.619	ER19	45.064	77.827
SW21	42.548	82.364	ER32	45.082	75.636
SW22	42.597	81.655	ER30	45.143	77.265
CR01	42.914	78.958	NR04	45.215	79.313
CR08	43.309	79.803	ER31	45.499	78.020
SW27	43.333	81.740	NR05	45.658	80.411
SW08	43.566	81.422	NR13	46.008	79.356
SW13	43.948	80.716	NR25	46.212	82.574
CR26	44.106	78.917	NR31	46.278	83.429

ER34	44.154	78.494	NR27	46.672	84.335
ER20	44.329	78.135	NR30	46.864	81.634
ER25	44.458	77.763	NR26	48.281	84.886
CR21	44.465	79.869	NR34	48.617	85.331
ER26	44.624	77.148	NW19	48.917	87.767
ER29	44.767	78.094	NR37	49.058	81.245
ER17	44.779	76.110	NR17	49.289	81.785
ER08	44.917	75.197	NW09	49.793	86.318
NR45	45.046	78.719	NW26	49.800	85.712

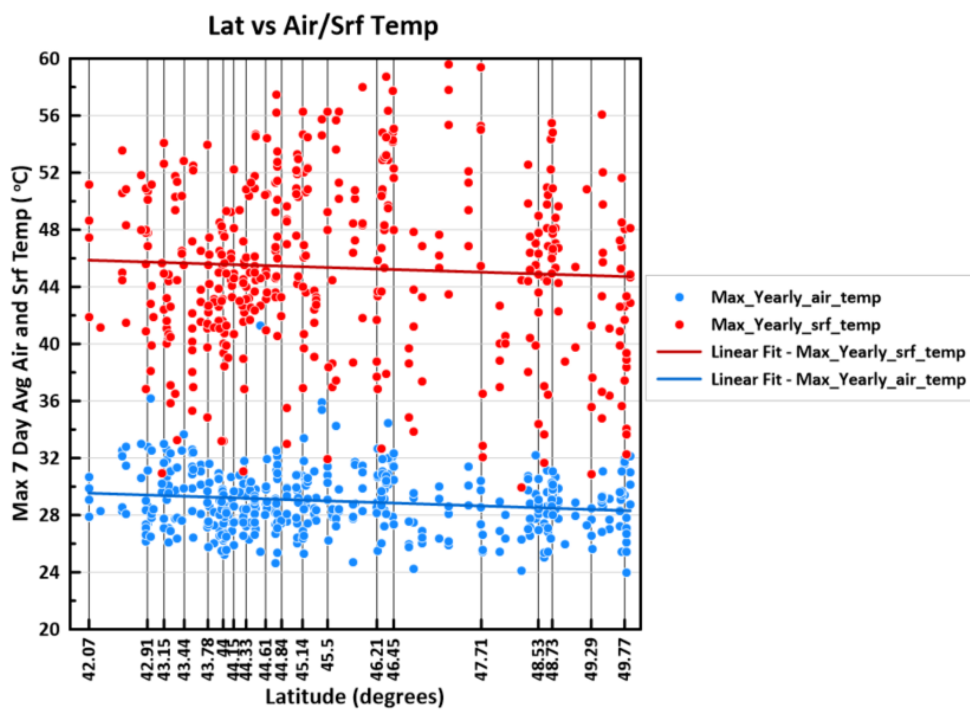

Figure 3.7 Maximum yearly 7-day avg air and surface temperature at various latitudes using data from the selected RWIS stations.

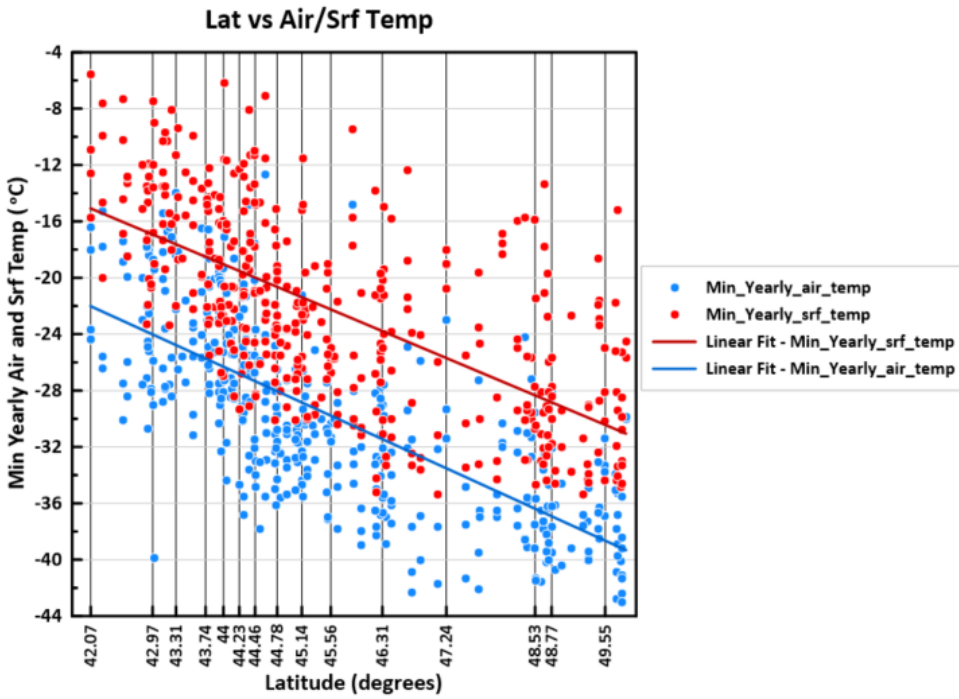

Figure 3.8 Minimum Yearly Air and Surface Temperature at various Latitudes using data from the selected RWIS stations

3.2. Network of Spring Load Adjustment (SLA) Stations in Ontario

To date, the MTO has installed and operates nine SLA stations located in the Northern Ontario. These weather stations contain a thermistor string which is set in a borehole to monitor temperatures and allow for the interpretation of freezing and thawing front depths. Thermistors are set vertically at depths of 5 cm, 15 cm, 30 cm, 45 cm, 60 cm, 75 cm, 90 cm, 105 cm, 135 cm, 165 cm, 195 cm, 225 cm, and 255 cm from the top of the pavement surface to create the thermistor string. The thermistors installed on these weather stations are semi conductors which measure temperature by monitoring the resistance (www.omega.ca). The data measured by these sensors is transmitted via buried cables to a datalogger stationed along the roadside. The information saved in the datalogger can then be downloaded to a computer. Along with the surface and subsurface temperatures, these stations also record air temperatures and precipitation data. The SLA stations are used by the authorities to gather sufficient information to determine road surface and sub surface conditions for Northern Ontario's Road network, which helps to minimize the winter road maintenance costs. Utilizing the data collected by SLA stations, MTO can better plan winter maintenance activities, minimise salt consumption, and provide better service. Figure 3.9 shows the approximate location of SLA stations in Ontario. Out of nine, five SLA stations are located in the Northwestern administrative region, whereas four are located in the North Eastern administrative region, as shown in Figure 3.9.

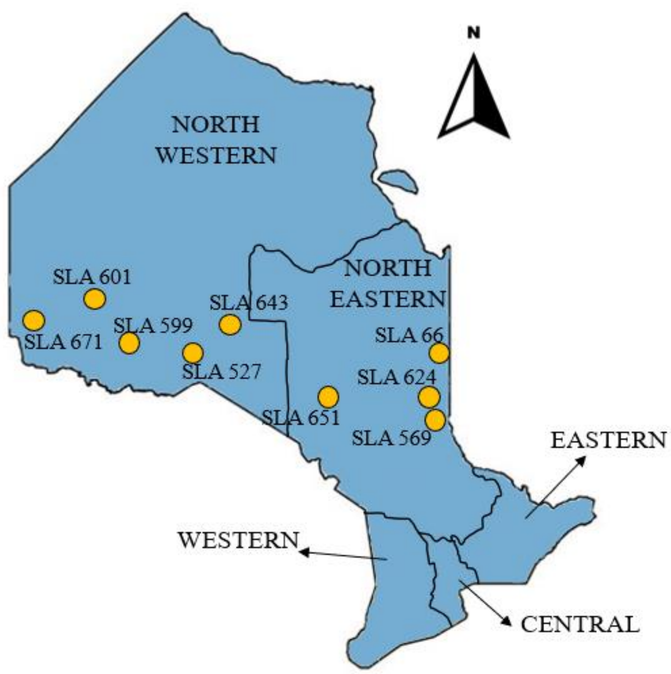

Figure 3.9 Approximate locations of SLA stations installed in Northern Ontario.

The climatic and subsurface temperature data were collected from all nine SLA stations for the period between 2012 and 2019. The data was then filtered and analyzed for missing values. As mentioned before, the missing data can be due to many different reasons such as broken sensors, damaged cables, broken data logger etc. Typically, when pavement repair works are being carried out, the temperature sensors get damaged and thus are unable to measure data anymore. In case of missing data for one or two days, the average was calculated. Where one day of temperature data was missing, the average of previous and next day temperature data was estimated to fill the missing day's data. For two days of missing data, the temperature data from the previous day and next day was utilized to fill the missing two days of data. Any data missing for more than two days was filtered and not considered in the study. Temperature data such as air temperatures and subsurface temperatures at depths ranging from 5 cm to 165 cm were considered for data analysis. The stations with data for two or more seasons of freezing and thawing were considered for the development and validation of a thawing depth model. Therefore, data from five stations i.e., SLA 527, 599, 624, 643 and 671 met the criteria and were considered in this study. The temperature data at specific depths was considered by keeping in view the MTO's guidelines for implementing and removal of SLR. These guidelines state that the most significant loss of pavement strength occurred when the thaw starts in the base, and the least significant loss occurred when the thaw reached a depth of around 106 cm. It is believed that the absolute thawing depth of 106 cm may not be considered for determining SLR removal date as temperature variation may fluctuate the thawing depth. For example, if the thawing depth reaches a depth of 106 cm one day, there may be a fair chance that it may go back to say 90 cm the very next day due to temperature drop. It is therefore believed that a thawing depth greater than 106 cm may be considered for SLR removal as it accounts for any fluctuations or errors. The MTO uses a thawing depth of 150 cm to 165 cm to determine the SLR removal dates across the province whereas, it uses a depth of 45 cm for determining the SLR start date. Since the 5 cm is the lowest depth where data is being monitored and recorded by these stations, therefore temperature data at this depth was considered to get an idea that how temperatures are changing in the near surface.

Figure 3.10 a to d represents temperature contours at different depths from March to May for the years 2013, 2016, 2017 and 2019, respectively. The data used for these temperature contour maps was taken from SLA 527. It was observed from these Figures that an initial, discontinuous thawing occurred up to a depth of less than 1 m before the continuous thawing started from surface to 165 cm depth. Moreover, it was also noted that the thawing occurred earlier in the years 2016, 2017 and 2019 as compared to 2013. In order to have a clearer picture of temperature variation at different depths, Figure 3.11 a to d were plotted. These Figures show temperatures at various depths from March to May for the year 2013, 2016, 2017 and 2019, respectively. The data was taken from SLA 527 and temperature at 5 cm, 45 cm and 165 cm depth were plotted. From Figure 3.11 (a to d), it was observed that the air temperature values frequently fluctuate whereas these fluctuations decrease with the increase in depth. At a depth of 165 cm, the temperature front is relatively smooth as compared to temperature fronts at 5 cm and 45 cm.

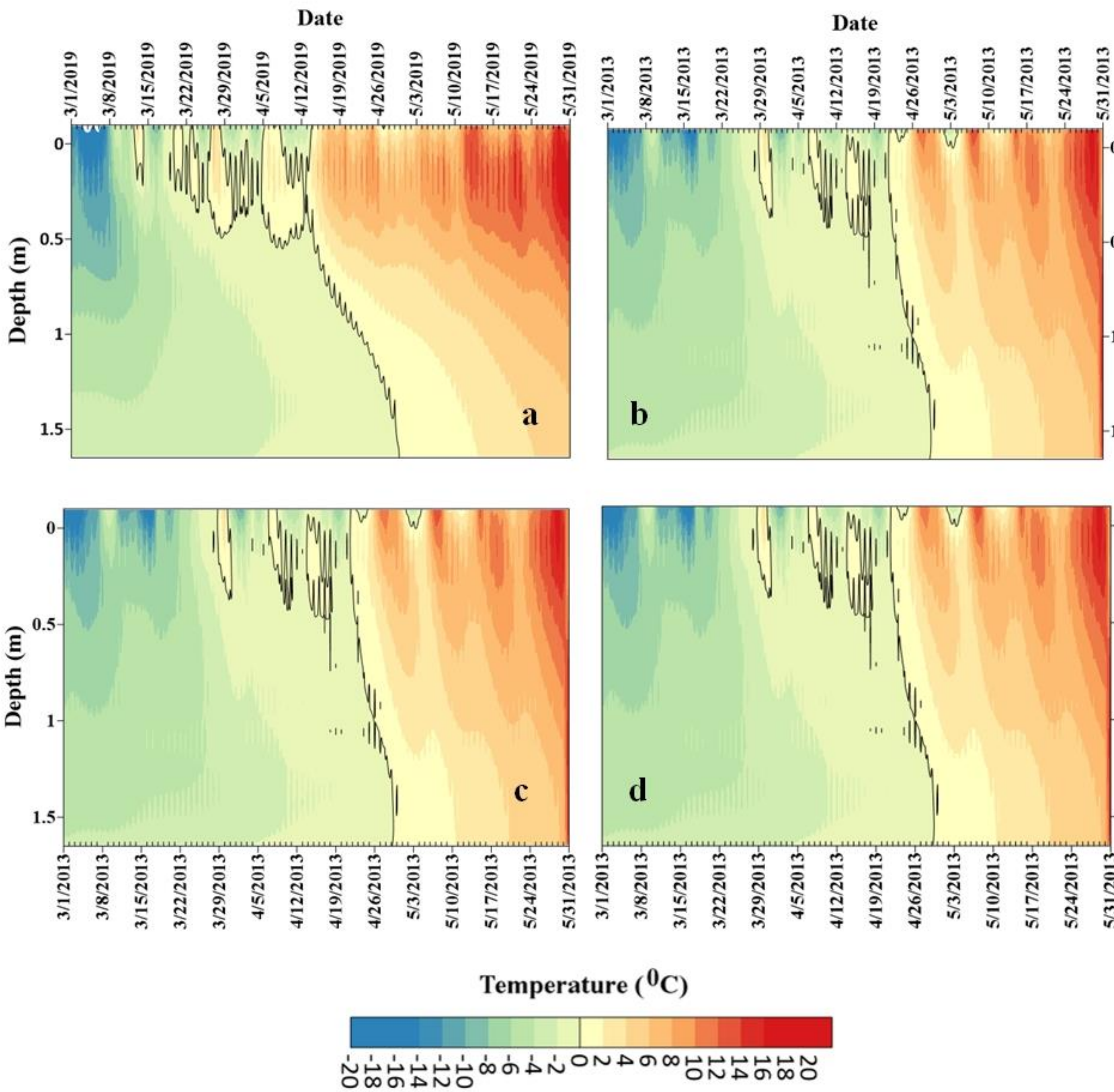

Figure 3.10 Temperature Contours at different depths from March to May for the years (a) 2013, (b) 2016, (c) 2017 and (d) 2019 using data from the SLA 527 station.

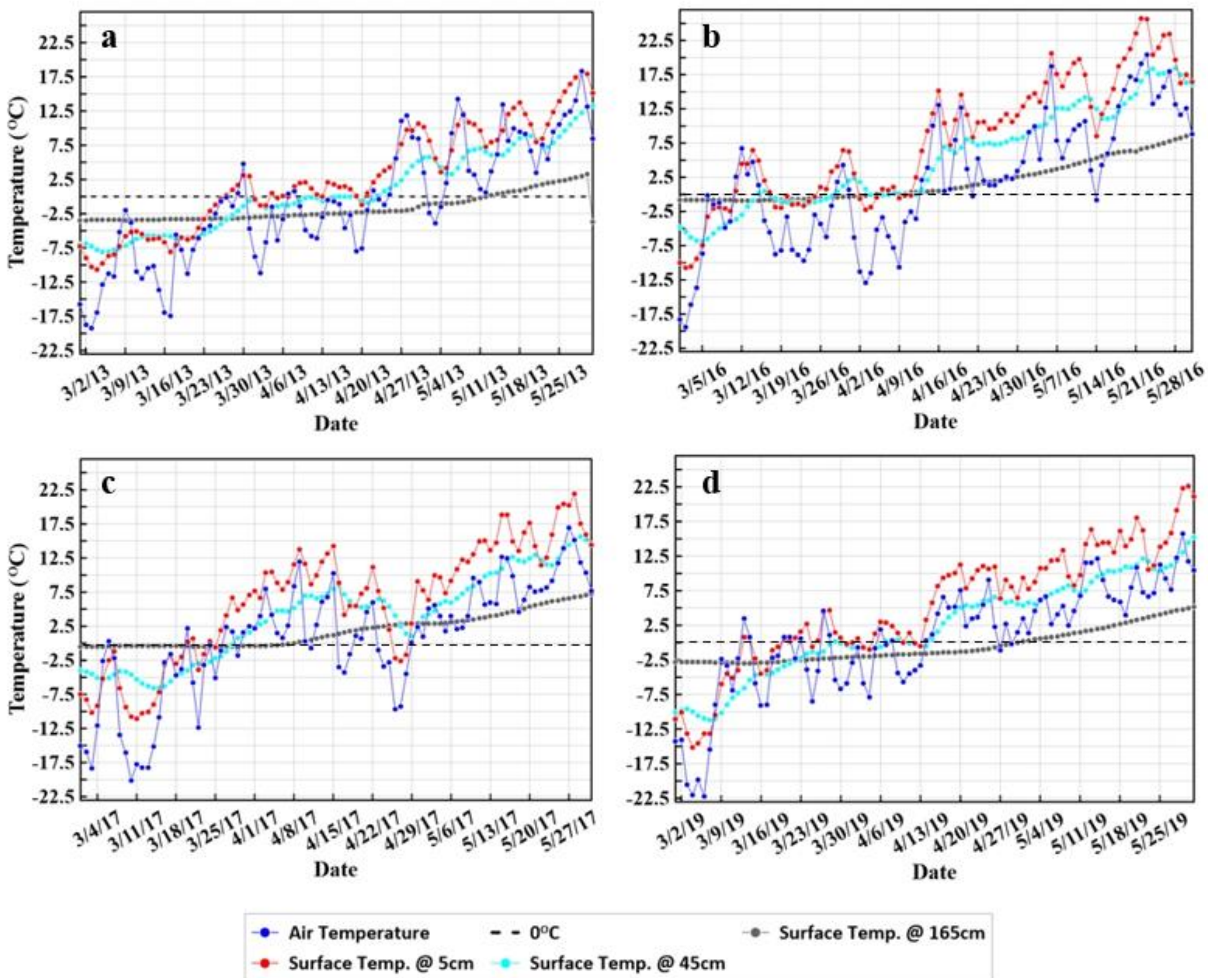

Figure 3.11 Temperature graphs from March to May for the years (a) 2013, (b) 2016, (c) 2017 and (d) 2019 using data from the SLA 527 station.

3.3. Weather Web Portal

The measured data obtained from the RWIS and SLA stations is automatically uploaded, in the raw form, to a web-based weather portal which was developed and is maintained by Wood PLC Canadian operations. This web portal displays the forecast and measured data on a map. The website is meant to be simple to use and show meteorological and subsurface data in a clear and concise manner. The graphical user interface of this website is the map of Ontario, with forecast sites and public weather sites shown on it. The user interface is simple and intuitive. By clicking on a site icon and/or utilising a site list, the user can gain access to information. Data is given in graphs and tables, with connections to other sources of information, such as data from Environment Canada. The data can be downloaded directly from this web portal for any desired range in the xlsx format. No challenges were faced while downloading data for this study. Figure 3.12 (a) presents the graphical user interface of this website, which shows different layers and legends for weather warning sites, forecast sites and public weather sites, whereas Figure 3.12 (b) shows some graphs and information which can be downloaded.

a

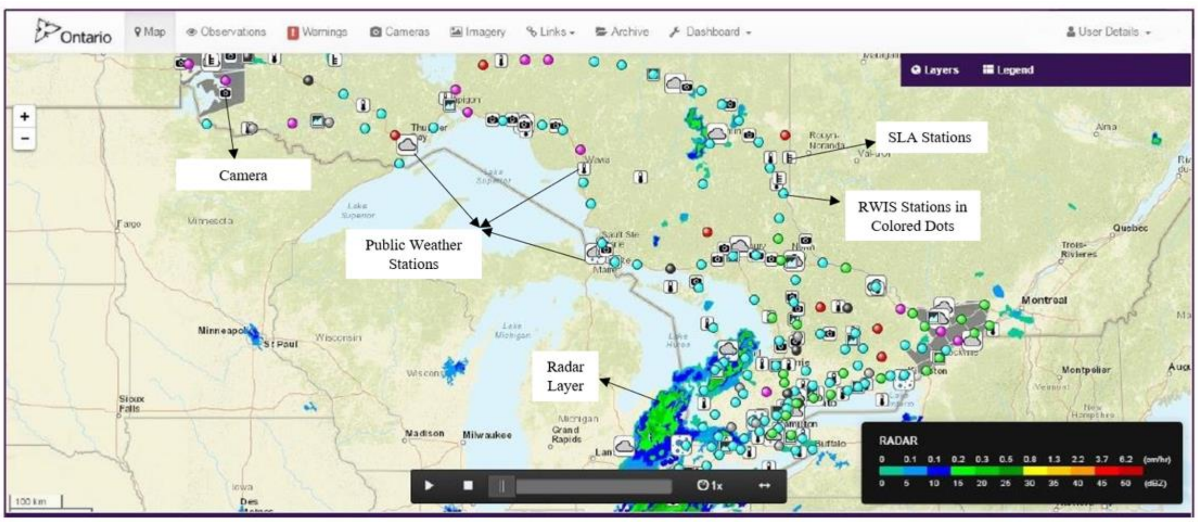

b

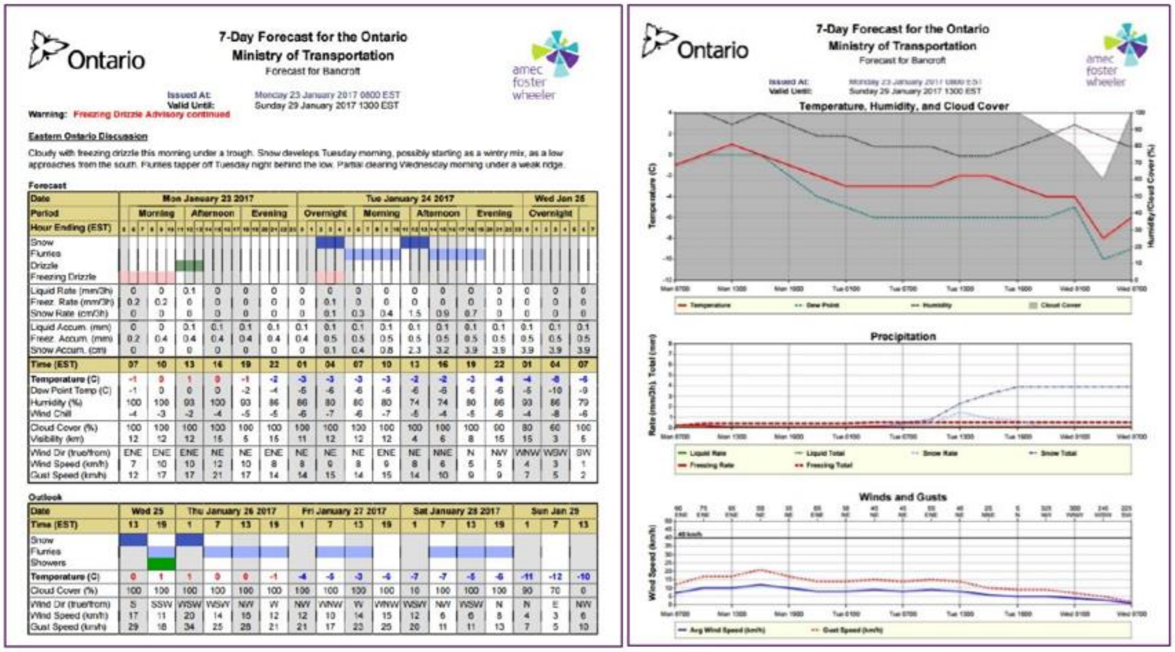

Figure 3.12 (a) Graphical User Interface of the Weather Web Portal. (b) Some Graphs and Information as it looks like on the web portal (Source: https://weather.amec.com)

3.4. Future Climate Data

The prediction of future climate is an effort to forecast the progression of climate changes with respect to time. The Global Circulation Models (GCMs) are the tools developed using past climate information to make future climate projections. The climate model simulations show how the climate system reacts to different greenhouse gas emission or concentration scenarios, as well as different radiative forcing scenarios (IPCC 2007, 2013). Representative Concentration Pathways (RCPs) are the pathways of total radiative forcing (van Vuuren et al. 2011). The fifth assessment report of the Intergovernmental Panel on Climate Change (IPCC) developed four alternative RCPs i.e., RCP2.6, RCP4.5, RCP6.0, and RCP 8.5 (IPCC 2013). Each RCP number represents a different cumulative radiative forcing by the year 2100. These RCPs are commonly used in climate-based research to determine the impacts of climate change in the future. The details on RCPs are provided in the next section.

GCMs are the tools used to estimate the quantitative change in the climate. These are the models in which the atmospheric and oceanic processes are represented in a mathematical form. In this way, internally consistent results are ensured (IPCC, 1994). In a GCM, the most significant characteristic is being internally consistent. This relates the changes in the climate variables in a consistent manner.

3.4.1. RCPs

When attempting to estimate how future global warming will contribute to climate change, several elements must be considered. A significant variable is the quantity of future greenhouse gas emissions. RCPs are basically the pathways to indicate time-dependent estimates of GHG concentrations in the atmosphere (IPCC, 2007). The IPCC's fifth assessment report recommends four alternative RCPs i.e., RCP2.6, RCP4.5, RCP6.0, and RCP 8.5 (IPCC 2013), which are emission scenarios. These RCPs were developed by creating scenarios of future's radiative forcing which is a measurement of the combined effect of greenhouse gases, aerosols, and other climate-influencing elements to trap additional heat. The data used in the RCP development was taken from the available literature. Each RCP represents a specific trajectory of emissions and the resulting radiative forcing. Table 3.2 presents the emissions and concentrations, radiative forcing and temperature anomalies for all the four RCPs.

Table 3.2 emissions and concentrations, radiative forcing and temperature anomalies for the RCPs. Source: Moss et.al. 2010

Name	Radiative Forcing	CO_2 equiv. (p.p.m)	Temperature anomaly (°C)	Pathway
RCP 8.5	8.5 W/m^2 in 2100	1370	4.9	Rising
RCP 6.0	6 W/m^2 post 2100	850	3.0	Stabilization
RCP 4.5	4.5 W/m^2 post 2100	650	2.4	Stabilization
RCP 2.6	3 W/m^2 before 2100, declining to 2.6 W/m^2 by 2100	490	1.5	Peak and decline

Out of these four pathways, the RCP 2.6 denotes the best-case scenario in which the radiative forcing fist reaches to 3.1 W/m^2 by mid century and then starts decreasing to reach 2.6 W/m^2 by the end century. To achieve such radiative forcing levels, GHG emissions must be significantly lowered over time (Van Vuuren et al. 2007a). The RCP 4.5 and 6.0 depicts the intermediate or the stabilization scenarios in which the radiative forcing stabilises at around 4.5 W/m^2 or 6 W/m^2, respectively, by the end-century. Whereas the RCP 8.5 represents the worst-case scenario in which radiative forcing reaches >8.5 W/m^2 by the year 2100. This RCP was developed by considering such a representative scenario from the literature which depicts high GHG emissions over time. As suggested using RCP 2.6, the GHG emissions must be significantly lowered and requires that carbon dioxide emissions start declining by 2020. However, even as of now i.e., year 2022, no such conditions have been observed. The RCP 2.6 suggest a global mean temperature rise below

2 °C whereas the global mean temperatures have already increased by a magnitude of around 1.2 °C as compared to the 1850-1900 baseline. This makes the RCP 2.6 least likely in order to provide more focused takeaway points for the reader. RCP 4.5 is an intermediate scenario which requires that carbon dioxide emissions start declining by around 2045 to reach half of the levels by 2100. This RCP suggests a global mean temperature rise between 2 °C to 3 °C by 2100. Whereas the RCP 8.5 depicts the worst-case scenario and suggests a continuous rise in emission throughout the 21st century. Therefore, RCP 4.5 and 8.5 are most likely in order to provide more focused takeaway points for the reader.

3.4.2. Future Data Collection and Analysis

The future climate data for Ontario was obtained from the Ontario Climate Change Data Portal (OCDP) published by York University's Laboratory of Mathematical Parallel System (LAMPS), available publicly. It is an easily accessible data portal with a user-friendly interface. This data portal offers high-resolution spatial projections of regional climate change for Ontario, Canada. The climate change data for the period 1981 to 2100 (120 years) with spatial resolution of ~10 km x ~10 km and temporal resolution of 1 day, UTC is available on this portal and it can be downloaded in .mat or .csv formats. Data for four different climate variables i.e., precipitation, maximum, minimum and average temperature is available for more than 20 GCMs and all 4 RCPs.

For this study, the climate change data was downloaded from 19 GCMs, as shown in Table 3.3, and 3 RCPs i.e., RCP 2.6, 4.5 and 8.5. Since both RCP 4.5 and 6.0 represent the intermediate case scenarios, only one was considered in this study. The data was downloaded for the period 1981 to 2100. The data period was divided into six 20-year intervals and were termed as the historical period (1981-2000), baseline (2001-2020), short-term future (2021-2040), mid-century (2041-2060), third-quarter century (2061-2080) and end-century (2081-2100). The temperature data obtained from the 19 GCMs were averaged and utilized in the research. The data was analyzed in Python 3.8, 64-bit version. Figure 3.13 represents the predicted Mean Annual Air Temperatures (MAAT) from 2021 to 2100 for the city of Toronto. The mean temperatures were determined using the average values from the selected GCMs under different RCPs. The predicted temperatures were then compared with the MAAT measured values and values measured and reported by Environment Canada. The data was collected from the Pearson International airport weather station having station ID 71624. Figure 3.13 gives an idea of how the temperatures may change by the end century under different RCPs. The RCP 8.5 represents the worst, whereas 2.5 depicts the best-case scenario.

Table 3.3 GCMs Utilized for the collection of Future Climate Data

Sr. No.	**GCM**	**Sr. No.**	**GCM**
1	bcc-csm1-1	11	IPSL-CM5A-LR
2	bcc-csm1-1-m	12	IPSL-CM5A-MR
3	BNU-ESM	13	MIROC5
4	CanESM2	14	MIROC-ESM
5	CCSM4	15	MIROC-ESM-CHEM
6	CNRM-CM5	16	MPI-ESM-LR
7	CSIRO-Mk3-6-0	17	MPI-ESM-MR

8	GFDL-CM3	18	MRI-CGCM3
9	GFDL-ESM2G	19	NorESM1-M
10	GFDL-ESM2M		

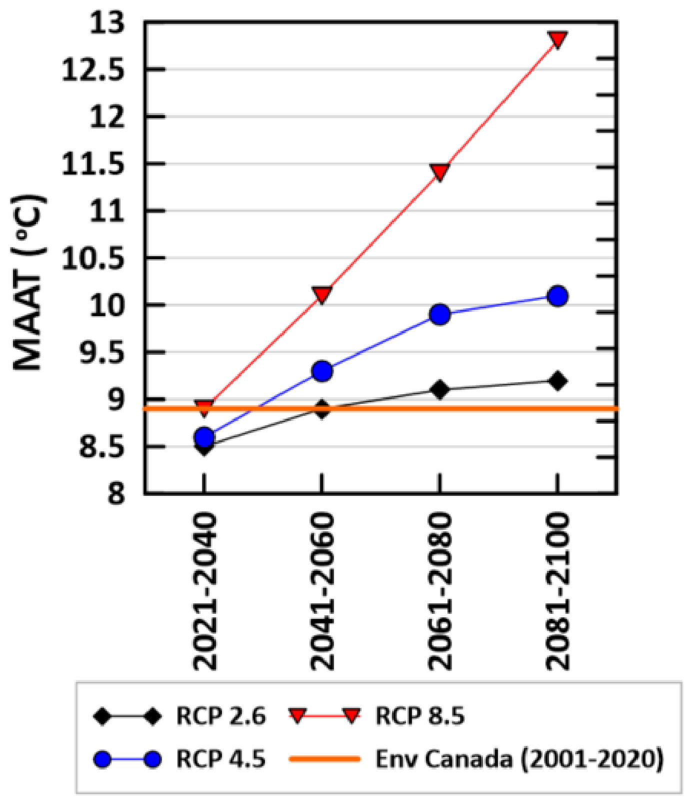

Figure 3.13 Mean Annual Air Temperatures for Toronto estimated by selected GCMs under different RCPs and the value recorded by Environment (Env) Canada.

3.5. Historical Climate Data Normals

The historical climate data normals for the period 1981-2010 were collected from the Environment and Climate Change Canada portal (Environment and Climate Change Canada 2018). These normals were collected for ten different cities located in all the five administrative regions of the

MTO. The approximate locations of these cities are provided in Figure 3.14. The purpose of collecting the historical climate data normals was to determine the accuracy of temperature data estimated by GCMs for different climate change scenarios or RCPs. The average of the Mean Monthly Air Temperatures (MMAT) from 19 GCMs for the 10 cities across Ontario, were then determined and used for the analysis. To validate the future climate data, the climate normals determined from the predicted historical data by the GCMs for selected cities were compared with that of climate normals reported by Environment Canada for the period of 1981 to 2010. This comparison, for selected 4 cities with lowest to highest latitudes, is shown in Figure 3.15 (a to d). It can be observed that, for all the considered cities, the GCMs predicted the historical measured data very well.

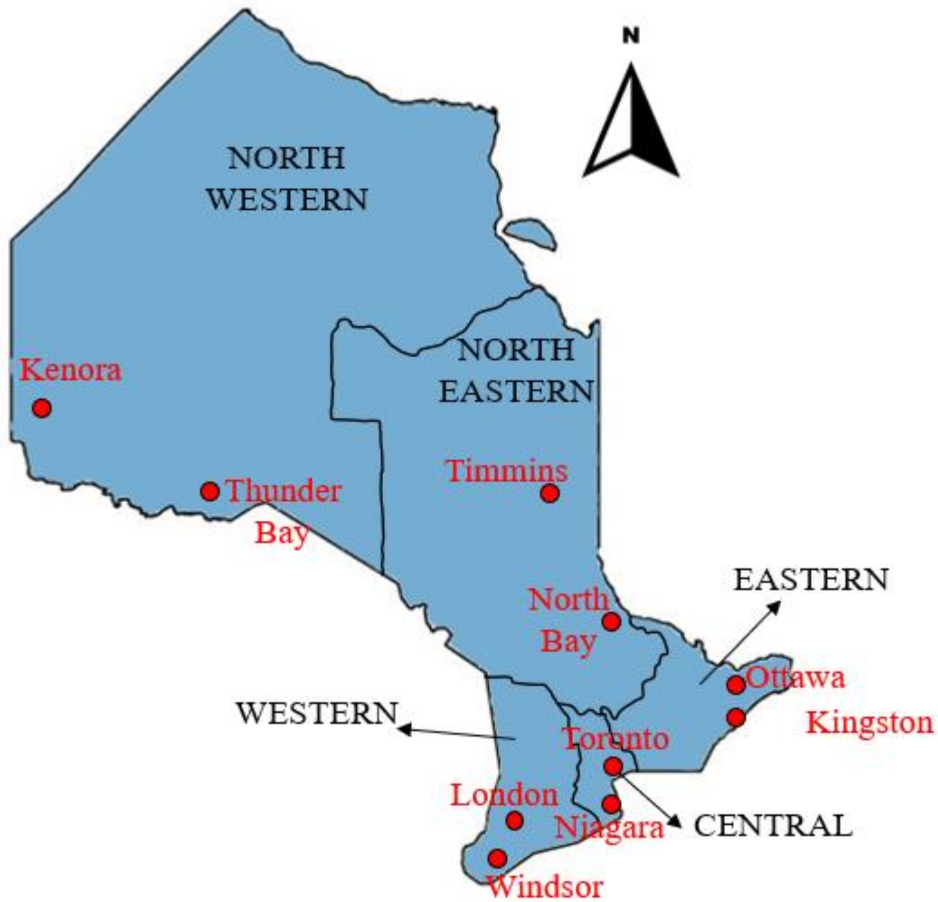

Figure 3.14 Approximate Locations of the 10 cities for which the climate normals determined from future climate data were compared with the climate normals reported by environment Canada

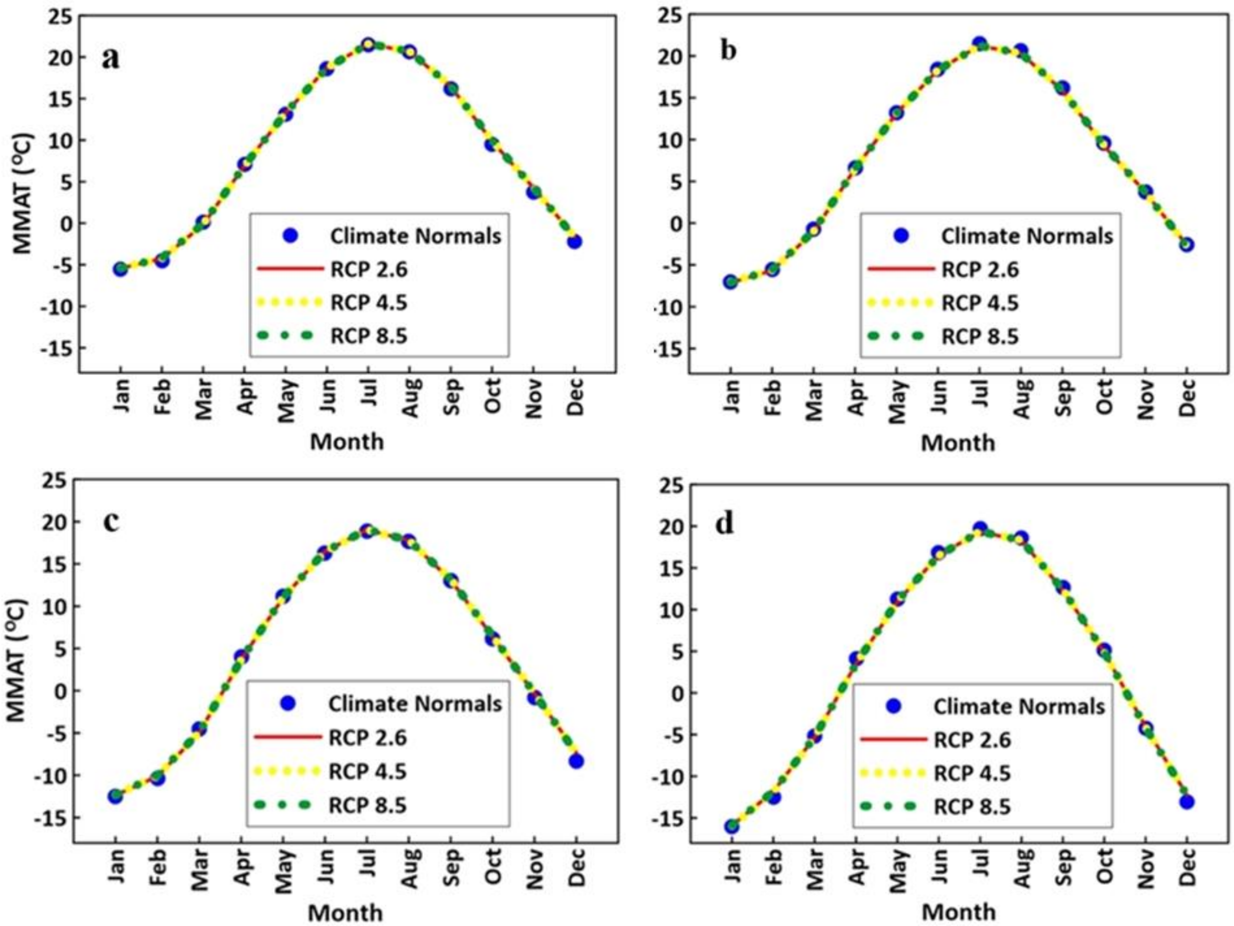

Figure 3.15 Comparison of Climate Normals for (a) Toronto (b) Kingston (c) North Bay (d) Kenora

3.6. Summary

This chapter covered the various data sources and techniques involved in the data analysis for this research. The climatic data was collected using data sources such as RWIS, SLA, OCDP, and Environment and Climate Change Canada stations. The meteorological and subsurface data collected from RWIS and SLA stations was analysed and utilised to develop and validate regression models for estimating asphalt PG and SLR periods. Furthermore, future climate data from 19 distinct GCMs were used to analyse changes in asphalt PG and SLR across Ontario up to the year 2100. Details on the development and validation of models for calculating asphalt PG and

SLR periods, as well as their use for analysing change in asphalt PG and SLR periods across Ontario by the end century are presented in chapters 4 and 5 respectively.

4. Climate Change and Asphalt Binder Selection across Ontario: A Quantitative Analysis Towards the End of the Century

4.1. Introduction

It is internationally acknowledged that the climate is changing, and the combined surface, air and sea surface temperatures are increasing (Stocker et al., 2013). Many climate change impacts are irreversible and have been identified with the expanded release of greenhouse gasses (GHG). Recent studies suggest a dangerous atmospheric deviation sooner rather than later in different parts of the world, for example, (Vincent et al., 2018) in Canada, (Meleux et al., 2007) in Europe, (Dash et al., 2007) in India and (Hughes et al., 2003) in Australia. Between the period of 1880 to 2012, the global surface temperature has increased by 0.85 degrees Celsius, and the pace of change has accelerated in recent decades (Vincent et al., 2012). As indicated by Canada's Changing Climate Report published in 2019 (Bush et al., 2019), Canadian urban areas are expected to encounter accelerated and more extreme climate changes than many other parts of the world. Furthermore, the variations in climate are not consistent across the country. The magnitude of daily low temperature has risen somewhat quicker than the daily maximum temperature. It is anticipated that these trends will worsen in the future if the GHG emission rates remain the same as they are at the present. These changes in climate could potentially result in increased precipitation and diminished snowfall sums affecting the winter season in Canada (Bush et al., 2019).

Changing climate is one of the most important issues that demonstrates the need for innovative changes that will reduce the GHG emission rates in the future (Plati, 2019). Climatic load is a significant factor while assessing the safe performance of a roadway. Furthermore, extreme temperatures may be utilized to evaluate a road structure’s damage (Sun et al., 2019). Higher air temperatures lead to higher pavement temperatures (Swarna et al., 2021) which may have a significant impact on both the functional and structural performance of the asphalt pavements (Li et al., 2018). With the rapidly changing climate, the probability of thermal distress may increase which is the most noticeable distress in asphalt concrete pavements (Dong et al., 2018). Toronto, the largest metropolitan city in the province of Ontario in Canada, faced a heat wave in July 2012 for an extended period, resulting in rutting in sections of Canada's busiest highway, the 401 (Fletcher et al., 2016). The change in climate and warmer temperatures may also cause early failure of pavements, thus necessitating more rehabilitation procedures (Qiao et al., 2015; Gudipudi et al., 2017; Chen et al., 2021). The asphalt binder is a temperature sensitive viscoelastic material. The accurate determination of asphalt binder is very critical to avoid rutting and cracking in pavements caused by seasonal temperature variations. To assess the relative effect of climate change on suitable binders for more durable pavement design, it is vital to examine how the potential atmospheric conditions may impact pavement surface temperatures.

Developed by the Strategic Highway Research Program (SHRP) in 1987, Superior Performing Asphalt Pavements (SUPERPAVE) requires Performance Graded (PG) binders based on site's historical climatic conditions (McGennis et al., 1995). Solaimanian and Bolzan (1993) and Robertson (1995) developed regression models for estimating high and low pavement temperatures respectively and are the original SHRP models. Due to limited data availability for validating SUPERPAVE specifications, SHRP initiated the (Long Term Pavement Performance (LTPP) Seasonal Monitoring Program (SMP) to collect air and pavement temperature data from additional locations (Mohseni, 1998). Utilizing this data, Mohseni (1998) developed pavement temperature models which were termed as the first-generation LTPP models. These models were replaced in 2005 by the second and third LTPP generation models (Swarna et al., 2020). The second-generation models used the traditional parameters i.e., lowest, and average 7-day highest annual air temperatures for low and high pavement temperatures, respectively. It was investigated that the average 7-day could not account for the extended hot periods thus a rut damage (third generation) model for high pavement temperatures was developed (Mohseni et al., 2005). This model used the average yearly degree days air temperature over 10°C and target rut depth for PG selection. Furthermore, a computer software, LTPPBind, was also developed under the same program. The latest version of this program i.e., LTPPBind V 3.1, guides the user in selecting the performance-based binder grade under different traffic load and speed limits by utilizing both, the LTPP second and third generation models.

A recent Canadian study on the subject used the data from five different climate models. The data was obtained from the Pacific Climate Impacts Consortium (PCIC) climate database for three Representative Concentration Pathways (RCPs) i.e., 2.6, 4.5 and 8.5 to measure the effect of climate change on the PG for ten cities around the country using the LTPP models (Swarna et al., 2020). In relation to the baseline climate of 1950–2040, it was determined that four cities would need high temperature PG upgrades, while five cities would need low temperature PG upgrades by 2070 under the RCP 8.5.

A research study conducted in the United States, analysed climate change data from 19 Global Circulation Models (GCMs) of the Coupled Model Intercomparison Project 5 (CMIP5) climate projection project (Underwood et al., 2017). This study concluded that, for 799 weather stations used in the study, around 35% of the weather stations suggested different PG based on 1985-2014 when compared to 1965-1996 weather data. It was also concluded that, by the year 2099, all the locations considered would have a different PG.

Another investigation related to PG was conducted in Italy, which included 71 different locations throughout the country (Viola et al., 2015). The historic climate data was collected from the Italian Air Force Meteorological service between 1984 and 2013, and the predicted temperature variations by 2033 were calculated using spatial interpolation. Using the original SHRP formulas, it was predicted that a rise of one grade in high temperature PG can be expected for more than 25% of the Italian regions by 2033 due to rising temperatures.

A similar analysis was recently conducted in Chile to investigate the expected changes in PG by climate change (Delgadillo et al., 2018). The researchers examined 94 weather stations across Chile and collected historical climate data from 1970 to 1999. The MICRO5 climate model was used to estimate future climate data from 2030 to 2059 (30 years) for RCP 2.6 and RCP 8.5 emission scenarios. According to the study, a significant number of stations may need to change their high temperature grade, while only a few stations may need to change their low temperature grade. The different studies, mentioned above, all indicate the increased cost of maintenance because of climate change thus highlighting the necessity for the road construction standards to be updated, despite the increased costs of adaptation measures (Hayhoe et al., 2010; Barros et al., 2014). These increased maintenance costs can be associated to the premature deterioration of roadways because of failure to update the material standards where heat extremes are predicted to increase (Fletcher et al., 2016).

Canada has one of the world's largest road networks, with over one million kilometres of two-lane equivalent public roads. The province of Ontario, on average, accounts for 38.55 percent of the overall national Gross Domestic Product (GDP) and its economy is heavily reliant on road surface transportation (Govt. of Canada Statistics Report, 2016). It has almost 116,000 km of municipal roads (Govt. of Canada Statistics Report, 2016) and 40,000 km of highways (FAO, 2019), which have a net book asset value of $26.7 billion (FAO, 2019). Due to Canada’s size and geographic dispersal of population centres, current road systems are subjected to a broad range of temperature conditions (Vincent et al., 2006; Zhang et al., 2000). To date, no such study, specifically for the whole province of Ontario, has been carried out. Most of the above studies relied on existing models. One of the objectives of this study is to develop regression models, specifically for Ontario, Canada, for pavement temperature determination as the existing LTPP models are for the whole of North America and their performance can be improved by using the measured pavement data in Ontario, Canada.

In terms of the PG requirements, the province of Ontario has been divided into three climatic zones by the Ministry of Transportation Ontario (MTO) as shown in Figure 4.1. The MTO recommends base PGs for these zones which can be changed depending on the traffic requirements for any given site. The recommended PGs are 52-34 for zone 1, 58-34 for zone 2 and 58-28 for zone 3 (ABC of PGAC, 1999).

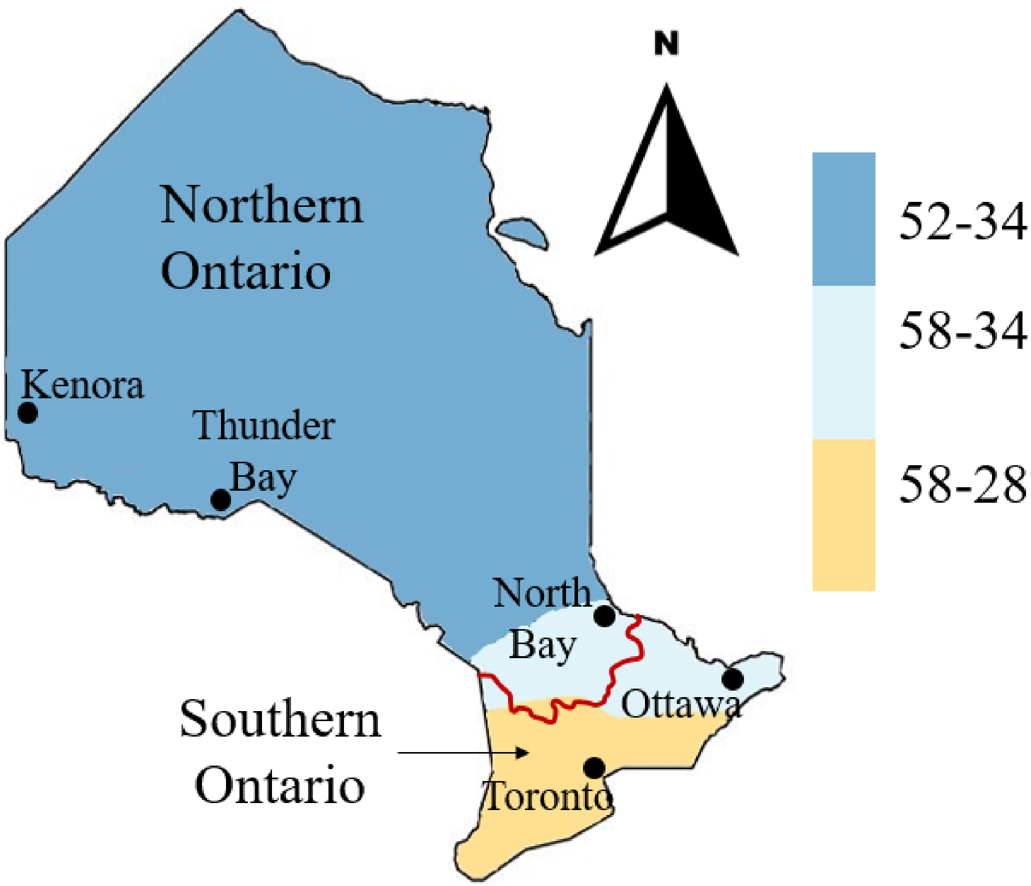

Figure 4.1 PG Zones and recommended PGs, with Zone 1 having a PG of 52-34, Zone 2 having a PG of 58-34, and Zone 3 having a PG of 58-28, as per MTO Guidelines.

In this study, the historical and projected climate data, within the context of rising temperatures, was reviewed for Ontario. In order to determine better relationship between asphalt pavement surface temperature and ambient weather data, regression models were developed by carrying out detailed review of the data obtained from the vast network of Road Weather Information System (RWIS) stations. The suitability of these developed models and the LTPP models were then assessed against the measured data collected from the RWIS stations. To assess the relative effect of climate change on PG across Ontario, the historical (2001 – 2020) and future climate data for four time periods: short-term future (2021-2040), mid-century (2041-2060), third quarter (2061-

2080) and end-century (2081-2100) for the province was collected from 19 different GCMs. Using the developed models and the climate data for the aforementioned time periods, the PGs were determined to quantify the change in PG in changing climate.

4.2. LTPP Models

The SHRP developed a performance-based system to specify asphalt materials known as SUPERPAVE (McGennis et al., 1995). This system selects the PGs based on the expected highest and lowest pavement temperatures in order to minimize cracking in winters and rutting in summers. The low and high pavement temperature models developed under this program are referred to as LTPP 2.1, in which the lowest pavement temperature is estimated using the lowest annual air temperature, whereas highest pavement temperature is estimated using the highest annual mean 7-day air temperature (Mohseni, 1998). The LTPP 2.1 models for the estimation of high and low pavement temperatures are provided below in equations 1 and 2, respectively (Mohseni, 1998; Mohseni et al., 2005).

$$T_{P\,max} = 54.325432 + 0.78T_{air\,max} - 0.0025{Lat^2}^{0.5} \\ -15.41\,log_{10}(H+25) + Z(9 + 0.61\sigma^2_{Tair\,max}) \tag{4.1}$$

$$T_{P\,min} = -1.56 + 0.72T_{air\,min} - 0.004{Lat^2}^{0.5} \\ +6.26\,log_{10}(H+25) - Z(4.4 + 0.52\sigma^2_{Tair\,min}) \tag{4.2}$$

Where $T_{P\,max}$ is the highest mean 7-day pavement temperature in °C, $T_{air\,max}$ is the highest mean 7-day air temperature in °C, $\sigma_{Tair\,max}$ is the standard deviation of highest mean 7-day air temperature in °C, $T_{P\,min}$ is the lowest pavement temperature in °C, $T_{air\,min}$ is the lowest air temperature in °C, $\sigma_{Tair\,min}$ is the standard deviation of lowest air temperature in °C, Lat is the latitude in degrees, H is the depth in mm and Z is the standard normal distribution value i.e., 2.055 for 98% reliability.

In 2005, the LTPP 2.1, for selecting high temperature PG, was superseded by the LTPP 3.1 model. This is the latest modification, and it uses the degree-days above 10 °C, instead of highest annual mean 7-day air temperature as mentioned before. The equations for determining high temperature PG are provided in equations 3, 4 and 5.

$$PG_{H,d} = 48.2 + 14DD - 0.96DD^2 - 2RD \tag{4.3}$$

$$CVPG = 0.000034(Lat - 20)^2 RD^2 \tag{4.4}$$

$$PG_{H,rel} = PG_{H,d} + (Z)(PG_{H,d})\frac{CVPG}{100} \tag{4.5}$$

Where $PG_{H,d}$ is the high temperature damage-based performance grade in °C at 50% reliability, DD denotes the average yearly degree-days with air temperature over 10 °C, x1000 °C, RD is the allowable rutting depth in mm, $CVPG$ represents the high temperature yearly PG coefficient of variation in %, $PG_{H,rel}$ denotes the high temperature PG at desired reliability in °C and Z represents standard normal probability for the desired reliability. These models are widely being used by road agencies and designers to predict pavement temperatures and determine suitable PG for any specific site.

4.3. Methodology

In this study, models to determine pavement temperatures, using the ambient temperatures and latitude of a location, were developed. For this, the ambient air and pavement subsurface temperature data was obtained from selected RWIS stations. The suitability of the developed and the LTPP models were then assessed using measured data. Utilizing the future climate data, the high and low pavement temperatures were predicted, and thus suitable PGs were selected by incorporating the latest LTPP and the developed models. The procedure for the models developed in this study is highlighted further in this section.

4.3.1. Development of Ontario-specific Models

The regression models were developed by using the air and soil temperature data from 36 weather stations within the Ontario Ministry of Transportation’s Road Weather Information System (RWIS) to determine the relationships between ambient weather data and asphalt pavement surface temperature. The Road Weather Information System stations use environmental sensors deployed on and around the highway to track existing road and weather conditions at specific locations. These RWIS stations have different sensors including meteorological sensors that measure air temperature, relative humidity, wind speed and direction, precipitation, and pavement sensors that measure pavement surface temperature, subsurface (40 cm and 150 cm) temperature, pavement state (wet, dry, or frozen), and the freezing point of a wet surface (Bernstein et al., 2003). In this study, air temperatures, pavement surface temperatures and subsurface temperatures at 40 cm depth were used for model development. The climatic variables used in the development of models are the same as used in the LTPP 2.1 models (equation 1 and 2). The utilization of extreme, instead of average, daily temperatures in models’ development is linked to the fact that average temperatures may skew the results, therefore they cannot be regarded as the most important component in determining the pavement temperature (Li et al., 2017). There are 165 RWIS weather stations across Ontario to date (Buchanan et al., 2005). The MTO has divided the province into 5 different regions namely Northern, North-western, Eastern, Central and Western regions and these weather stations are installed in each region. In this study, the weather stations used for models' development were taken from all these regions.

The low pavement temperature model was developed by utilising the climate data from 2012 to 2014. The data was analysed to identify erroneous values and outliers. The parameters, such as lowest yearly air temperatures, latitude of site and depth were considered in the model development. The multiple linear regression analysis was then carried out using forward selection regression approach in the Statistical Analysis System (SAS) software 9.4 (SAS, User's Guide, 2013). The model was evaluated based on its goodness of fit i.e., R^2 and RMSE value. The equation developed for the low pavement temperature determination is as follows.

$$T_{P\,min} = 24.88 + 0.73T_{air\,min} - 0.61Lat + 0.047D - Z(2.98^2 + \sigma^2_{Tair\,min})^{0.5} \tag{4.6}$$

The R^2 value of the model was found to be 91% with an RMSE value of 2.98. Figure 4.2 shows the statistical outlook of the developed model. The first panel of this figure (Figure 4.2 a) shows the quality of the developed regression model. This graph plots the predicted versus actual low surface and subsurface temperatures for each observation. As it can be seen from this graph that the points are close to the 45-degree line, thus suggesting that the developed model predicts the surface and subsurface temperatures quite well. The second panel of this figure (Figure 4.2 b) plots the residual versus percent graph which shows that the residuals are normally distributed. This is confirmed by the normal quantile-quantile plot as shown in Figure 4.2 c. Since most of the data points lie on or close to the diagonal line, thus suggesting that the residuals for the model are normally distributed. It can also be seen from this plot that both left and right ends of pattern are above the diagonal line which suggest a short tail on both ends, which can be confirmed by looking at the Figure 4.2 b. The third, fourth and fifth panel of this figure i.e., Figure 4.2 c through Figure 4.2 e, includes the residuals plotted against the value of each explanatory variable. These graphs show that whether the residuals contain a signal or are randomly distributed. The residual plotted against the low air temperatures, latitude and depth does not show a systematic pattern thus indicates that the model adequately captured the dependence of the response on all the explanatory variables.

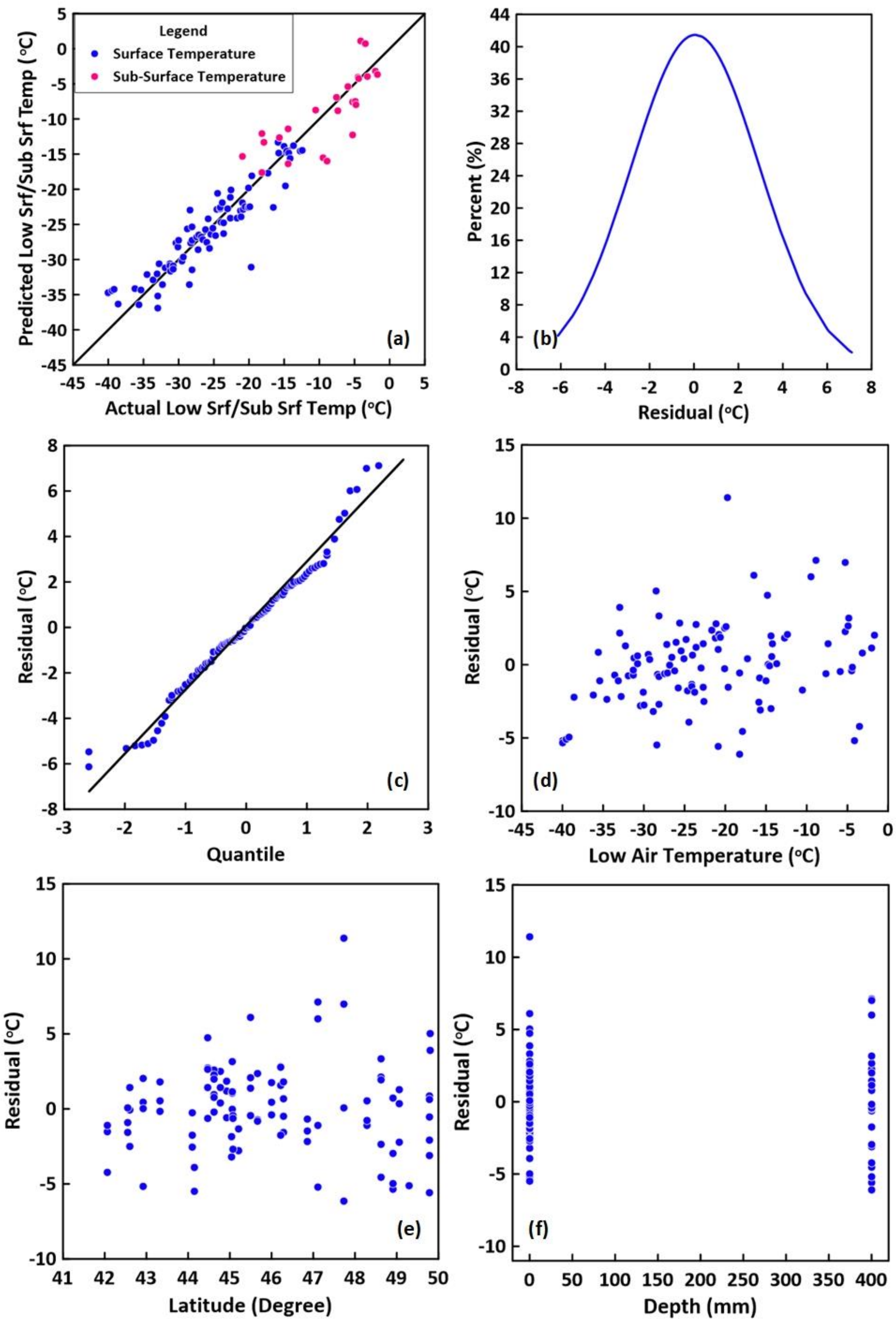

Figure 4.2 Statistical Outlook for the Low Pavement Temperature Model (Colour should be used in print)

The last term in the equation 6 is the error term, which is defined in the same way as described by Mohseni et al., (2005). This term is related to the uncertainty in predicting the correct pavement temperature. To improve efficiency, the error term was subtracted from the low pavement temperature equation (Mohseni et al., 2005). The uncertainty is caused by two separate variables: mean air temperature and the model (Mohseni et al., 2005). The standard deviation of mean air temperature ($\sigma_{Tair\ min}$) and the root mean square error of the model ($\sigma_{min\ model}$) were used to define this uncertainty. The variability in the estimated pavement temperature ($\sigma_{TP\ min}$) and the error term ($\varepsilon_{min\ model}$) at any desired reliability was calculated as follows:

$$\sigma_{TP\ min} = (\sigma^2_{min\ model} + \sigma^2_{Tair\ min})^{0.5} \tag{4.7}$$

$$\sigma_{TP\ min} = (2.98^2 + \sigma^2_{Tair\ min})^{0.5} \tag{4.8}$$

$$\varepsilon_{min\ model} = Z(2.98^2 + \sigma^2_{Tair\ min})^{0.5} \tag{4.9}$$

For the high pavement temperature model, the data from year 2012 to 2014 was considered in model development. The regression model development procedure was the same as described above for the low pavement temperature model. The model developed for determining the average 7-day high pavement temperature is presented in equation 4.10, and Figure 4.3 exhibits the statistical outlook of the developed model. The first panel of this figure (Figure 4.3 a) plots the predicted versus actual average 7-day high surface and subsurface temperatures for each observation. As it can be seen from this graph that the points are close to the 45-degree line, thus suggesting that the developed model predicts the surface and subsurface temperatures quite well.

The second panel of this figure (Figure 4.3 b) plots the residual versus percent graph which shows that the residuals are normally distributed. This is confirmed by the normal quantile-quantile plot as shown in Figure 4.3 c. Since most of the data points lie on or close to the diagonal line, thus suggesting that the residuals for the model are normally distributed. The third, fourth and fifth panel of this figure i.e., Figure 4.2 c through Figure 4.2 e, includes the residuals plotted against the value of each explanatory variable. The residual plotted against all the explanatory variables does not show a systematic pattern thus indicates that the model adequately captured the dependence of the response on the explanatory variables.

$$T_{P\ max} = 64.05 + 0.72T_{air\ max} - 0.77Lat - 0.074D + Z(2.99^2 + \sigma^2_{Tair\ max})^{0.5} \tag{4.10}$$

The R^2 value of the model was estimated as 95% with an RMSE value of 2.99. The last term in equation 10 is the error term, which is related to the uncertainty in predicting the correct pavement temperature (Mohseni et al., 2005). To improve efficiency, the error term was added to the high pavement temperature equation (Mohseni et al., 2005). This term was defined in the same manner as for the low temperature model. The variability in the estimated pavement temperature ($\sigma_{TP\ max}$) and the error term ($\varepsilon_{max\ model}$) at any desired reliability was estimated as provided in equations 11 to 13.

$$\sigma_{TP\ max} = (\sigma^2_{\max model} + \sigma^2_{Tair\ max})^{0.5} \tag{4.11}$$

$$\sigma_{TP\ max} = (2.99^2 + \sigma_{Tair\ max}^2)^{0.5} \tag{4.12}$$

$$\varepsilon_{max\ model} = Z(2.99^2 + \sigma_{Tair\ max}^2)^{0.5} \tag{4.13}$$

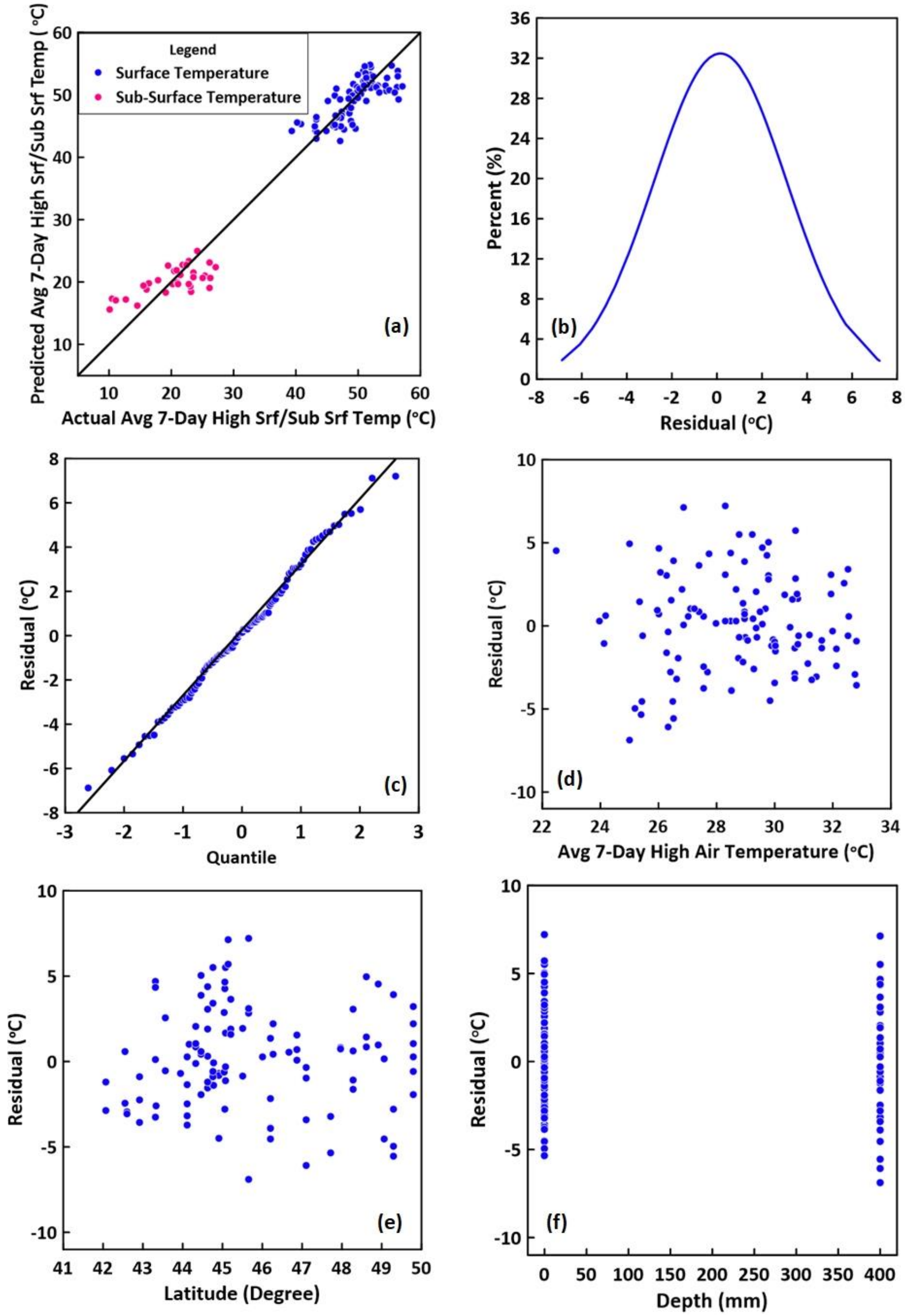

Figure 4.3 Statistical Outlook for High Pavement Temperature Model

4.3.2. Validation of Models

The developed models were validated by comparing the predicted pavement temperatures with the measured temperatures as shown in Figure 4.4 and Figure 4.5. The validation was carried out at 98% reliability. A different dataset was used for models' validation and the climate data from year 2015 was utilised for this purpose. The data used for the validation of low pavement temperature model was collected from 55 RWIS stations, whereas for high pavement temperature model, data from 44 stations were used. These stations were selected based on the availability of data. Since more stations had complete dataset for low air and surface temperatures, therefore a greater number of stations were used for low pavement temperature model as compared to high pavement temperature model. The performance of these models was compared against the LTPP models as shown in Figure 4.4 and Figure 4.5. From Figure 4.4, it can be seen that the LTPP 2.1 model predicts higher lowest annual air temperatures compared to observed for all the considered locations. On the other hand, the developed model predicted the lowest annual temperatures which were either very close or lower than the actual temperatures thus suggesting a better temperature to consider for PG determination.

The actual versus predicted highest mean 7-day annual pavement temperatures are shown in Figure 4.5 and it was observed that the pavement temperatures predicted by the developed model for the considered locations were better or equivalent to the measured pavement temperatures as compared to the LTPP 2.1 model. It was also observed, for almost all the locations, that the developed model did not estimate lower pavement temperatures whereas, the LTPP 2.1 predicted lower pavement temperatures as compared to the actual ones for locations with latitudes between 42 and 43 degrees.

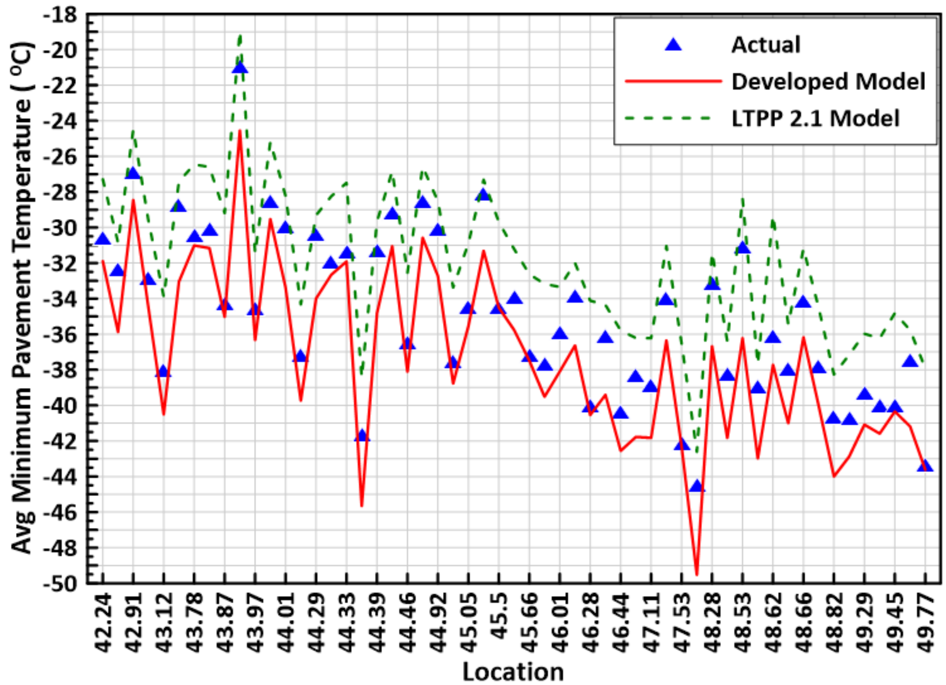

Figure 4.4 Actual versus Predicted Lowest Annual Pavement Temperature

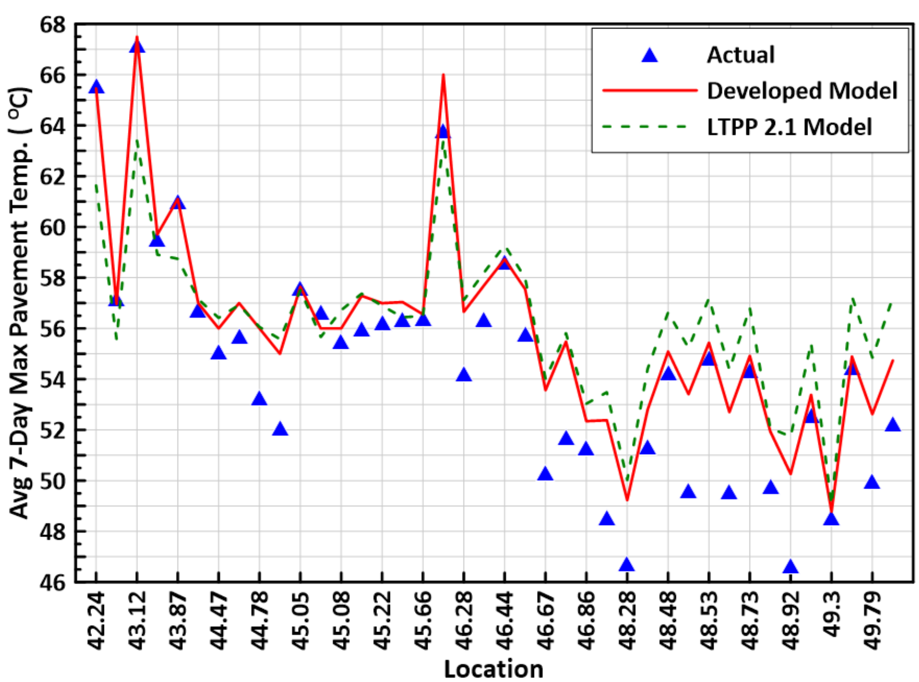

Figure 4.5 Actual versus Predicted Highest Mean 7-Day Annual Pavement Temperature.

4.4. Discussion and Results

The climate data, namely daily maximum, and minimum air temperatures, obtained from GCMs, was used to quantify the change in air temperatures due to climate change across Ontario. The average of air temperatures from all these GCMs was then computed, for which a code was written. This code was also utilized to plot map charts as shown in Figure 4.6 and Figure 4.7. The code was written in Python 3.8, 64 bit version and different packages, such as numpy, pandas, geopandas, shapely.geometry, scipy.io, matplotlib.pyplot were utilised to compute results and plot maps.

The predicted highest 7-day mean annual air temperature for the province by the end-century for different RCPs under consideration are highlighted in Figure 4.6. It is expected that, for RCP 2.6, the magnitude of highest 7-day mean annual air temperatures may increase by 3 to 4 °C for many locations in Northern and Southwestern Ontario by the end-century. It can be observed that, using the RCP 4.5 data, most of the Northern and Southern Ontario may have their highest temperatures increased by a magnitude of 3 to 5 °C. The analysis also indicates that, under no climate change policy or RCP 8.5, many locations in the Northern Ontario may have an increase of around 8 to 10 °C whereas, Central and Southern parts of the province may have an increase of 4 to 5 °C by the end-century.

The mean annual minimum air temperatures (MAMAT) using average data from GCMs for the baseline and future time periods for different RCPs are shown in Figure 4.7. From this figure it can be observed that by the year 2100, it is expected that, for RCP 2.6, a considerable number of locations in northern Ontario may show an increase of around 5 °C in the magnitude of their lowest annual air temperatures. The same increase in magnitude may expand to some of the regions in Central Ontario as well for the RCP 4.5 scenario. For the RCP 8.5, most of the Southern and Northern Ontario may see a 5 °C and 8 to 10 °C increase in magnitude respectively by the end-century.

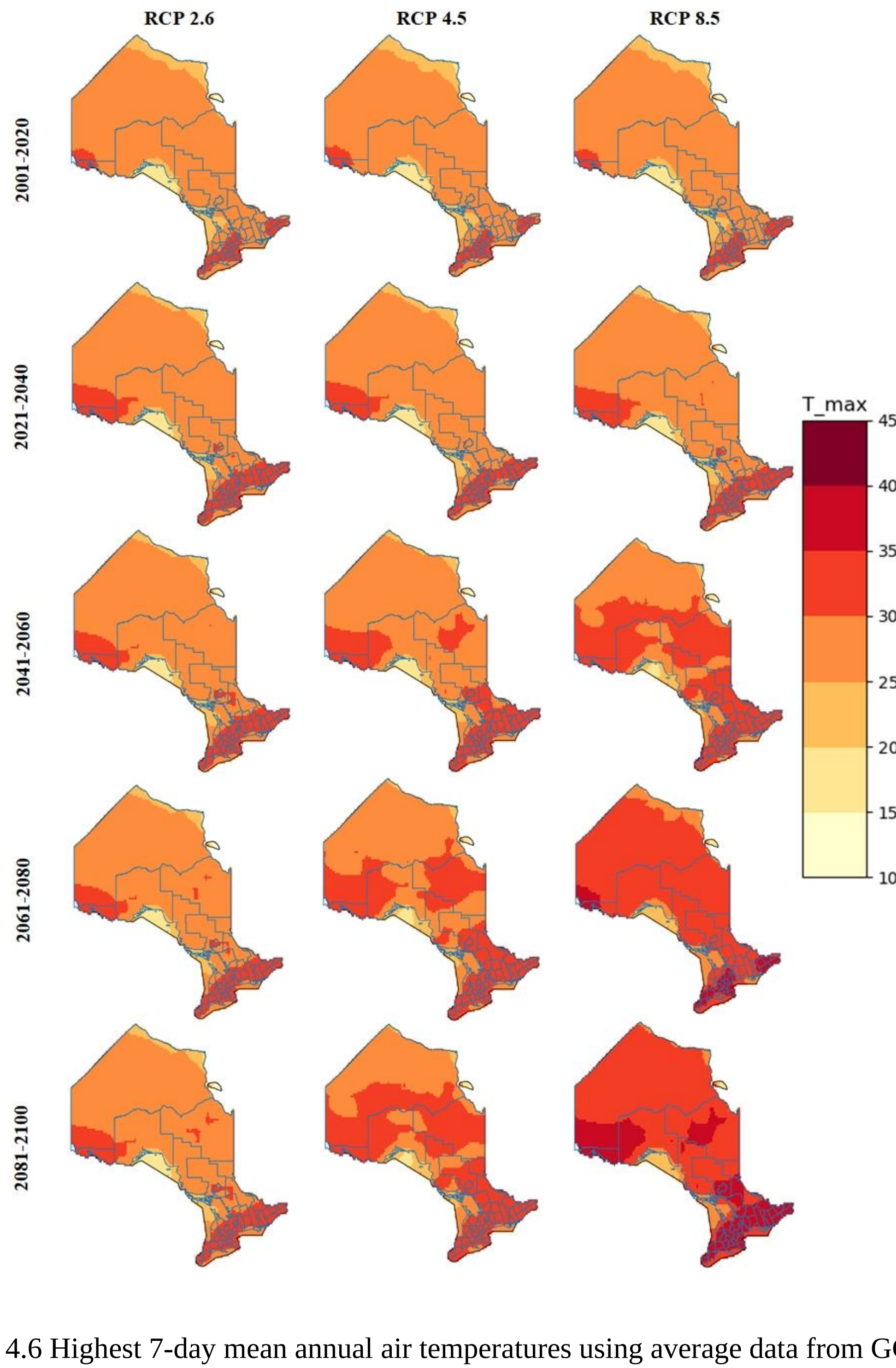

Figure 4.6 Highest 7-day mean annual air temperatures using average data from GCMs for baseline and future time periods for different RCPs, °C

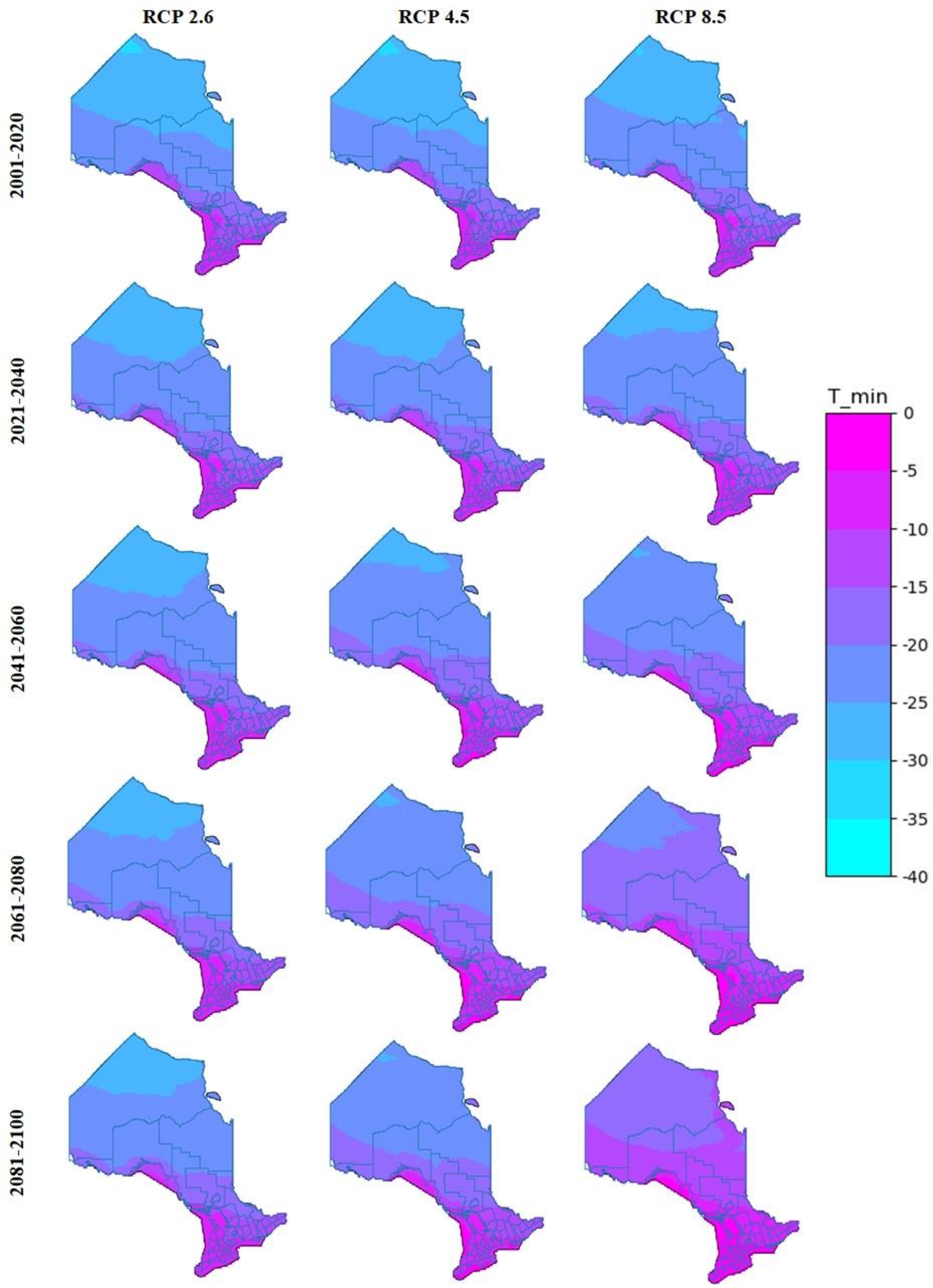

Figure 4.7 MAMAT using average data from GCMs for baseline and future time periods for different RCPs, °C.

The averages of both daily high and low air temperatures, across all the considered GCMs, was used to determine the high and low temperature PGs respectively, for the considered time periods. For the selection of PG and plotting map charts, a code was written in python 3.8 using the same packages as mentioned earlier. The estimated mean annual highest 7-day (Figure 4.8) and the minimum pavement temperatures maps (Figure 4.9) for different time periods and RCPs considered in this research. These maps were plotted using the models developed in this study. The selected PGs, across Ontario, using the developed models were also compared with that of latest LTPP models as shown in Figure 4.10. For the LTPP 3.1 model, a target rut depth of 12.5 mm, which is typical for primary roads, was used. The results were estimated using standard loading, which is less than 3 million Equivalent Single Axle Load (ESAL) with fast traffic speed (> 70 km/h) and the PGs were predicted at 98% reliability. The results were then round off to the nearest 6 °C increment to estimate the required PG.

By the year 2040 and with the best-case scenario (RCP 2.6), the results indicate that some locations in the northern part of the province are expected to see up to 5 °C increase in their highest 7-day and minimum mean annual pavement temperatures. This leads to a suggestion that those locations may require a completely different PG in the near future. It is also worth noting that no significant change in pavement temperatures is projected after the mid-century. The results generated using the developed models also suggest that, for RCP 4.5, more locations in north-eastern and north-western Ontario are expected to see a change in their highest 7-day mean annual pavement temperatures. This increase may result in the highest pavement temperatures to reach 55 °C and 60 °C for the most part of northern and southern Ontario, respectively, by the end-century. Whereas, for the mean annual minimum pavement temperatures, it can be interpreted that northern

Ontario may face more intense change than southern Ontario. The results suggest that the increase in magnitude can be as high as 5 °C by the year 2100. It can also be observed from Figure 4.8 and Figure 4.9 that under the worst-case scenario, RCP 8.5, almost the whole province may undergo a change in the highest and lowest pavement temperatures by the end-century. The 7-day mean annual pavement temperatures may reach up to 55 °C to 60 °C for northern Ontario, whereas they may reach 60 °C to 65 °C for southern Ontario. The mean annual minimum pavement temperatures may increase to -30 °C to -25 °C for northern and -20 °C to -10 °C for southern Ontario. The change in both the highest and lowest pavement temperatures suggest that the whole province may require a completely different set of PGs by the year 2100.

The pavement temperatures estimated using the developed models and the LTPP models, were utilised to determine PG maps, as shown in Figure 4.10. This figure shows the estimated PGs under RCP 8.5 and compares the estimated results with that suggested by MTO. It can be observed from Figure 4.10 that, by the mid-century, using the developed models, a change in PG may be required for southern and major parts of northern Ontario, thus suggesting 52-40, 58-28, 64-28 and 70-22 for the whole of Ontario. The LTPP models, on the other hand, suggest 52-34, 58-34, 58-28 and 64-28 by the year 2060. The results generated using both, the developed and LTPP, models highlight that, by the year 2100, almost all the locations across Ontario may require 1 to 2 grades increase in both high and low temperature PG. It can also be noted that the most suitable PG suggested by both models may be 52-34, 58-28, 64-28 and 70-22 by the end-century.

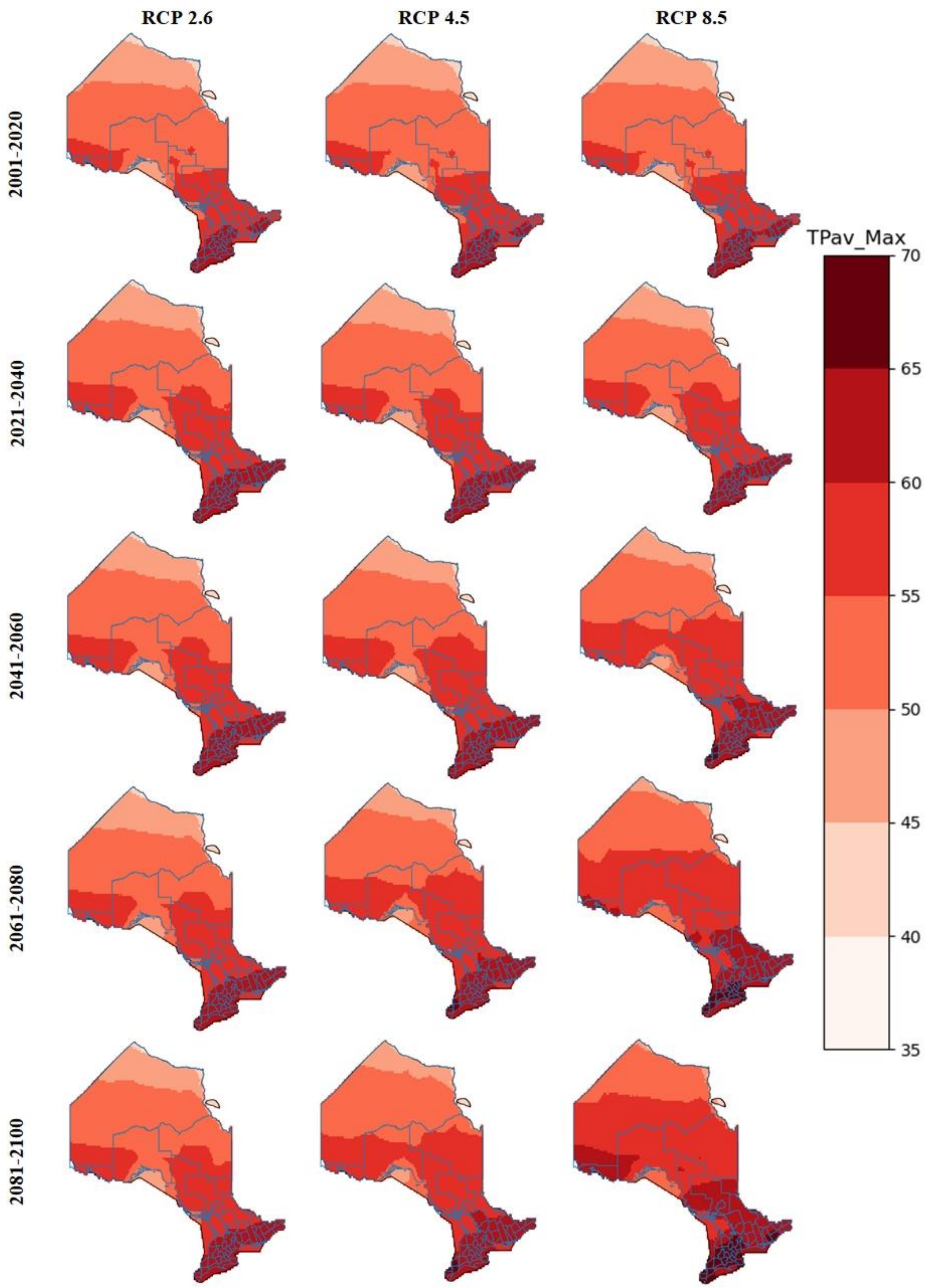

Figure 4.8 Estimated Highest 7-day mean annual pavement temperatures using developed model, °C

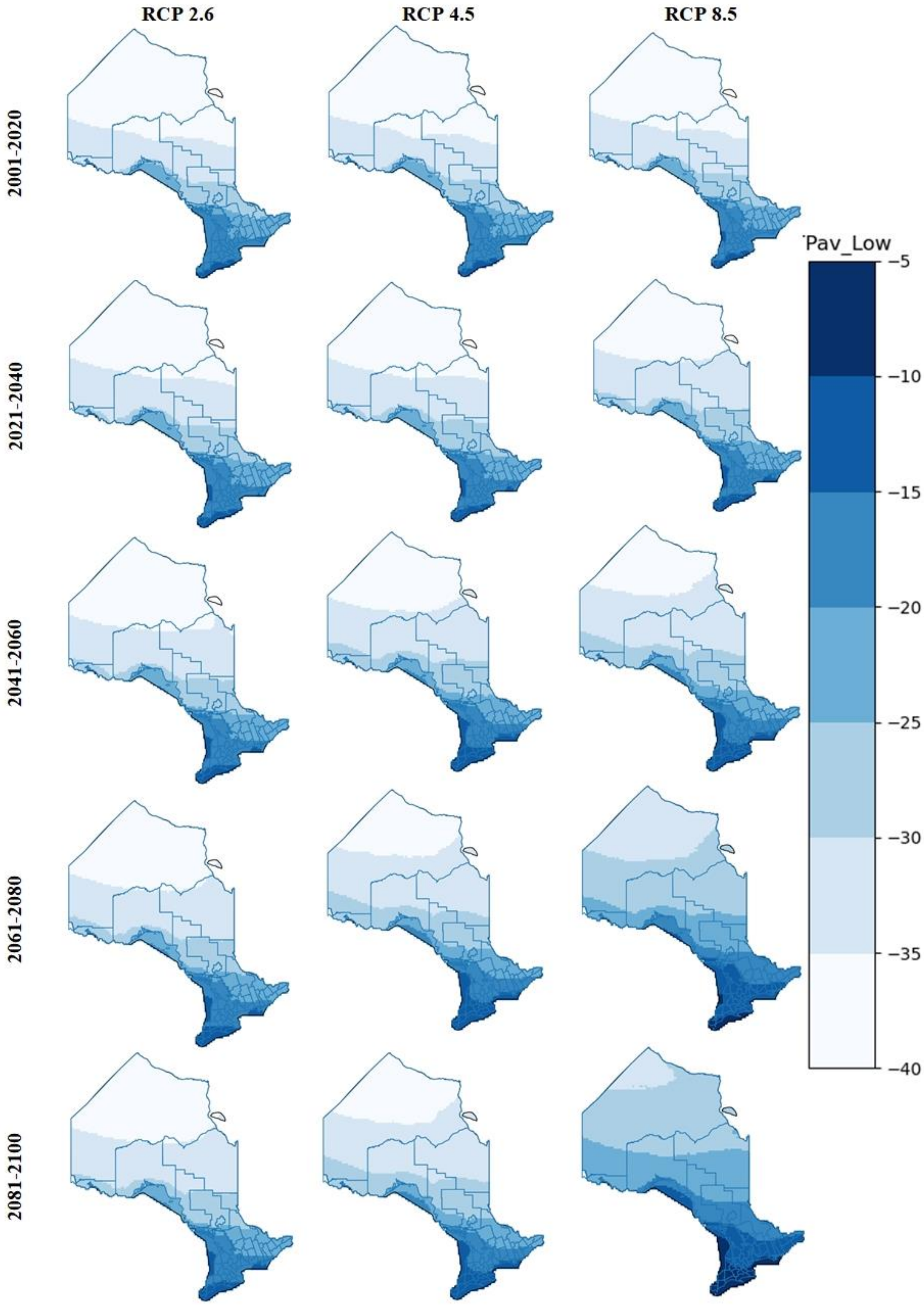

Figure 4.9 Estimated MAMPT using developed model, °C.

It was observed that the results predicted by the developed models, for the locations under consideration performed better than that of LTPP 2.1 models, as shown in Figure 4.4 and 4.5. These Figures also show that the LTPP 2.1 model estimated lower minimum pavement temperatures, whereas it estimated higher values for maximum pavement temperatures for most of the locations investigated. From Figure 4.5, the developed model substantially predicted higher values, as compared to actual, for the highest 7-day mean pavement temperatures for some of the locations. This is an indication that there is a room for improvement in the high pavement temperature model. The PGs estimated using these models, as shown in Figure 4.10, suggest that there may be a need to change the current PG set for the whole province by end-century. It is also worth mentioning that the results generated using the LTPP models suggest the same PG set for the province as the developed models. It is also expected that incorporating the changes in PG may result in less rutting and cracking due to climate change, thus increasing the service life of flexible pavements throughout Ontario.

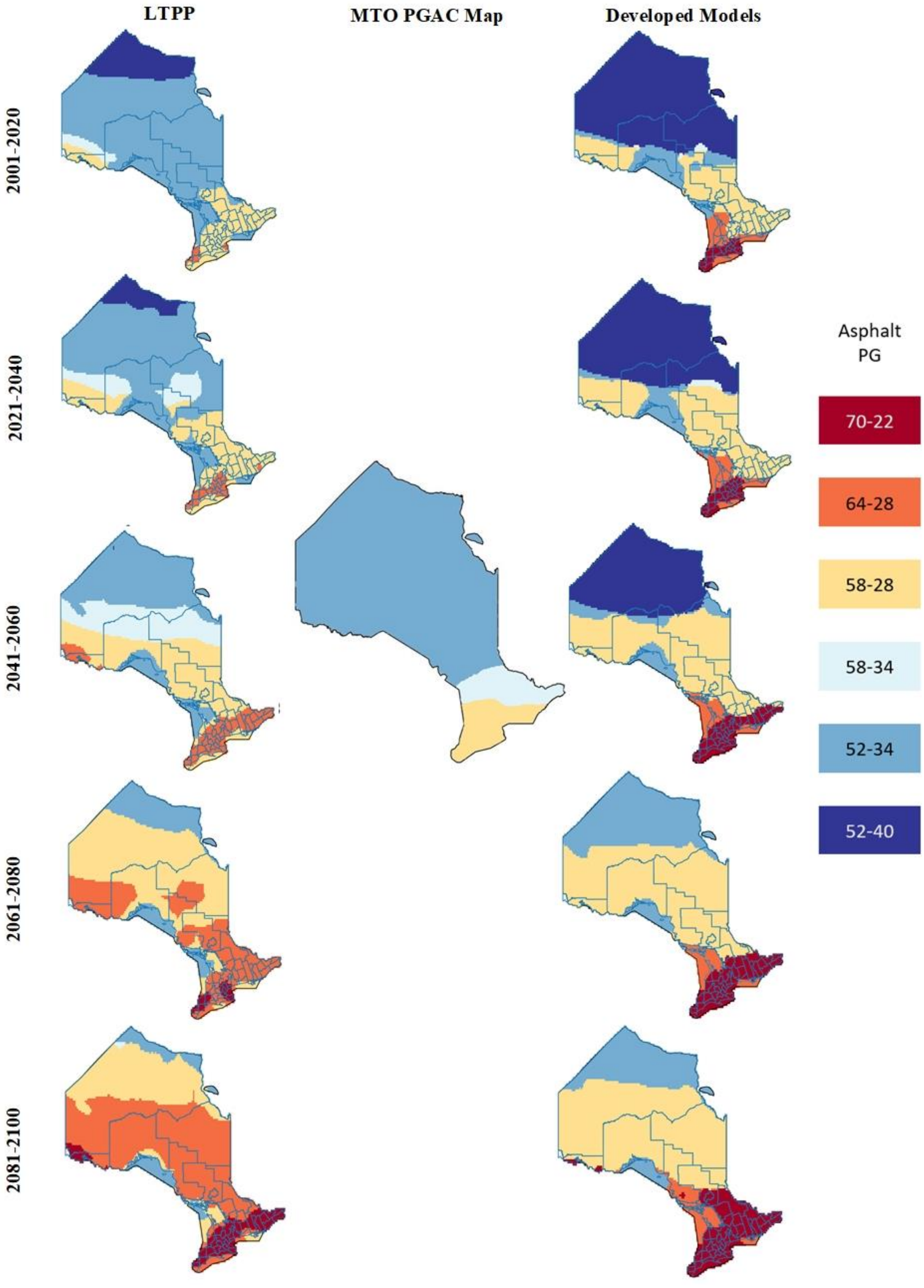

Figure 4.10 Estimated PG under RCP 8.5 using the latest LTPP and developed models, °C

4.5. Summary and Conclusions

This study examines the impacts of climate change on asphalt binder selection across the province of Ontario. For this purpose, regression models to predict pavement temperature from air temperature were developed. The models were developed using measured climatic variables and pavement surface temperatures. The climatic data used for model development and validation was obtained from various RWIS stations located in Ontario. A comparison between the models developed as part of this research indicates a superior performance over models proposed by LTPP.

To quantify the climate change impact on PG selection, the climatic data from 19 GCMs for 3 different RCPs was collected. The average based on all these GCMs was calculated and the data was compiled for 5 time periods i.e., baseline (2001 to 2020), short-term future (2021 to 2040), mid-century (2041 to 2060), third quarter (2061 to 2080) and end-century (2081 to 2100). Detailed review and analysis of the data indicates that mean annual air temperatures will increase throughout the century. Under no climate change policy or RCP 8.5, the province is expected to see up to 7.5 °C increase in the mean annual air temperatures whereas, the highest 7-day mean, and lowest annual air temperatures may rise by a magnitude of 7 to 9°C by the year 2100.

This study also leads one to conclude that, with the expected increase in air temperatures, pavement temperatures would increase. These temperatures may reach as high as 55 °C to 60 °C for northern Ontario and 60 °C to 65°C for southern Ontario for the scenario RCP 8.5 by the end-century. The rise in pavement temperatures may lead the province to face challenges in terms of revising their current PG guideline on a regular basis. The result of this study also suggests that the PG may change drastically by the end-century. It can be concluded that, by the end-century, under the worst-case scenario i.e., RCP 8.5, the current PG suggested for each MTO zone may require at least one and for some locations two grade increases in their high and low temperature PG by the end-century. The results of this study also suggest that, under no climate change policy or RCP 8.5, the most suitable PG set for the province should be 52-34, 58-28, 64-28 and 70-22 using both the developed and LTPP models. The models developed in this study are limited to Ontario, as these were generated and validated using the measured climate and pavement temperature data obtained from various weather stations located in the province. These models can be further improved as more data becomes available. Furthermore, these models were developed and tested using climatic, surface and sub surface data from no permafrost locations and are therefore limited to no permafrost locations of the province. The result of this study provides valuable recommendations that road agencies and designers can take into consideration to adjust pavement construction materials in response to changing climate conditions.

5. Evaluating the Effects of Climate Change on Spring Load Restrictions Across Ontario

5.1. Introduction

Over the last century, climate change has had a significant impact on the planet and our infrastructure. This refers to the exceptionally rapid rise in the average land and water surface temperature, which is primarily attributable to the greenhouse gases as a result of anthropogenic activities. The Intergovernmental Panel on Climate Change (IPCC) has reported that its consequences on specific locations will vary over time (IPCC, 2014). Canada is a prime example of a country whose climate has been severely affected. Canada's western and northern areas have seen more significant warming over the winter and spring than the rest of the country (Vincent et al., 2012). Furthermore, Canada’s changing climate report issued in 2019 highlighted that Canada may experience more rapid and dramatic climate change affects than many other regions around the globe in the future (Bush et al., 2019).

Pavements in cold climates are exposed, and impacted by frost, ice, and snow over extended periods of time. These pavements are expected to maintain good structural and functional performance by resisting environment-related stresses and displacements, in addition to transmitting loads from the traffic to the subgrade materials (Dore’ et al., 2008). During the winter, these pavements are subjected to negative temperatures for extended periods of time, resulting in frost penetration into the layers of pavement and the subgrade soil. Water gathers in the pavement structure throughout the year, primarily due to lateral moisture transfer, precipitation penetration, and capillary rise from the water table, and begins forming ice lenses. During the spring thaw, the frozen water converts back to a liquid state, resulting in a very high saturation within the pavement structure. During the thawing phase the upper layers thaw first, resulting in excess moisture trapped between the upper layer and the frozen or impermeable soil layers underneath it, raising the water content of the pavement structure (Janoo, 2002). During this phase, moisture can also rise in the unbound pavement layers, resulting in loss of structural stiffness and a reduction in the load bearing capability. Water saturation and excess pore water pressure develops owing to the passage of large axle loads, resulting in a loss of internal frictional forces between the aggregates, thus decreasing the shear strength in the unbound layers (Huang, 2003). In the thawing or weakened periods; authorities implement Spring Load Restrictions (SLR) for the truck traffic to reduce the load on the pavement structure. These SLR, on one hand, increase the life expectancy of the pavement structure by ensuring the truck load does not exceed the strength of the pavement structure, while on the other hand, impacts the trucking industry financially due to lower loads requirements per truck. Restrictions on the maximum payloads of trucks lead to a greater number of trips resulting in increased costs and fuel use. Therefore, it is extremely important to accurately determine the SLR application and removal dates. The accurate implementation and removal of the SLR period ensures minimum pavement damage due to truck traffic loading and economic hardships faced by the trucking industry (Chapin et al., 2013).

The SLRs are enforced based on predetermined dates and/or visual inspection methods by various transportation authorities. The issue with utilizing predetermined or fixed dates is that, the subsurface freezing and thawing patterns change from year to year. Therefore, dates and durations that are good for one year might not be appropriate for future years (Miller et al., 2014). The observation and inspection technique involves, field employees noticing changes in the pavements in the early spring, such as deflection, cracking, and/or other signs of pavement distress. By the time these pavement distresses are reported, the structural strength has already been compromised, since the SLRs often require three to five days' notice prior to application for legislation by the authorities (Miller et al., 2014). Over the years, many road agencies and authorities have started using science-based methods to determine the SLR application date and duration rather than fixed dates or individual judgement based on field observations. Quantitative methods, such as measuring the pavement deflections using a falling weight deflectometer (FWD) or estimating different indices based on climatic data are becoming increasingly common to track spring thaw processes. Furthermore, several agencies monitor the subsurface temperatures during the spring thaw period using sensors installed underneath the highways. Despite the fact that these quantitative methodologies provide a reasonable foundation for making SLR decisions, the FWD testing and accompanying analyses are expensive and time consuming. Installing sensors to monitor subsurface temperatures and/or moisture profiles, collecting and storing data obtained from these sensors, and maintaining these instruments can also be expensive. Increasingly, many road agencies and authorities have started to consider the use of weather-based indices and/or frost-thaw depth prediction models to determine the SLR thresholds. The measured weather data being readily available and much more cost effective to measure, as compared to FWD data and/or subsurface temperature data, makes these prediction models more practical. These prediction models can also be used with air temperature forecasts to provide advance warning for SLR application and duration.

The province of Ontario has an enormous 116,000 km of municipal roads (Gov. of Canada Stats, 2018) and 40,000 km of highways (FAO, 2019). Furthermore, this province is the largest contributor to the overall national Gross Domestic Product (GDP) of Canada (Gov. of Canada Stats, 2016). Almost 20% of Ontario’s entire road network are low volume roads (Chapin, 2010) and are in a seasonal frost zone. The Ministry of Transportation Ontario (MTO) owns Spring Load Adjustment (SLA) and Road Weather Information System (RWIS) stations which are used to monitor the road network. The SLA stations measure and record soil temperature and moisture data at depths ranging from 5 cm to 255 cm, whereas the RWIS stations measure subsurface temperatures at the depths of 40 and 150 cm. In addition, both stations also measure and record weather variables, such as air and surface temperatures, relative humidity, wind speed, and precipitation data. The soil temperatures at different depths obtained from these stations can be utilized to impose SLR periods on most provincial highways. In contrast, fixed SLR start dates and durations are used for the municipal roads.

Climate plays a vital role in the design and service life of the pavements. While assessing the performance of pavements, the climatic load is considered the most significant factor (Sun et al., 2019). Almost 50% of the pavement structure degradation is linked to climatic factors (Dore' et al., 2005, Watson and Rajapakse, 2000). The changing climate has been regarded as a threat to infrastructure, including pavements, by many researchers (Amy Schweikert et al., 2014, Hoyoung et al., 2017, Haslett et al., 2021). Recent studies have highlighted that climate change will result in increased stresses on pavements, thus compromising their performance and reducing their service lives (Dong et al., 2018, Jacobs et al., 2018, Stoner et al., 2019). Therefore, earlier, and frequent reconstruction and rehabilitation of pavements will be required (Mills et al., 2007). In the Permafrost regions, increased rainfalls and decreased snowfall due to climate change will affect the water balance impacting pavements (Woo, 1990). Climate change is expected to increase the number of freeze and thaw cycles (Haas et al., 2004), accelerating pavement deterioration (Haas et al., 1997, Mills et al., 2009, Erik et al., 1997, Shafiee et al., 2021). Therefore, it is vital to assess the implications of climate change on Spring Load Restrictions (SLR) periods to ensure the sustainability of low volume roadways.

Most of the analytical models developed to predict SLR start, and duration are either developed for a specific type of climate and/or require site specific calibration. Most of them have been developed using very limited climate data. Therefore, it is very important to develop a network level model that can predict SLR periods using readily available information such as air temperatures. The main objective of this study is to determine better correlations between air temperature, thawing index, and thawing depth for the province of Ontario, Canada, and then use these correlations to predict the future SLR under changing climate scenarios. Thus, this study comprises of two phases. In the first phase, network level regression models were developed utilizing data from selected SLA and RWIS stations to correlate air and surface thawing indices. Two different regression models were developed to determine the SLR periods for Northern and Southern Ontario separately. The performance of the models developed in this study were subsequently evaluated using measured subsurface data from SLA and RWIS stations. The second phase of the study involved estimating the potential implications of climate change on the SLR periods across Ontario. The climate data was collected from 19 different General Circulation Models (GCMs) for 3 Representative Concentration Pathways (RCPs) for historical (2001–2020) and future time intervals: short-term future (2021-2040), mid-century (2041-2060), third quarter (2061-2080) and end-of-century (2081-2100). The SLR periods for these time intervals were estimated by utilizing models developed in phase 1 to assess the change in these time intervals for different emission scenarios. The models developed in this study and the SLR outlook by the end-century is of interest and use for the designers and policy makers in order to ensure maximum road structure life and minimum financial hardships faced by trucking industry during the spring season.

5.2. Existing Models

Several studies have been carried out, and different techniques have been used for the SLR predictions using air temperatures. Two different types of models i.e., models based on trigger thresholds and models based on frost and thaw depth predictions, are presented in this section. The models based on trigger thresholds use a CTI threshold values whereas the frost and thaw depth prediction models use TD for application and removal of SLR. Some of the widely used models are presented in this section.

5.2.1. Based on Trigger Thresholds

Mahoney et al. (1986)

One of the earliest analyses on this subject was carried out by Mahoney et al., 1986, in which analytical models were developed to determine the start and duration of SLR. A correlation between air temperature and surface thawing index was developed, and it was proposed that the thawing season begins when the daily average air temperature exceeds 1.67 °C. The proposed relationship can be expressed as follows:

$$CTI = \sum_{i=1}^{N}(T_{avg,i} + 1.67) \quad (5.1)$$

Where, CTI is the cumulative thawing index in °C days, T_{avg} is the average daily temperature in °C and N is the number of cumulative days. In the above equation, the constant 1.67 is the reference temperature (T_{ref}) which is defined as the magnitude of air temperature at which the surface temperature fluctuates around 0 °C. If a thawing phase is interrupted by a substantial refreezing event, the CTI cannot be negative and is consequently reset to zero (Mahoney et al., 1986). This method suggests that SLR should be applied as soon as CTI reaches 15 °C days and must be applied when CTI reaches 28 °C days. The authors suggest two approaches for the lifting of SLR i.e., duration threshold and CTI threshold. The cumulative air freezing index (AFI), computed as the difference between the freezing temperature and the daily average air temperature, is used in determining the end of SLR. The duration threshold and CTI threshold can be determined using equations 2 and 3, respectively.

$$Duration\,Threshold = 25 + 0.01(AFI) \quad (5.2)$$

$$CTI\,Threshold = 0.3(AFI) \quad (5.3)$$

Bradley et al (2012)

In this method, models for initiating and terminating SLRs were developed by corelating weather-based indicators to when pavements began to lose their strength and when they have considerably regained their strength in the spring. This method recommends a CTI threshold value of 15 °C days for the SLR application (Bradley et al., 2012). This approach uses a T_{ref} for the determination of CTI.

$$CTI = \Sigma[T_{ref} + \frac{T_{max}+T_{min}}{2}] \quad (5.4)$$

Where T_{max} and T_{min} are the maximum and minimum daily air temperatures in °C. Starting March 1st, T_{ref} is taken equal to 1.7 °C with a daily increase of 0.06 °C until May 31st (Bradley et al., 2012). If the MDAT becomes negative, then TI for that particular day should be calculated as follows to compensate for the time when the ambient air temperature goes below 0 °C.

$$CTI = \Sigma[T_{ref} + \frac{T_{max}+T_{min}}{4}] \quad (5.5)$$

It is recommended that SLR should be removed either eight weeks following the application date, or when the CTI hits 350 °C-days, whichever comes first, (Bradley et al., 2012).

Mn/DOT Research (2014)

The Minnesota Department of Transportation (Mn/DOT) model was derived from the concepts developed by Ovik et al. (2000). This method also uses reference temperatures and measured air temperatures to calculate daily FI and TI values. The reference temperature in this method is a variable value which is used to convert the air temperatures into corresponding surface temperatures. The value of this reference temperature is taken as -1.5 °C, which begins on 1st February, and it decreases by 0.5 °C every week until it reaches a value of -9.5 °C during 24th – 30th May (Mn/DOT, 2014). The values of TI and FI are then used to determine the cumulative thawing index as shown in the following equations (Mn/DOT, 2014):

CTI = $\sum_{i=1}^{n}(Daily\ Thawing\ Index - 0.5 * Daily\ Freezing\ Index)$ (5.6)

- Case A: when $\left(\frac{T_{max} + T_{min}}{2} - T_{reference}\right) > 0°C$ (The pavement structure is thawing)

  Then, $Daily\ Thawing\ Index = \left(\frac{T_{maximum} + T_{minimum}}{2} - T_{reference}\right)$

  and $Daily\ Freezing\ Index = 0°C$

- Case B: when $\left(\frac{T_{maximum} + T_{minimum}}{2} - T_{reference}\right) < 0°C$

  And $CTI_{n-1} \leq 0.5 \text{ x } \left(0°C - \frac{T_{max} + T_{min}}{2}\right)$, (Significant thawing has not yet occurred)

  Then, $Daily\ Thawing\ Index = 0°C$ and $Daily\ Freezing\ Index = 0°C$

- Case C: When $\left(\frac{T_{maximum} + T_{minimum}}{2} - T_{reference}\right) < 0°C$

  And $CTI_{n-1} > 0.5 \text{ x } \left(0°C - \frac{T_{max} + T_{min}}{2}\right)$, (Pavement structure is refreezing)

  Then, $Daily\ Thawing\ Index = 0°C$ and $Daily\ Freezing\ Index = \left(0°C - \frac{T_{max} + T_{min}}{2}\right)$

Where CTI is the cumulative thawing index calculated over a period from 1 to n days in °C -days, CTI resets to zero on January 1st, T_{max} is the maximum daily air temperature in °C, T_{min} is the minimum daily air temperatures in °C and T_{ref} is the reference air temperature in °C. As mentioned before, the reference temperatures are utilized to adjust for the temperature difference between the air and asphalt temperatures (Mn/DOT, 2004). While determining the CTI, the 0.5 factor is applied to the FI which accounts for the partial phase change of water and therefore known as the refreeze factor.

This method suggests that the SLRs should be implemented when a 3-day forecasted temperature period gives a CTI greater than 14°C -days. There is no specific value of CTI, suggested by this method, which corresponds to the removal of SLRs however, some variables such as cumulative spring precipitation, accumulated fall precipitation measured during the preceding year and CTI are used to provide a better judgement for SLR removal. Generally, it is recommended that SLRs should remain in place for a minimum of 4 weeks and a maximum of 8 weeks.

5.2.2. Based on Frost-Thaw Depth Predictions

Chapin et al., (2013) and Pernia et al., (2014) Research

Chapin et al. (2013) and Pernia et al. (2014) proposed a model corelating frost and thaw depths with temperature indices. For determining freezing and thawing indices, they proposed the utilization of MnDOT equations and reference temperatures. The CFI and CTI were then used to estimate frost and thaw depths using an empirical model which was developed through regression analysis. The calibration coefficients for the prediction model were determined by plotting the measured frost or thaw depth against the day's matching CFI or CTI value. Chapin et al. (2013)

and Pernia et al. (2014) compared the R-squared values of a linear and polynomial trend functions and found that the polynomial model provided higher R-squared value for their research sites. As a result, their prediction model is based on a second-order quadratic equation which is given below:

$$y = ax^2 + bx + c \tag{5.7}$$

Where, y is the frost or thaw depth, x is CFI or CTI and a, b, c are the regression coefficients.

5.3. Development of a Network Level SLR Model for Ontario

In order to develop an Ontario specific network level SLR model, air and pavement temperatures data was obtained from various SLA and RWIS stations located across Ontario, Canada. The approximate locations of these stations and data utilized in models' development are provided in Figure 5.1 and Table 5.1 SLA and RWIS Stations used for Development of Modelsrespectively. Regression models were developed to obtain the relationship between Thawing Depth (TD) and CTI using the similar concept used by Chapin et al. (2013) and Pernia et al. (2014). In order to obtain a single equation for the SLR determination across different regions in Ontario, latitudes of sites were included as an explanatory variable. The models were based on second-order quadratic equations developed using regression analysis. The models were evaluated based on the R-squared, Root Mean Squared Deviation (RMSD) and Mean Absolute Deviation (MAD) values.

In Ontario, the MTO have constructed and operate 9 SLA stations. Temperature sensors are installed at these SLA stations, which detect the temperature of the subsurface at various depths (Chapin et al., 2010). The SLA data is used by MTO to monitor subsurface freeze-thaw cycles during the autumn and spring seasons, as well as to implement the SLR on the roadways in order to minimize road damage.

The MTO also manages 165 RWIS stations located in different regions across Ontario, Canada (Buchanan et al., 2005). An RWIS station is a combination of different sensors, such as pavement and meteorological sensors, and a monitoring and prediction system (Bernstein, 2003). These stations measure and record data such as air temperature, relative humidity, wind speed and direction, precipitation, pavement surface temperature, subsurface temperature, pavement state, and the freezing point of a wet surface (Bernstein, 2003).

As a part of this study, different models were developed for Northern and Southern Ontario in order to account for the difference in climatic conditions. While analysing the air and surface temperature data, it was observed that the Northern and Southern Ontario have different trends of temperature with latitudes. It was impossible to capture different temperature trends in a single model therefore two different models for Northern and Southern Ontario were developed in this study. The model for Northern Ontario was developed using the data from 5 SLA stations, while the model for Southern Ontario was developed by utilizing data from 6 RWIS stations. While selecting the RWIS stations for model development, only those stations were considered which are located in Southern Ontario and had a complete air and surface temperature data set from September of one year to June of the following year. The period from September to June was considered as it encapsulates the freezing and the following thawing season. Furthermore, any station having more than two consecutive days of missing data was not considered in the model's development. The air and subsurface temperature data at depths 5, 15, 30, 45, 75, 90, 105, 135 and 165 cm from SLA stations, and at 0, 40, and 150 cm depths from RWIS stations, were utilized to corelate TD and CTI. The data obtained from these stations was cleaned of any statistical outliers and erroneous values. These were identified as the data points that differ significantly from other observations. A forward selection regression technique was employed in the Statistical Analysis System (SAS) software version 9.4 for the multiple second-order regression analysis. The prediction models are presented as equations 5.8 and 5.9, whereas the location map and pertinent details of stations and data are presented in Figure 5.1 and Table 5.1 SLA and RWIS Stations used for Development of Models, respectively.

$$TD_N = -3.85 - 0.0006CTI^2 + 0.66CTI + 0.2Lat \quad (5.8)$$

$$TD_S = 22.8 - 0.0061CTI^2 + 2.46CTI - 1.11Lat \quad (5.9)$$

Where, TD_N is the thaw depth for Northern Ontario and TD_S is the thaw depth for Southern Ontario. The R-squared value for the Northern Ontario model was 92%, whereas its RMSD and MAD was found to be 4.9 and 0.2, respectively. For the Southern Ontario model, the R-squared value was 94%, however its RMSD and MAD values were found to be 16.6 and 4.2, respectively. It is important to mention here that the CTI was determined using the reference temperatures as prescribed by MnDOT (2014). As mentioned earlier, the developed models do not require any site-specific calibration, unlike previously developed models.

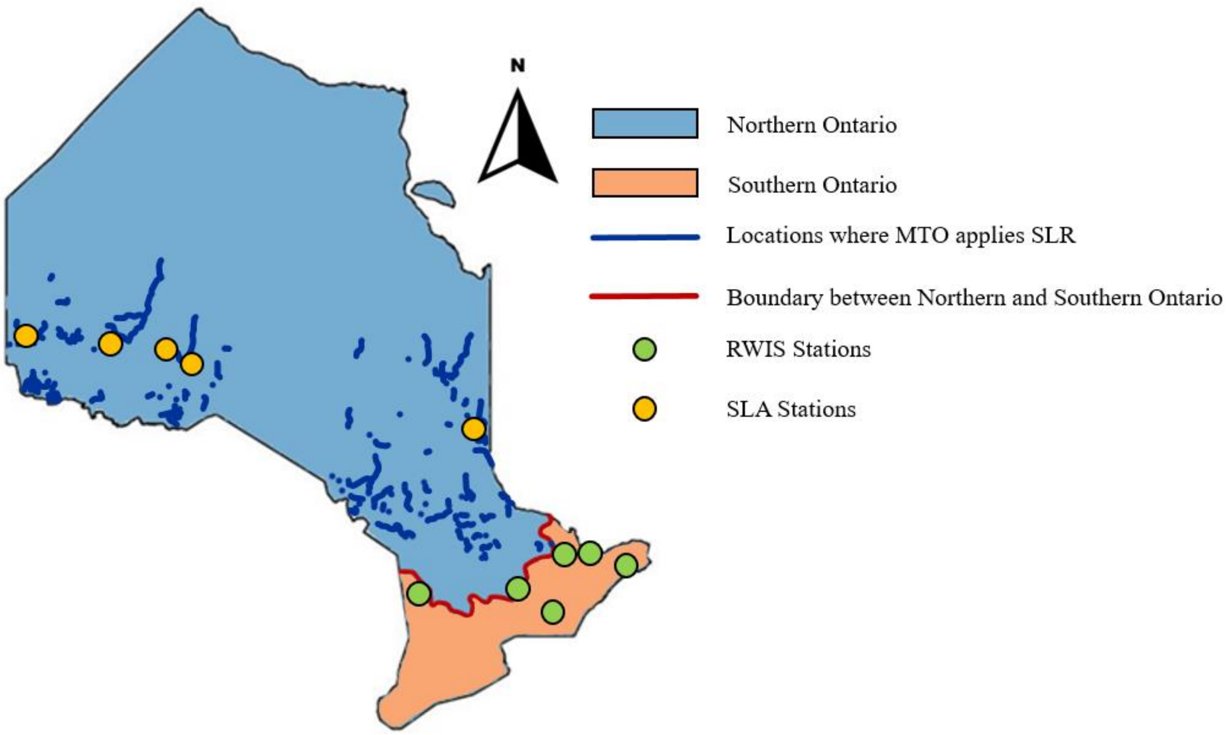

Figure 5.1 The approximate locations of SLA and RWIS stations across Ontario used in this study.

Table 5.1 SLA and RWIS Stations used for Development of Models

Station ID	Latitude	Longitude	Data used for Models' Development	Data used for Models' Validation
ER 25	44.5°	77.8°	2017 (Feb – Apr)	2017 (Feb – Apr)
ER 08	44.9°	75.2°	2017 (Feb – Apr)	2017 (Feb – Apr)
ER 32	45.1°	75.6°	2017 (Feb – Apr)	2017 (Feb – Apr)

ER 30	45.1°	77.3°	2017 (Feb – Apr)	2017 (Feb – Apr)
NR 13	46.1°	79.4°	2017 (Feb – Apr)	2017 (Feb – Apr)
NR 27	46.7°	84.3°	2017 (Feb – Apr)	2017 (Feb – Apr)
SLA 624	47.9°	79.8°	2014 – 2015 (Feb – May)	2016 (Feb – May)
SLA 527	49.4°	89.4°	2013 (Feb – May)	2019 (Feb – May)
SLA 671	49.8°	94.3°	2013 (Feb – May)	2014 (Feb – May)
SLA 599	49.8°	91.2°	2013 – 2014 (Feb – May)	2017 (Feb – May)
SLA 643	50.2°	88.8°	2014 – 2016 (Feb – May)	2017 (Feb – May)

5.4. Network Level Models' Validation

5.4.1. Comparison of the Developed Models with Actual SLR Periods

The duration of data over which the models were validated is presented in Table 5.1 SLA and RWIS Stations used for Development of Models. The data utilized for models' validation is different than that used for of models' development. The SLR periods were estimated using the recommendation from MTO, which states that the most significant loss of pavement strength occurs when the thaw starts in the base, and the least significant loss occurs when the thaw reached a depth of around 1 meter.

From the results presented in Figure 5.2, Figure 5.3 and Table 5.2, it can be observed that both models predicted the SLR periods quite well. The Northern Ontario model, as presented in Figure 5.2, predicted SLR start dates very close to the actual dates for all the locations except for SLA 671 where the prediction was around four days late. Whereas this model suggested conservative results for SLR removal, thus predicting around 6 to 8 days of delay in the SLR removal dates for most of the locations with the exception of station SLA 643 where there is delay of around 17 days. It can also be observed that, unlike the other sites, the model predicted around 6 days earlier SLR period for SLA 671 as compared to the measured value.

The comparison of the model developed for southern Ontario, presented in Figure 5.3, shows that the model predicted a 1 to 3 days delay in SLR application date for stations NR 27, NR 13, ER 32, and ER 25, whereas a 7 to 8 days earlier prediction is made for stations ER 30 and ER 08. The results also indicate that for four out of six locations, the model suggested a 2 to 4 days of delayed SLR removal date. It can also be observed that for two locations i.e., ER 08 and ER 30, the model predicted around 15 to 18 days longer SLR period in comparison to the SLR period predicted from ground temperature measurements.

5.4.2. Comparison of the Developed Models with Existing Models

The previously developed, widely used models, were also used to determine the SLR periods by utilizing the climate data obtained from selected stations. The results were then compared with that of the models developed in this study as also shown in Figure 5.2, Figure 5.3 and Table 5.2.

For the Pernia et al. (2014) method, the regression coefficients for each site were estimated in the SAS software 9.4 using the data obtained from the relevant stations.

From Figure 5.2, it can be observed that the MnDOT (2014) model predicted earlier SLR application dates for most of the locations particularly for SLA 527 where the prediction was around 23 days earlier than the measured. Whereas, for SLA 624, this model suggested a delayed SLR application date. Figure 5.2 and Table 5.2 also shows that the MnDOT (2014) model predicted 12 days later SLR removal date for SLA 643 and 6 days sooner removal date for SLA 599, however this model predicted reasonable results for the rest of sites. It can also be observed that the MnDOT model predicted conservative results for most of the RWIS stations' location while predicting around 16 to 26 days of delayed SLR removal dates than the measured. The model predicted around 8 to 10 days earlier SLR application date for ER 25 and ER 32 locations whereas, the prediction was reasonable for the rest of locations.

In Figure 5.2 and Table 5.2, it can be observed that the Bradley et al. (2012) model predicted longer SLR periods while predicting around 15 to 20 days earlier SLR application dates for SLA 624 and 527. Moreover, this model suggested an approximately 6 to 16 days delay in the SLR removal date for all the locations except SLA 671. From the results estimated from RWIS stations' data (Figure 5.3 and Table 5.2), it can be noted that this model predicted a delayed SLR application date for ER 08, 25 and 32 stations and suggested SLR application dates close to the actual SLR removal dates. It can also be observed that this model produced very conservative results while predicting SLR removal dates approximately 22 to 28 days delayed from the actual SLR removal.

The results also suggest that the Pernia et al. (2014) model was found to be predicting lower temperature values compared to observations for most of the locations under consideration.Figure

5.2, Figure 5.3 and Table 5.2 shows an 8 to 12 days sooner SLR removal date was predicted using this model for Northern Ontario locations such as SLA 671, 599 and 543 whereas 4 to 7 days of delayed SLR application date was anticipated for Southern Ontario locations including ER 30, 32, NR 13 and 27.

The Mahoney et al. (1986) model, on the other hand, showed better results as compared to the Pernia et al. (2014) model. For Northern Ontario locations, as shown in Figure 5.3 and Table 5.2, the Mahoney et al. model predicted late SLR application dates for SLA 599 and 643 by 3 to 6 days whereas it predicted slightly early dates for the remaining locations. However, this model suggested a 6 to 16 days of delayed in SLR removal date for most locations. The Southern Ontario locations showed a different trend (Figure 5.3 and Table 5.2) with three stations showing 3 to 6 days later and two showed around 9 to 12 days sooner SLR application date. It can also be observed that this model anticipated 6 to 16 days later SLR removal dates for all the Southern locations. It can be concluded that, for most of the locations, the models developed in this study predicted more accurate SLR start dates and durations when compared to other widely used models. However, in Figure 5.2 and 5.3, there are some locations where developed model predicted late SLR start dates, which can be considered anomalous. It may be due to the reason that the regression models may not entirely capture the thawing depth trend for those locations as compared to other locations. This limitation may be removed by calibrating the models with more data for such locations.

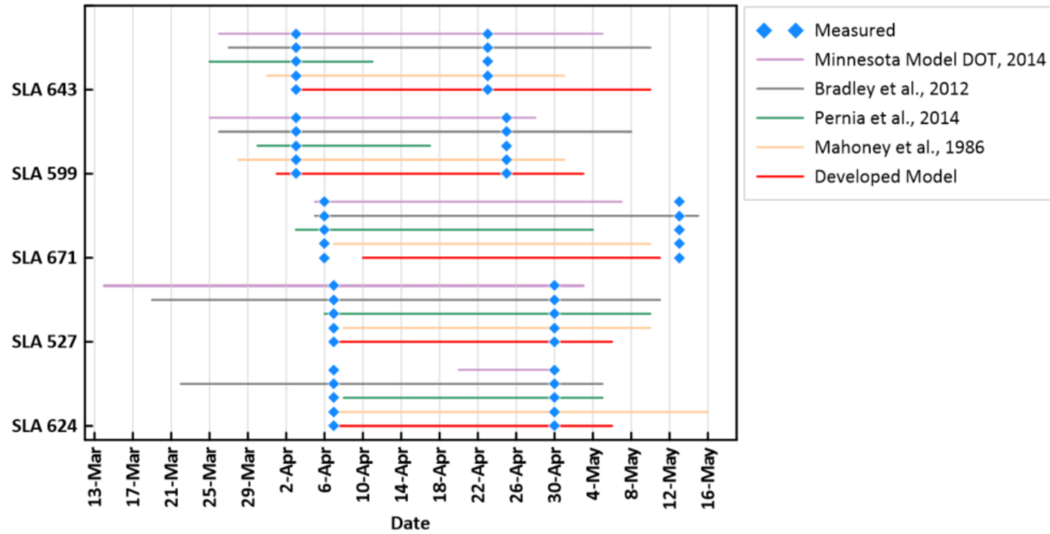

Figure 5.2 Measured and Predicted SLR Periods for Northern Ontario for various models from the literature and the model developed in this study. Stations are sequenced according to descending order of Latitude.

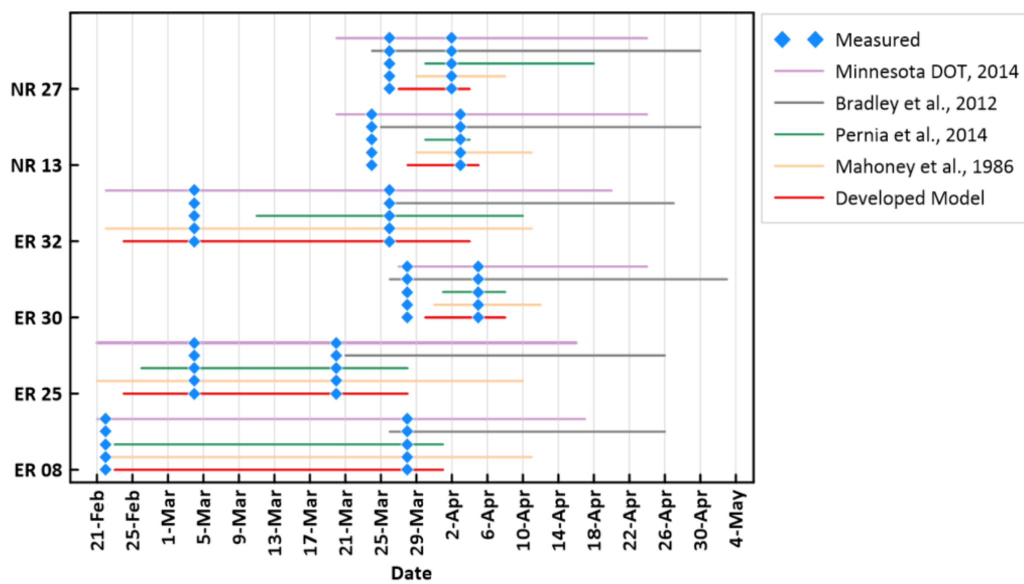

Figure 5.3 Measured and Predicted SLR Periods for Southern Ontario for various models from the literature and the model developed in this study. Stations are sequenced according to descending order of Latitude.

Table 5.2 Number of Days that the predicted SLR start, and end dates fell Early (-) or Late (+) for various models from the literature and the model developed in this study.

Station ID	Minnesota		Bradley et al.		Pernia et al.		Mahoney et al.		Developed	
	SLR Start	SLR End	SLR Start	SLR End	SLR Start	SLR End	SLR Start	SLR End	SLR Start	SLR End
NR 27	-7	+22	-2	+28	+4	+16	+3	+6	+1	+2
NR 13	-4	+21	+1	+27	+6	+1	+5	+8	+3	+1
ER 32	-10	+25	+22	+32	+7	+15	-10	+16	-7	+8
ER 30	-1	+19	-2	+28	+4	+3	+3	+7	+2	+3
ER 25	-11	+27	+17	+36	-6	+8	-11	+21	-8	+8
ER 08	-1	+20	+32	+29	0	+4	0	+14	0	+4
SLA 643	-8	+12	-7	+17	-9	-12	-3	+8	0	+17
SLA 599	-9	+3	-8	+13	-5	-8	-6	+6	-2	+8

SLA 671	-1	-6	-1	+2	-3	-9	+1	-3	+4	-2
SLA 527	-24	+3	-19	+11	-1	+10	+1	+11	0	+6
SLA 624	+13	0	-16	+5	+1	+5	0	+16	0	+6

5.5. Future Climate Impact

5.5.1. Temperature Projections and Potential Impacts

Climate data was obtained from 19 distinct GCMs for the baseline (2001 to 2020) and the future, i.e., short-term (2021 to 2040), mid-century (2041 to 2060), third quarter (2061-2080) and end-of-century (2081 to 2100). The datasets consist of mean daily air temperatures (MAAT). The data was obtained from the OCDP website (lamps.math.yorku.ca/OntarioClimate). This website provides data with a spatial resolution of 10 km x 10 km that has been downscaled by members of the North American Coordinated Regional Downscaling Experiment Program (NA-CORDEX), Pacific Climate Impacts Consortium (PCIC), Laboratory of Mathematical Parallel Systems (LAMPS) York University, University of Toronto, and University of Regina using various statistical and dynamical downscaling techniques. Three different climate change scenarios i.e., RCP 2.6, 4.5, and 8.5 were investigated in this study to assess the impact of climatic change. An RCP is a GHG concentration trajectory that is used to describe concentration changes by the year 2100. The RCP 2.6 route portrays the climate change scenario with the strictest climate policies and the lowest GHG emissions, with radiative forcing reaching 3 wm^{-2} before 2100. RCP 4.5 is an intermediate pathway in which the radiative forcing peak around 2040, and then decline and stabilized at around 4.5 wm^{-2} via intermediate stabilization mechanisms. Whereas the RCP 8.5 depicts a high trajectory in which radiative forcing exceeds 8.5 wm^{-2} by 2100 and continues to grow for some time and represents the highest emission scenario in the absence of climate policy (Meinshausen et al., 2011). To check the adequacy of the climate data collected from the GCMs, the climate normals for the historical period were compared with that of climate normals reported by Environment Canada (climate.weather.gc.ca) for the period of 1981 to 2010. This comparison, for selected cities located across Ontario, Canada, is shown in Figure 5.4. Two of these cities are located in Northern Ontario while the other two are located in Southern Ontario. This figure clearly indicates that the GCMs predicted the historical temperature data very well. It is pertinent to mention here that SLR increases the number of trips required to transport the same load and as such further studies should aim to try and find a balance between GHG emissions and the load restriction times. This points to the need to have site specific SLR periods and a way to update those durations effectively.

5.5.2. SLR Assessment by the End of Century

The change in air temperatures due to climate change in Ontario, Canada, was quantified using the Mean Daily Air Temperatures (MDAT) collected from 19 different GCMs. A code was written to determine the average of MDAT across all the GCMs. This code was developed in Python 3.8, 64-bit version, and a variety of packages, such as numpy, pandas, geopandas, shapely.geometry, scipy.io, matplotlib, and pyplotlib, were utilized to calculate results and plot maps. Figure 5 depicts Mean Annual Air Temperatures (MAAT) for RCP 2.6, 4.5, and 8.5 for five time periods: baseline (2001-2020), short-term future (2021-2040), mid-century (2041-2060), third quarter (2061-2080) and end-century (2081-2100). By the end of the century, the strictest climate change policy, i.e., RCP 2.6, may result in an average increase of 1-1.5°C in MAAT, whereas RCP 4.5 is predicted to result in an average increase of 3-4°C in MAAT. It's also worth noting that with no climate change strategy, i.e., RCP 8.5, MAAT can be expected to rise by 6.5-7.5°C on average across the province by the year 2100. Figure 5.5 also illustrates that the southern and north-western sections of Ontario may have a greater rise in MAAT than the rest of the province, implying that these areas may experience more pronounced changes in their SLR periods than the rest of the province.

For the time periods under consideration, SLR start dates and durations were determined using average MDATs collected from GCMs. Again, a code was created in Python 3.8 to compute SLR periods and plot map charts, using the same packages as mentioned above. The predicted maps showing SLR start dates and durations for various time periods and RCP scenarios are shown in Figure 5.6 and Figure 5.7. Different colours in this figure show the dates whereas the lines show the highway network where MTO imposes these restrictions in the spring. The models established in this study were utilized to forecast these SLR periods. The Southern Ontario model was utilized for locations with latitude 46° and less whereas, Northern Ontario model was used for locations with latitude greater than 46°.

The results suggest a trend of SLR start dates falling earlier by the end century as compared to the baseline period. It can be observed from Figure 5.6 that, considering the temperature changes predicted using emission scenario RCP 2.6, many locations in the Northern Ontario may require these restrictions to start around 20 days earlier by the year 2100 as compared to the baseline period. Whereas, only a few locations in Southern Ontario may need such change. It can also be observed that, using the RCP 4.5 scenario, more locations in both Southern and Northern Ontario may require the SLR to be imposed about 20 days earlier by the year 2100. Furthermore, under the RCP 8.5, whole of the province may require an earlier SLR start date. It is expected that most of the locations in Northern Ontario may need the restrictions to start by the end of March and April. Whereas, for the locations in Southern Ontario, these restrictions may start from January to mid of February by the year 2100.

The results also suggest that under the strictest climate change policy, i.e., RCP2.6, the SLR period for many Northern and a few Southern Ontario's locations may reduce by 5 to 10 days by the end-century. Under these circumstances, most of the Northern regions may require a 30 to 35 days while the rest may need 35 to 40 day SLR period. Whereas for the Southern Ontario, by the year 2100, most of the locations are expected to see SLR periods of 10-15 with few Southern locations requiring a 15-20 days SLR period.

It can also be observed from Figure 5.7 that under the moderate climate change circumstances, i.e., RCP 4.5, more regions in the North may require a 5 to 10 days shorter SLR period when compared to RCP 2.6. Thus, by the end-century, most of the regions may need a 10-15, 30-35 and 35-40 days of SLR period with a few locations in Southern Ontario exhibiting 15-20 days of SLR period. Whereas, under the worst-case scenario, i.e., RCP 8.5, it is expected that almost whole of the Northern and Southern Ontario may require a 30-35 days and 10-15 days of SLR period respectively.

Maps for selected dates in a year showing locations across the province which may need the SLR to be in effect on or before that date are presented in Figure 5.8. These maps were created using the RCP 8.5 data by using the similar approach as used in plotting Figure 5.6 and Figure 5.7. The results from this analysis indicate that, by the mid-century, some of the Southern Ontario locations may need the SLR to start by March 15. Whereas almost all the locations in Southern Ontario may need these restrictions to be in effect by March 31 and/or April 15. Furthermore, it is expected that almost all the locations across Ontario, where MTO applies SLR, may require these restrictions to start as early as April 30 and/or May 15. It can also be observed that, by the end century, a considerable number of locations in Southern Ontario may have the SLRs starting by mid of February. Whereas all the locations in Southern Ontario may have the restrictions in effect by March 15 and/or 31. Furthermore, locations in the Northern Ontario, may require these restrictions in effect by April 15 and/or 30.

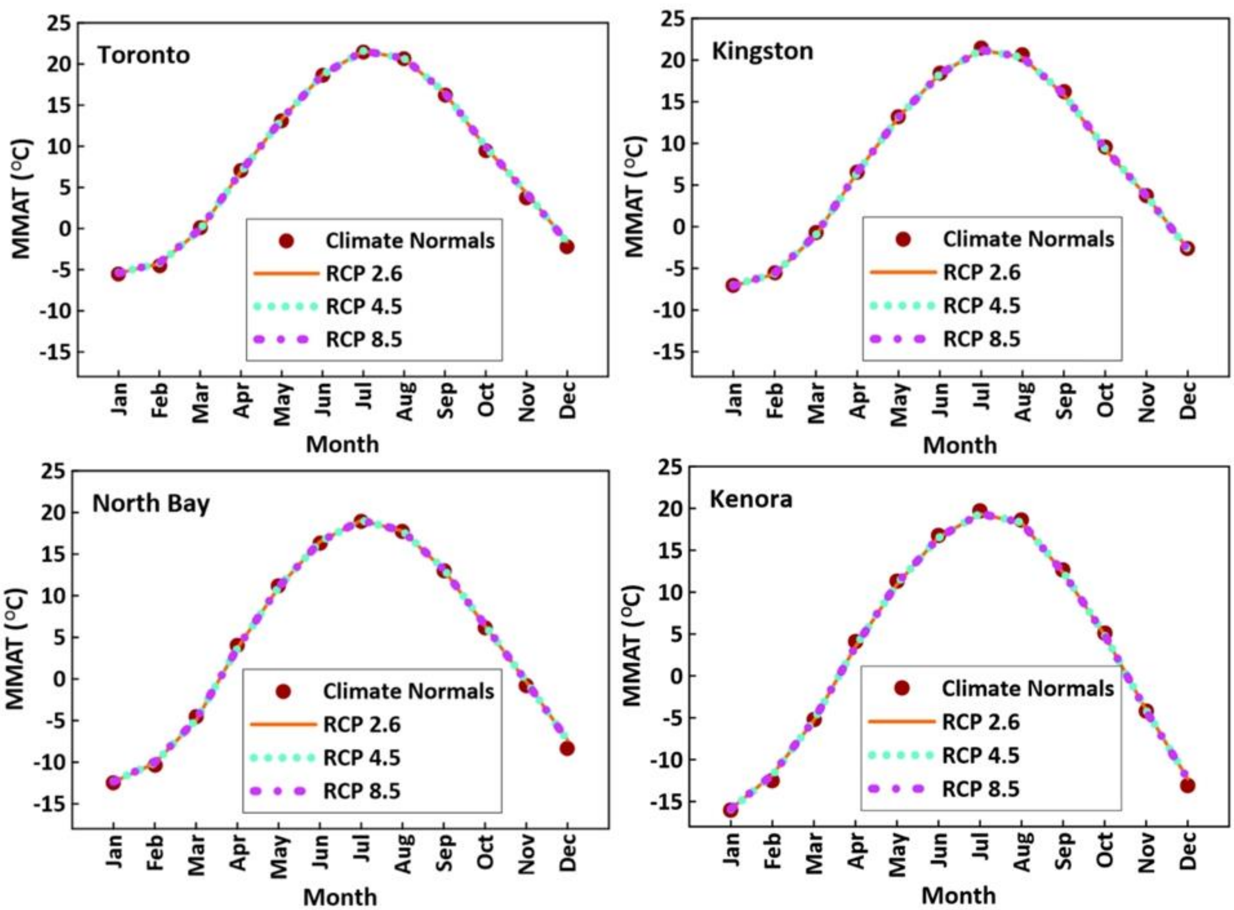

Figure 5.4 Comparison of Climate Normals and Mean Monthly Air Temperatures (MMAT) Under RCP 2.6, 4.5 and 8.5 for various Ontario cities for the period 1981-2010.

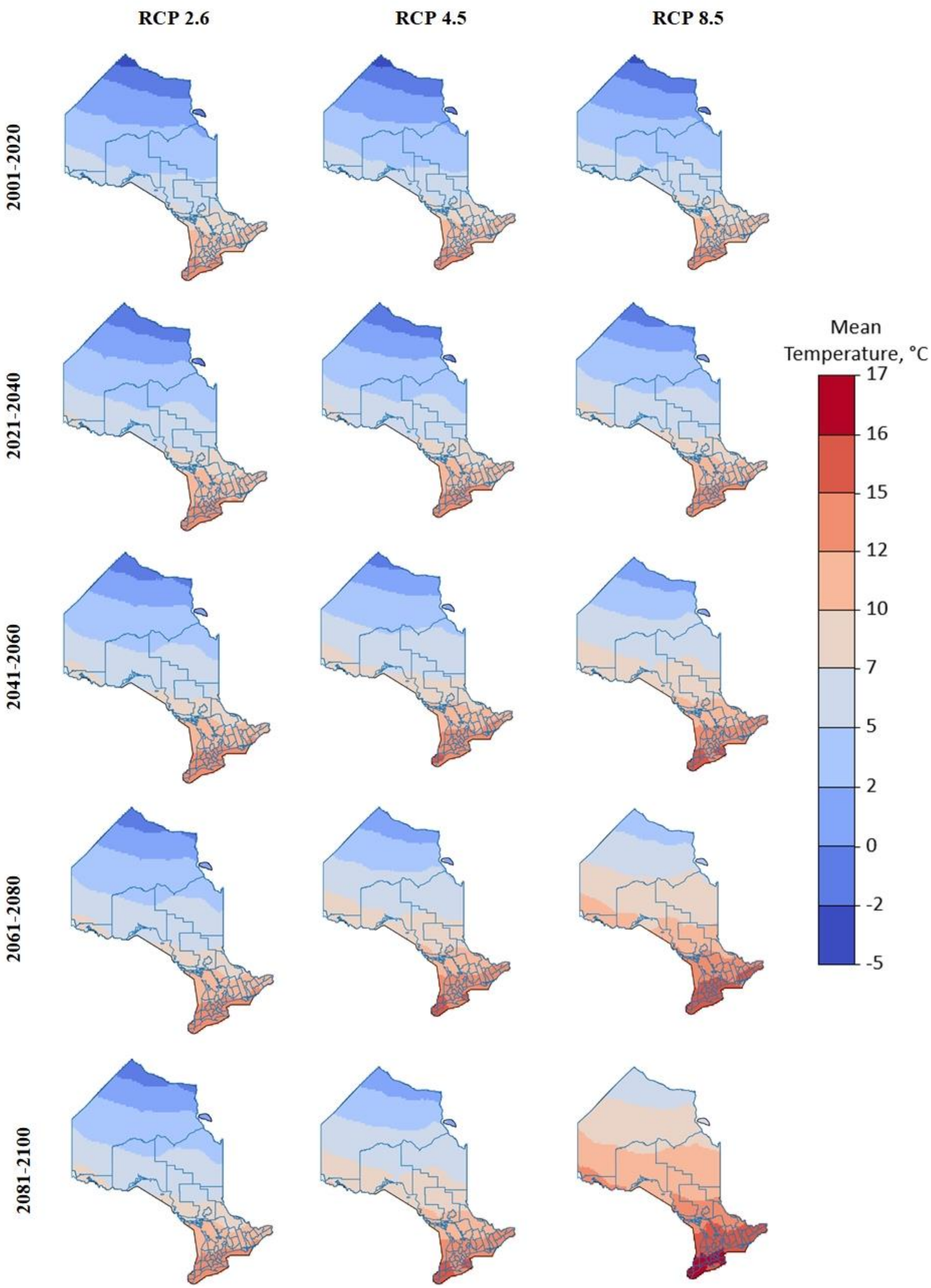

Figure 5.5 MAAT using average data from GCMs for baseline and future time periods for different RCPs, °C.

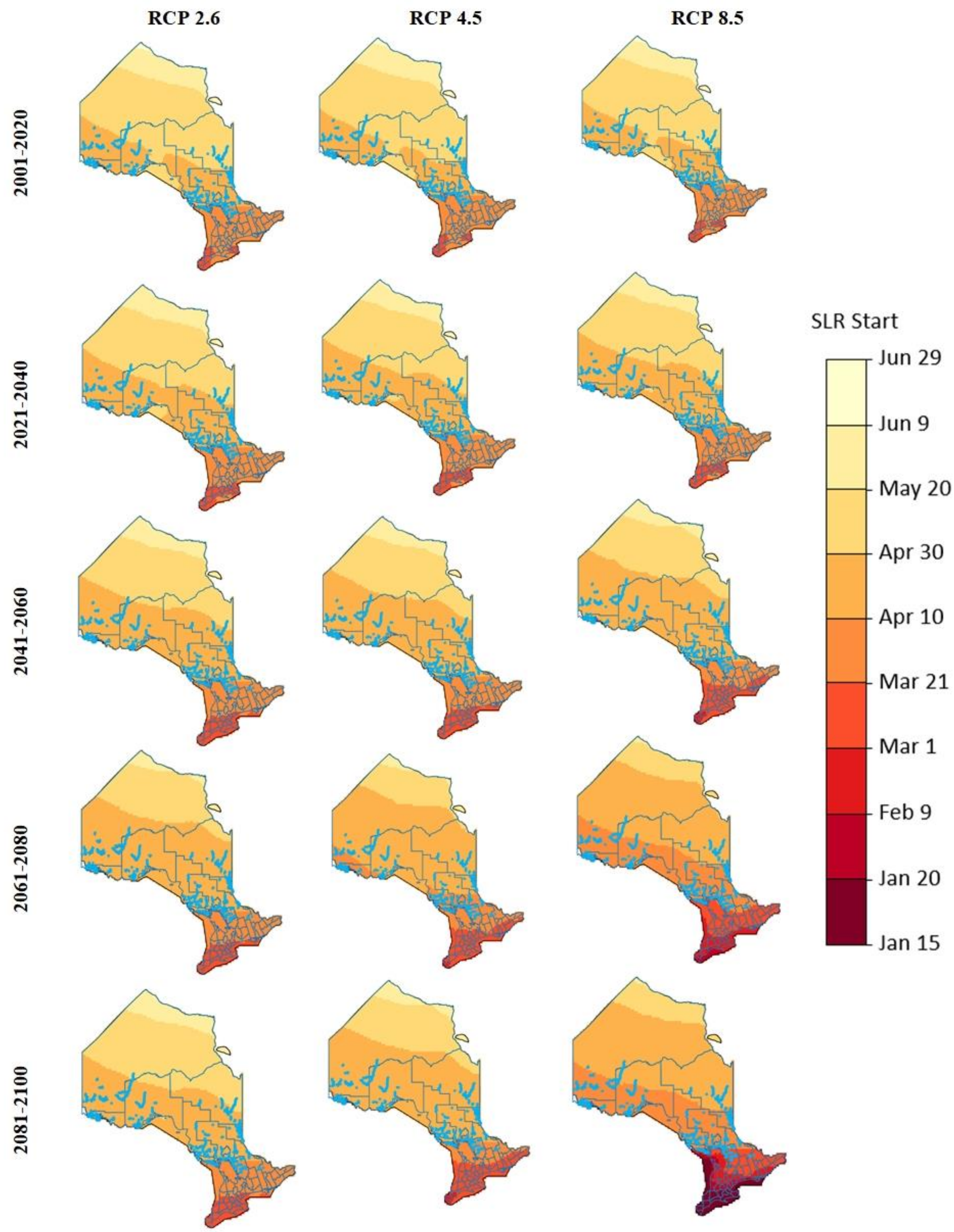

Figure 5.6 Prediction of SLR Start Dates using the Developed Models.

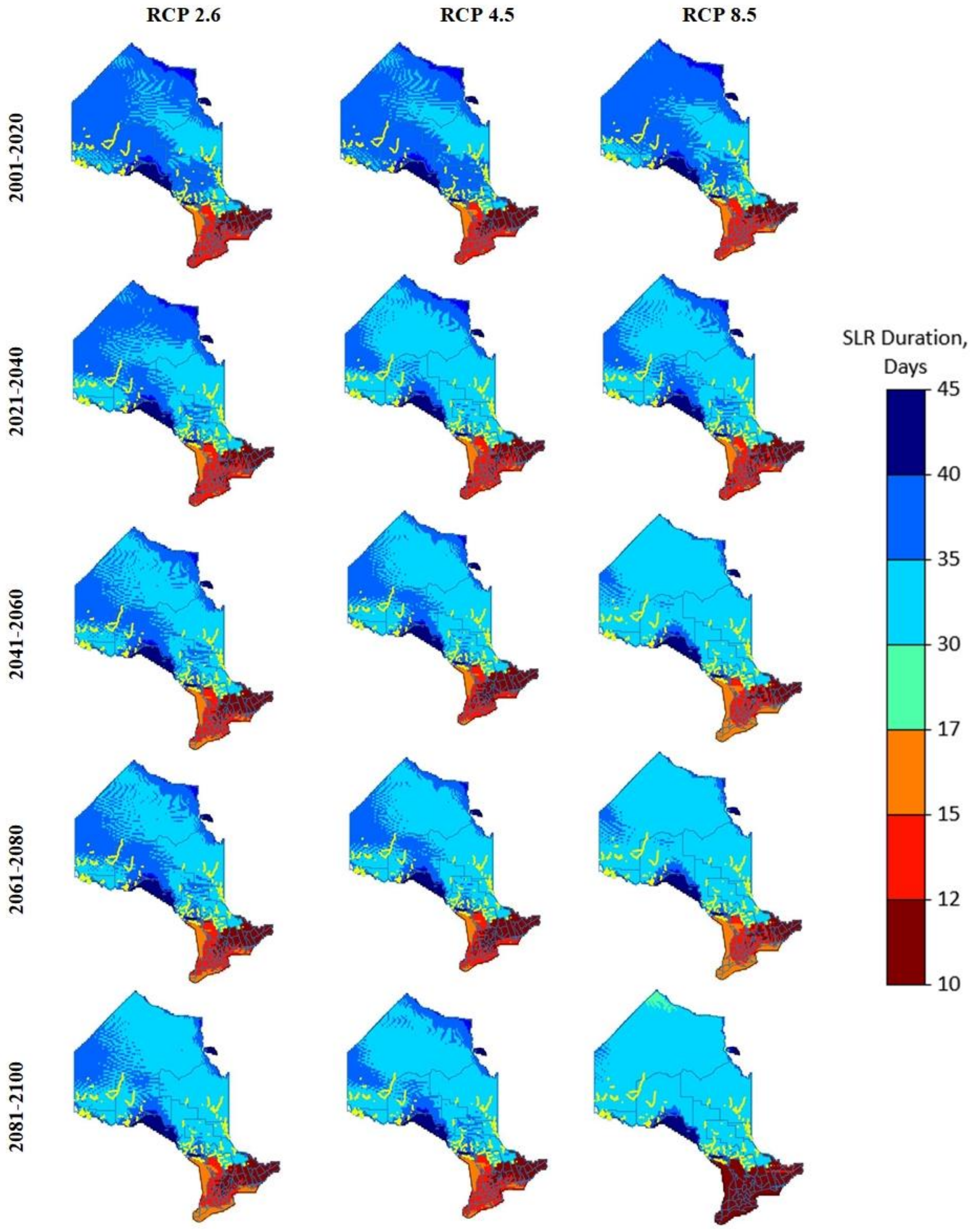

Figure 5.7 Duration in days, of the Predicted SLRs using the developed models.

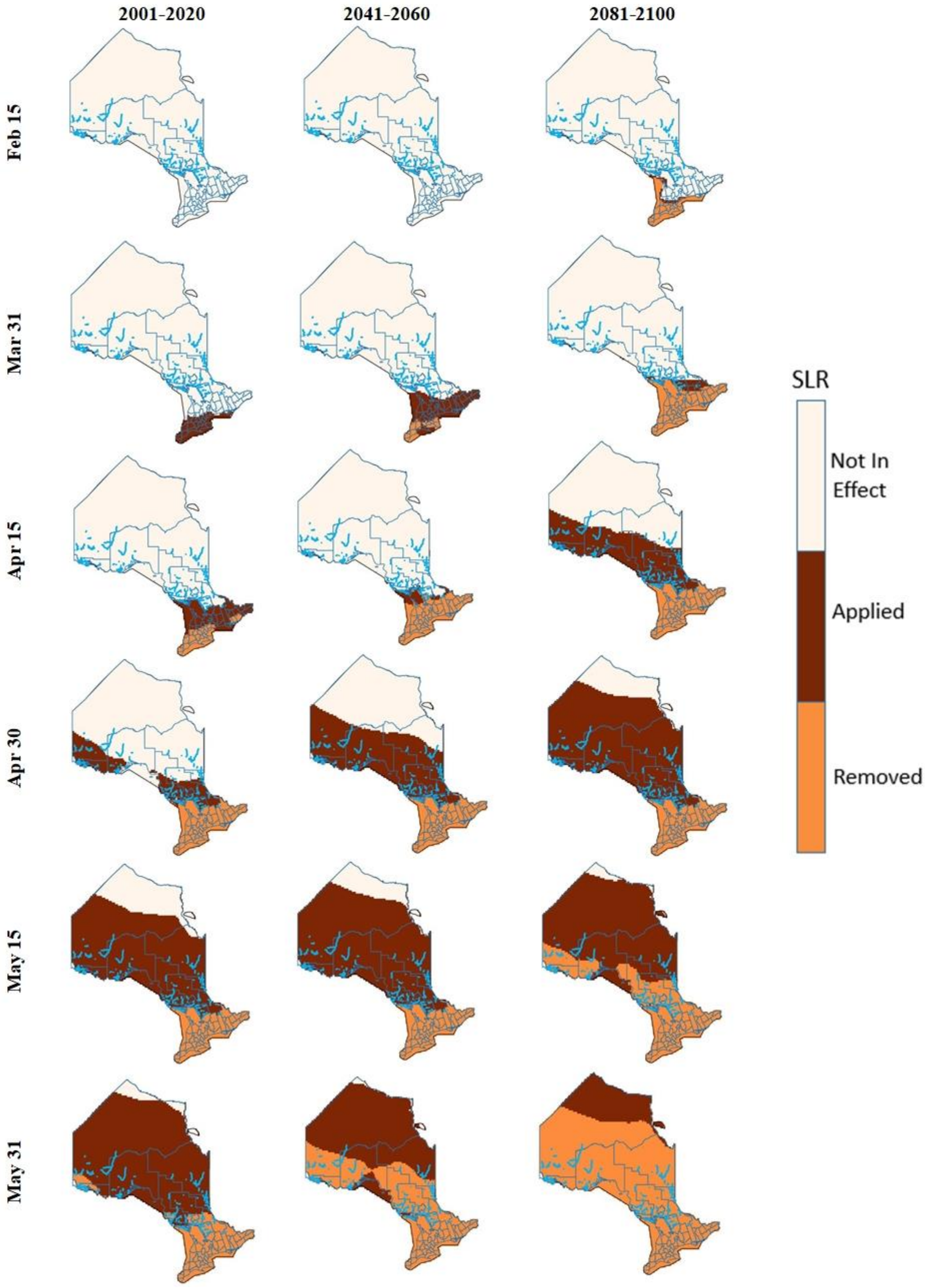

Figure 5.8 Locations requiring SLR to be in effect for the selected dates in a year using RCP 8.5

5.6. Discussion

To account for the climatic differences in Northern and Southern Ontario, two separate models are proposed in this study. As it can be seen in Figure 5.2, Figure 5.3 and Table 5.2, the predictions by the developed models are superior to other models reported in the literature. The findings also indicate that, for some locations, the developed models predicted higher and/or lower temperature values as compared to observations but in no instance, these predictions would have a detrimental effect on the pavements. It is expected that improvements to these models can be made as more surface data becomes available.

These developed models were used to predict SLR periods across Ontario as shown in Figure 5.7. while analyzing the results during model predictions, it was observed that some locations, particularly from the Southern Ontario, showed initial thawing period. The initial thawing period was considered when the thawing front reached a depth of slightly more than 45 cm, and after some days, went back to 0 cm. In the results, the initial thawing period was ignored and only the continuous thawing period was considered. The continuous thawing period was considered when the thawing front, after reaching 45 cm depth, went all the way to 165 cm.

From the results presented in Figure 5.7, a rather abrupt transition between northern and southern portions of the province can be observed. One of the reasons for this abrupt transition is the fact that none of the SLA stations are located close to the boundary between the regions. Additionally, SLA stations are better equipped to measure subsurface variables to greater depth. This transition can be improved by considering some of the RWIS stations in the northern region as more data becomes available.

5.7. Summary and Conclusions

The effects of climate change on SLR periods in Ontario, Canada, were investigated in this study. To determine the start and end dates for the SLR, network level regression models were developed. Climate variables, as well as soil surface and subsurface temperatures, were used in the model development. The climatic data used for model development and validation were obtained from selected SLA and RWIS stations located across Ontario, Canada. A comparison of the models generated as part of the research with those currently used or proposed in the literature indicates a superior performance.

To quantify the impact of climate change on SLR durations, climatic data for the baseline (2001 to 2020) and future, short-term (2021 to 2040), mid-century (2041 to 2060), third quarter (2061 to 2080) and end-century (2081 to 2100), were compiled by averaging daily temperature data from 19 different GCMs for three different RCPs (2.6, 4.5, and 8.5). Detailed review of this data indicates that the mean annual air temperatures are expected to increase throughout the century It is anticipated that, under the RCP 8.5, Northern and Southern parts of the province will see an increase in MAAT of 4-7 and 8-12°C respectively by the end of the century.

The research also led to the conclusion that, as air temperatures are likely to rise, surface temperatures would also rise, posing issues for the province in terms of implementing SLRs i.e., early start dates and shorter periods. The early SLR start dates require one to be cautious in starting them early, otherwise the consequences would be in terms of pavement damage and loss. Whereas shorter SLR periods, if not taken into consideration, results in increased cost, delays in transportation and increase in use of fuels. The findings of this study imply that, depending on the emission scenario, the SLR start dates and durations may alter in the future. The results suggest the optimum SLR start date to fall earlier in the future as compared to the baseline period. It can be concluded that a considerable number of locations across the province, under RCP 2.6 and 4.5, may need up to a 20-day shift in their SLR start dates by the end of the century. Moreover, under RCP 8.5, this change in SLR start dates may be required by all the locations by the year 2100. The results lead one to conclude that, under the worst-case emission scenario by the year 2100, almost all the locations, where MTO or other authorities apply SLR, may need the restrictions to start by the mid of April. The results of this study also lead one to conclude that the Northern regions may require more changes in the SLR periods than the Southern regions. It can be expected that, with the toughest climate change strategies as those outlined for RCP 2.6, towards the end of the century, the province may be divided into three parts on the basis of the SLR periods. These parts may require a 10 to 15, 30 to 35 and 35 to 40 days long SLR period. Furthermore, these results suggest that most of the regions in Northern Ontario may need a 5 to 10 days shorter SLR periods by the year 2100 as compared to the baseline period. Whereas a few regions in Southern Ontario are also expected to have different SLR start dates and periods. The predictions under the intermediate emission scenario, RCP 4.5, indicate that the regions with 30 to 35 days of SLRs may increase in number thus limiting the regions with 35 to 40 days of SLRs. The results of the study also suggest that for emission scenario RCP 8.5, most of the regions with the 35 to 40 days long SLR periods may require a shorter SLR period by the end-century thus leaving almost whole of the province with two regions in terms of SLRs i.e., 30 to 35 days and 10 to 15 days.

The models developed in this study were generated and tested using the climatic data obtained from selected stations located in Ontario and therefore, the adequacy of these models should be evaluated for other locations using site specific measured data. Also, these models were developed and tested using climatic, surface and sub surface data from no permafrost locations and are therefore limited to no permafrost locations of the province. These models can be further improved as more data becomes available. The addition of data from additional stations and/or removing data from existing ones, which were used in the model development, may cause an impact on the latitude and constant terms thus making it a limitation of this model. For the Southern model, the sign for all model parameters remains constant with an additional or removal of a station, however, for the Northern model, the constant and latitude signs reverse since those terms are close to zero. This may also impact the accuracy of this model and should be investigated in future studies.

6. Summary, Conclusions and Recommendations for future research

The purpose of this research effort was to study the effects of climate change on pavements in the province of Ontario. More specifically, this study quantifies the effect of rising temperatures on the selection of asphalt PG and changes in the SLR periods in the future.

To address quantification of the effects of rising temperature, regression models were developed and applied to asphalt PG and SLR application periods in a three staged process in this study. The first section involves compilation and analysis of historic and future climate data for the period 1981 to 2100 from 19 different GCMs and 3 RCPs. In order to determine the accuracy of temperature data estimated by the GCMs for different climate change scenarios or RCPs, the historical climate data normals for the period 1981-2010 were collected from the Environment and Climate Change Canada portal. Furthermore, this section also involves the compilation and analysis of climate, surface and subsurface temperature data from selected RWIS and SLA stations. Section two highlights the effects of climate change on asphalt PG selection across the province. For this quantification, new regression models, to predict pavement surface temperatures, were developed using air temperatures and latitude of a site. These models were developed to determine the relationships between asphalt pavement surface temperature and ambient weather data collected from RWIS stations, in section one. The developed models were used to predict the pavement temperatures for future climate data compiled in section one, and the results were compared with that of the latest LTPP models. Whereas the third section of this study talks about the implications of climate change on SLR periods across Ontario by the end century. For this, network level regression models were developed which correlate the surface CTI and thawing depth of a site. These models were developed by utilizing atmospheric, surface, and sub-surface data collected from different SLA and RWIS stations located at various locations across

Ontario, Canada. The developed models were then utilized to predict the SLR periods for future time scenarios using the future climate data compiled in section one. The performance of this model was evaluated by comparing the model's generated results with those commonly used or proposed in the literature. The results suggested a superior performance of the model developed in this study compared to those commonly used or proposed in the literature.

6.1. Conclusions

The examination of historical and projected temperature data showed that the climate in Ontario will change significantly in the future. For the whole province of Ontario, a rising trend in air temperature is expected in the future, with the mean annual air temperature (MAAT) projected to increase between 1.5 °C to 7.5 °C. The lower increase is projected for the strictest climate change policies (RCP 2.6) and the higher increase for no climate change policy (RCP 8.4). The data review also suggested that the locations in the Southern and Northwestern part of Ontario may experience a higher increase in the MAAT than the rest of the province. Furthermore, the locations near lakes may also experience a higher increase in the MAAT, as compared to the locations further away from lakes. This may be attributed to the lake effect. The results of this study lead one to conclude that, with the expected increase in air temperatures in the future, pavement temperatures would also increase. The results suggested that by the end of century for the best-case scenario (i.e., RCP 2.6), many Northern Ontario locations, and under the worst-case scenario (i.e., RCP 8.5), almost the whole province may have the maximum 7-day mean annual pavement temperatures increase by 5 °C. By the end century the mean annual minimum pavement temperatures may increase by a magnitude of up to 5 and 10 °C, under the RCP 2.6 and 8.5, respectively.

The existing LTPP models and the models developed as part of this study for determining pavement temperatures, were utilized to assess the impact of climate change on asphalt PG across

Ontario. The results suggest that the widely used pavement temperature models i.e., the LTPP models, predict higher values for average 7-day maximum pavement temperatures and lower values for minimum pavement temperatures for a considerable number of locations across Ontario. Based on the results of this study it can be concluded that by the end of the century, under the worst-case climate change scenario, i.e., RCP 8.5, the in practice current PG suggested for each the MTO zones may require at least one, and in some cases two, grade increases in their current high and low temperature PG. Furthermore, the results also suggested that the province can be divided into 4 instead of the current 3 zones on the basis of asphalt PG. The most suitable PG sets can potentially be 52-34, 58-28, 64-28 and 70-22 within the 4 new regions.

The study's findings suggested that SLR start dates and durations may change in the future, depending on the emission scenario. The results indicated that the optimal SLR start date may be sooner in the future than the baseline period. Many jurisdictions across Ontario use the prescheduled dates to apply and remove SLR period. The results of this study concluded that the changing climate would change the sub-surface thawing periods thus making this approach unreliable for determining the SLR periods in the future. This study also concludes that the expected rise in air temperatures will result in a rise in surface temperature indices thus making the SLR to start earlier and have a shorter duration. The early SLR start dates need to be considered by the relevant agencies as implications of not applying the SLR earlier could result in pavement damage and loss in strength. The shorter SLR durations, on the other hand, result in less costs for the trucking industry, if determined accurately. For emission scenarios RCP 2.6 and 4.5, it can be expected that a significant number of places across the province would require the SLR to start approximately 20 days earlier by the end of the century. Furthermore, for emission scenario RCP 8.5, all localities may have to revise the SLR start dates. The results imply that, in the worst-case emission scenario by the year 2100, virtually all places where MTO or other agencies impose a SLR period, the restrictions need to be in place by mid-April. The findings also showed that the northern regions may require greater SLR period adjustments than the southern regions. This study proposed network level models to predict pavement surface temperatures and SLR periods across Ontario. These models utilize only the air temperatures and latitudes to predict pavement surface temperatures and SLR periods. Furthermore, this study also quantified the impacts of climate change on asphalt PG and SLR periods across the province.

6.2. Contributions of the Research

The findings of this study provide valuable contributions that road agencies, municipalities and pavement engineers may use to modify the asphalt PG and SLR periods in response to the changing climatic conditions in the province of Ontario. Some of these contributions are as stated below:

- Researchers and practitioners attempting to quantify the influence of climate change on other projects and/or structures may find the prediction of changes in air and pavement temperatures of interest and value. This finding was published in the ASCE-ICTD conference paper, Basit et al., (2021).
- One of the novelties of this study is the development of network level models, specifically for Ontario. Specific models are developed for determining the asphalt PG and SLR periods, using only the air temperatures and latitudes of a location. These models perform better then models currently in use that may require site specific calibration. This finding was published in Basit et al., (2022) and Basit et al. (to be submitted to ASCE Journal of Cold Regions Engineering).
- Another contribution of this study is the development of the asphalt PG and SLR period maps for the province of Ontario, for changing climate. For this purpose, the PG maps were

generated using the LTPP models as well as the models developed in this study. The SLR period maps were created by utilizing only the developed models. These maps may help the pavement engineers, designers, road agencies and authorities to better understand how climate change may affect the selection of appropriate asphalt PG for the pavement design and the SLR period for the future. This finding was published in Basit et al., (2022) and Basit et al. (to be submitted to ASCE Journal of Cold Regions Engineering).

- This is one of the first studies that quantified the change in the SLR periods specifically for Ontario, by the end century. The results of this study highlighted how the approach of prescheduled dates, for the imposition and removal of SLR periods, may lead to inaccurate results due to changing climate in the future. The results of this study will be beneficial for different road authorities and municipalities in understanding the how climate change may affect the SLR periods across the province. This finding was published in Basit et al. (to be submitted to ASCE Journal of Cold Regions Engineering).

6.3. Recommendations for Future Research

The objectives of this study were to develop network level models for prediction of pavement temperature and SLR periods from ambient air temperature data and to predict the effect of climate change on asphalt PG selection and future SLR periods across Ontario, Canada. The findings of this study indicate that climate change may have an impact on the asphalt PG and SLR periods across the province. Based on the findings of this study, the following recommendations for further research are made:

- The current study utilized a few years of climatic, surface, and sub-surface data from a limited number of SLA and RWIS stations for the development of regression models. It is therefore recommended that the amount of data and the number of SLA and RWIS stations, considered for model development, should be increased in the future research to further improve the models.

- Since the models developed in this study were generated and tested using the climatic data obtained from selected stations located in Ontario, therefore these models are limited to Ontario, Canada. It is recommended that the area under consideration should be increased and incapsulate other provinces for future research.
- Air temperature is the most significant factor in determining pavement temperature. However, climatic factors such as precipitation, solar radiation and wind can also affect the surface temperature especially in the winter season. Precipitation and wind may tend to decrease the surface temperature whereas solar radiation may increase it. It is therefore recommended that a parameter may be added in the model which can address heat transfer between the environment and pavement due to precipitation, solar radiation, and wind. Furthermore, traffic volume greatly impacts the pavement temperatures, especially in the summer season, as it contributes to rutting in the pavement. It is recommended to develop a relation which can predict rut depth or rut damage by utilizing traffic volume and HMA stiffness. This rut damage can be added as a parameter in the surface temperature model. In this way the accuracy of models can be increased substantially.
- Current stations collect climatic data such as precipitation, wind speed etc. however, these stations do not record any solar radiation data such as solar irradiance and solar flux density. These stations may need solar radiation sensors or pyranometers to record this data.

- It is also recommended that the developed model, for determining SLR periods, should be calibrated and validated using the Falling Weight Deflectometer (FWD) or Light Weight Deflectometer (LWD) tests results in the future research to increase the model's capability.

It is believed that all the items which were recommended for future research may enhance the robustness and capability of developed models. In this way the limitations of these developed models may be minimized, and predictions can be made more accurate.

Bibliography

- Baïz S, Tighe SL, Haas CT, Mills B, Perchanok M. Development of Frost and Thaw Depth Predictors for Decision Making about Variable Load Restrictions. Transportation Research Record. 2008;2053(1):1-8. doi:10.3141/2053-01
- Basit, A., Shafiee, M., Bashir, R., & Perras, M. A. (2021). Climate Change Implications for Asphalt Binder Selection in Pavement Construction across Ontario. In International Conference on Transportation and Development 2021 (pp. 289-301).
- Basit, A., Shafiee, M., Bashir, R., & Perras, M. A. (2022). Climate Change and Asphalt Binder Selection across Ontario: A Quantitative Analysis Towards the End of the Century. Construction and Building Materials.
- Basit, A., Shafiee, M., Bashir, R., & Perras, M. A. (2022). Evaluating the Effects of Climate Change on Spring Load Restrictions Across Ontario. To be submitted to ASCE Journal of Cold Regions and Engineering.
- Barros, V.R., C.B. Field, D.J. Dokken, M.D. Mastrandrea, K.J. Mach, T.E. Bilir, M. Chatterjee, K.L. Ebi, Y.O. Estrada, R.C. Genova, B. Girma, E.S. Kissel, A.N. Levy, S. MacCracken, P.R. Mastrandrea, and L.L. White (eds.), IPCC, 2014: Climate Change 2014: Impacts, Adaptation, and Vulnerability. Part B: Regional Aspects. Contribution of Working Group II to the Fifth Assessment Report of the Intergovernmental Panel on Climate Change. Cambridge University Press, Cambridge, United Kingdom and New York, NY, USA, 688 pp.
- Batenipour, H., Kurz, D., Alfaro, M., Graham, J., & Ng, T. N. S. (2009). Highway embankment on degrading permafrost. In Cold Regions Engineering 2009: Cold Regions Impacts on Research, Design, and Construction (pp. 512-521).

- Bernstein, B.C., Wolff, J.K., Myers, W., Verification of the road weather forecasts system run during the 2003 demonstration at the Iowa Department of Transportation, Sixth Annual symposium on Snow Removal and Ice Control Technology, Transportation Research Board, Spokane, WA, 109-126, 2004.
- Bradley, A.H., M.A Ahammed, S. Hilderman, and S. Kass. 2012. Responding to Climate Change with Rational Approaches for Managing Seasonal Weight Programs in Manitoba. Proceedings of the American Society of Civil Engineers, 15th International Conference on Cold Regions Engineering. August 19–22, Quebec City, Quebec, Canada
- Brian N Mills, Susan L Tighe, Jean Andrey, James T Smith, Ken Huen. 2009. Climate change implications for flexible pavement design and performance in southern Canada. Journal of Transportation Engineering, Volume 135, Issue 10, pp: 773-782. DOI: 10.1061/(ASCE)0733-947X(2009)135:10(773)
- Buchanan, F. and Gwartz, S.E., Road Weather Information Systems at the Ministry of Transportation Ontario, Annual Conference of the Transportation Association of Canada, Calgary, Alberta, 2005.
- Bush, E. and Lemmen, D.S., editors (2019): Canada's Changing Climate Report; Government of Canada, Ottawa, ON. 444 p.
- C. Plati, (2019), Sustainability factors in pavement materials, design, and preservation strategies: A literature review, Construction and Building Materials 211, 539-555, https://doi.org/10.1016/j.conbuildmat.2019.03.242
- Cascione, A., (2018). The future of asphalt binder specification, a presentation. Minnesota Department of Transportation. http://mndot.org/mnroad/nrra/pavement-workshop/archive/2018/2018-cascione-future-of-binder-testing.pptx

- Chapin, J., J. Pernia, and B. Kjartanson. 2013. Optimization of Seasonal Frost-Thaw Depth and Pavement Strength Predictions on Low Volume Highways in Ontario. Phase 1 Report. HIIFP-099. Ministry of Transportation Ontario (MTO), St. Catherines, Ontario, Canada.
- Chen, X., Wang, H., Horton, R., DeFlorio, J., 2021. Life-cycle assessment of climate change impact on time-dependent carbon-footprint of asphalt pavement. Transp. Res. Part D Transp. Environ. 91, 102697. https://doi.org/10.1016/j.trd.2021.102697.
- Clark, B., York, R. Carbon metabolism: Global capitalism, climate change, and the biospheric rift. Theor Soc 34, 391–428 (2005). https://doi.org/10.1007/s11186-005-1993-4
- Dash, S.K., Jenamani, R.K., Kalsi, S.R. et al. Some evidence of climate change in twentieth-century India. Climatic Change 85, 299–321 (2007). https://doi.org/10.1007/s10584-007-9305-9
- Delgadillo, Rodrigo & Arteaga, Leandro & Wahr, Carlos & Alcafuz, Ricardo. (2018), The influence of climate change in Superpave binder selection for Chile. Road Materials and Pavement Design, 21, pp. 607-622, DOI: 10.1080/14680629.2018.1509803.
- Doré, G., and Zubeck, H. (2008). “Cold Regions Pavement Engineering”. ASCE Publications.
- Doré, G., Drouin, P., Pierre, P., and Desrochers, P. (2005). “Estimation of the relationships of road deterioration to traffic and weather in Canada.” Transport Canada, Ottawa.
- Environment and Climate Change Canada. 2018. Historical Climate Data - Environment and Climate Change Canada. https://climate.weather.gc.ca/historical_data/search_historic_data_e.html. (Last accessed: Jun 2021).

- Erik Simonsen, Vincent C. Janoo, Ulf Isacsson. 1997. Prediction of Pavement Response during Freezing and Thawing Using Finite Element Approach. Journal of Cold Regions Engineering, pp: 308-324, Vol 11, issue 4. doi:10.1061/(ASCE)0887-381X(1997)11:4(308)
- Financial Accountability Office of Ontario, (2019). "Provincial highways capital asset inventory". https://www.fao-on.org/en/Blog/Publications/expenditure-estimates-transportation-2019#_ftnref13. (Last accessed: Nov 2021).
- Fletcher, C. G., Matthews, L., Andrey, J., & Saunders, A. (2016). Projected Changes in Mid-Twenty-First-Century Extreme Maximum Pavement Temperature in Canada, Journal of Applied Meteorology and Climatology, 55(4), 961-974. DOI: https://doi.org/10.1175/JAMC-D-15-0232.1
- Francesco Viola, Clara Celauro, Effect of climate change on asphalt binder selection for road construction in Italy, Transportation Research Part D: Transport and Environment, Volume 37, 2015, Pages 40-47, ISSN 1361-9209, https://doi.org/10.1016/j.trd.2015.04.012.
- Frederik Meleux, Fabien Solmon, Filippo Giorgi. Increase in summer European Ozone amounts due to climate change. Atmospheric environment, Elsevier, 2007, 41 (35), pp.7577-7587. ff10.1016/j.atmosenv.2007.05.048. hal-00342309f
- G.D. Airey (2003) State of the Art Report on Ageing Test Methods for Bituminous Pavement Materials, International Journal of Pavement Engineering, 4:3, 165-176, DOI: 10.1080/1029843042000198568
- Giddens, A. (2009). Politics of climate change. Polity.

- Goodman, S., Eng, M., Eng, P., Bekheet, W., Hassan, Y., & Abd El Halim, A. O. (2002, May). Rapid in-situ shear testing of asphalt pavements for runway construction quality control and assurance. In Proceedings 2002 FAA airport technology transfer conference. USA: Atlantic City.
- Gough, W. A.; Anderson, V.; and Herod, K. Ontario Climate Change and Health Modelling Study: Report. Technical Report Ministry of Health and Long-Term Care Public Health Policy and Programs Branch, August 2016. bibtex\ p̌hantom\ doi: 10.13140/RG.2.2.35542.96327 p̌hantom\\
- Government of Canada, Statistics, 2016, Gross domestic product, expenditure-based, provincial, and territorial, annual, https://www150.statcan.gc.ca/t1/tbl1/en/cv.action?pid=3610022201. (Last accessed: Dec 2021).
- Government of Canada, Statistics. (2018) "Canada's core public infrastructure survey: Roads, Bridges and Tunnels". https://www150.statcan.gc.ca/n1/en/daily-quotidien/201026/dq201026a-eng.pdf?st=vNarm8PN. (Last accessed: Nov 2021).
- Gundla A, Salim R, Shane Underwood B, Kaloush KE. Implementation of the AASHTO M 332 Specification: A Case Study. Transportation Research Record. (2020);2674(9):959-971. doi:10.1177/0361198120933266
- Haas, R. (ed.) 1997. Pavement Design and Management Guide. Transportation Association of Canada, Ottawa, ON.
- Haas, R., L.C. Falls, D. MaxLeod and S. Tighe. 2004. Climate impacts and adaptions on roads in Northern Canada, Cold Climates Conference, Regina, AB. 18 pp.

- Hartmann, D. L., Tank, A. M. K., Rusticucci, M., Alexander, L. V., Brönnimann, S., Charabi, Y. A. R., ... & Zhai, P. (2013). Observations: atmosphere and surface. In Climate change 2013 the physical science basis: Working group I contribution to the fifth assessment report of the intergovernmental panel on climate change (pp. 159-254). Cambridge University Press.
- Hoyoung Jeong; Hongjo Kim; Kyeongseok Kim; and Hyoungkwan Kim, (2017). “Prediction of Flexible Pavement Deterioration in Relation to Climate Change Using Fuzzy Logic”. Journal of Infrastructure Systems 23(4):04017008 DOI: 10.1061/(ASCE)IS.1943-555X.0000363
- Huang, Y.H. Pavement Analysis and Design. Second Edition, Englewood Cliffs, NJ: Prentice Hall, 2003.
- Hughes, L. (2003), Climate change and Australia: Trends, projections and impacts. Austral Ecology, 28: 423-443. https://doi.org/10.1046/j.1442-9993.2003.01300.x
- Jacobs, J. M., Culp, M., Cattaneo, L., Chinowsky, P., Choate, A., DesRoches, S., Douglass, S., & Miller, R. (2018). Transportation. In D. R. Reidmiller, C. W. Avery, D. R. Easterling, K. E. Kunkel, K. L. M. Lewis, T. K. Maycock, & B. C. Stewart (Eds.), Impacts, risks, and adaptation in the United States: Fourth national climate assessment (Vol. II, pp. 479–511). U.S. Government Publishing Office. https://doi.org/10.7930/NCA4.2018.CH12.
- Janoo, V.C. “Performance of Base/Subbase Materials under Frost Action” Proceeding of the Eleventh International Conference on Cold Regions Engineering, American Society of Civil Engineers, Anchorage, Alaska, 2002, pp. 878–889.
- Katharine Hayhoe, Mark Robson, John Rogula, Maximilian Auffhammer, Norman Miller, Jeff VanDorn, Donald Wuebbles, An integrated framework for quantifying and valuing

climate change impacts on urban energy and infrastructure: A Chicago case study, Journal of Great Lakes Research, Volume 36, Supplement 2, 2010, Pages 94-105, ISSN 0380-1330, https://doi.org/10.1016/j.jglr.2010.03.011.

- Katie E. Haslett, Jayne F. Knott, Anne M. K. Stoner, Jo E. Sias, Eshan V. Dave, Jennifer M. Jacobs, Weiwei Mo & Katharine Hayhoe (2021) Climate change impacts on flexible pavement design and rehabilitation practices, Road Materials and Pavement Design, 22:9, 2098-2112, DOI: 10.1080/14680629.2021.1880468
- L.A. Vincent, X. Zhang, É. Mekis, H. Wan & E.J. Bush, (2018) Changes in Canada's Climate: Trends in Indices Based on Daily Temperature and Precipitation Data, Atmosphere-Ocean, 56:5, 332-349, DOI: 10.1080/07055900.2018.1514579
- Lekarp, F., Isacsson, U., & Dawson, A. (2000). State of the art I: Resilient response of unbound aggregates. ASCE Journal of Transportation Engineering, 126(1), 76–83.
- Lucie A. Vincent & Éva Mekis (2006) Changes in Daily and Extreme Temperature and Precipitation Indices for Canada over the Twentieth Century, Atmosphere-Ocean, 44:2, 177-193, DOI: 10.3137/ao.440205
- M. Solaimanian and P. Bolzan, 1993, "Analysis of the Integrated Model of Climatic Effects on Pavements: Sensitivity Analysis and Pavement Temperature Prediction", SHRP-A-637.
- Mahoney, J., M. Rutherford, and R. G. Hicks. 1986. Guidelines for Spring Highway Use Restrictions. Report No. WA-RD-80.2, Washington State Department of Transportation, Olympia, WA.
- McGennis R.B., R.M. Anderson, T.W. Kennedy, M. Solaimanian, Background of SUPERPAVE Asphalt Mixture Design and Analysis, 1995, United States. Federal

Highway Administration. Office of Technology Applications, FHWA-SA-95-003, https://rosap.ntl.bts.gov/view/dot/42577.

- Meinshausen, M., Smith, S.J., Calvin, K. et al. The RCP greenhouse gas concentrations and their extensions from 1765 to 2300. Climatic Change 109, 213 (2011). https://doi.org/10.1007/s10584-011-0156-z.
- Miller, H., Kestler, M., Berg, R., Cabral, C., (2014). Demonstration and Inter-Comparison of Seasonal Weight Restriction Models - Phase I. USDA Forest Service, Aurora Project 2012-05 https://intrans.iastate.edu/app/uploads/2019/01/seasonal_weight_restriction_models_w_cvr.pdf.
- Mills, B., S. Tighe, J. Andrey, J. Smith, S. Parm, and K. Huen. 2007. Road well-traveled: Implications of climate change for pavement infrastructure in southern Canada. Ottawa, ON: Environment Canada, Adaptation and Impacts Research Division.
- Ming-ko Woo. 1990. Consequences of Climatic Change for Hydrology in Permafrost Zones. Journal of Cold Regions Engineering, P 15-20, doi:10.1061/(ASCE)0887-381X(1990)4:1(15)
- MnDOT. 2014. Process for Seasonal Load Limit Starting and Ending Dates. Engineering Services Division Technical Memorandum No. 14-10-MAT-02. Minnesota Department of Transportation, St. Paul, MN.
- Mohseni, A., 1998, LTPP Seasonal Asphalt Concrete (AC) Pavement Temperature Models, FHWA-RD-97-103. Vol. 7, https://www.fhwa.dot.gov/publications/research/infrastructure/pavements/ltpp/97103/

- Mohseni, A.,Carpenter, S. H., and D'Angelo, J., 2005, Development of Superpave High-Temperature Performance Grade (PG) Based on Rutting Damage (With Discussion and Closure), Journal of the Association of Asphalt Paving Technologists, 74 (1), pp. 197-254.
- Ness, Ryan, Dylan G. Clark, Julien Bourque, Dena Coffman, and Dale Beugin. 2021. Under Water: The Costs of Climate Change for Canada's Infrastructure. Canadian Institute for Climate Choices. Ottawa, ON.
- News Staff, 2012: Toronto heat reaches record high 34.4C on Thursday. 680News, https://toronto.citynews.ca/2012/07/04/toronto-breaks-long-standing-heat-record (Last accessed: Dec 2021)
- Ningyuan, L., Kazmierowski, T., Lane, B. (2006), "Long-Term Monitoring of Low-Volume Road Performance in Ontario", 2006 Annual Conference of the Transportation Association of Canada, Charlottetown, Prince Edward Island
- OCDP. 2018. OCDP - Ontario Climate Change Data Portal. Available from http://www.ontarioccdp.ca/. (Last accessed: Jun 2021).
- Omran Maadani, Mohammad Shafiee, Igor Egorov. 2021. Climate Change Challenges for Flexible Pavement in Canada: An Overview. Journal of Cold Regions Engineering, P 03121002, Ver 35, issue 4. doi:10.1061/(ASCE)CR.1943-5495.0000262
- Padmini P. Gudipudi, B. Shane Underwood, Ali Zalghout, (2017), Impact of climate change on pavement structural performance in the United States, Transportation Research Part D: Transport and Environment, Volume 57, Pages 172-184, ISSN 1361-9209, https://doi.org/10.1016/j.trd.2017.09.022.

- Pernia, J., R. Timoon, and S. Esmeailazad. 2014. Seasonal Load Adjustments in Northern Ontario. Phase 2 Draft Report. Provided by Max Perchanok, Ministry of Transportation Ontario (MTO), Canada.
- Robertson, W.D., 1995, “Using the SHRP Specification to Select Asphalt Binders for Low Temperature Service”, Proceedings of The Fortieth Annual Conference of The Canadian Technical Asphalt Association, Charlottetown, P.E.I., Transportation Research Board, pp. 170-195.
- Salour, Farhad & Erlingsson, Sigurdur. (2013). Investigation of a pavement structural behaviour during spring thaw using falling weight deflectometer. Road Materials and Pavement Design. 14. 141-158. 10.1080/14680629.2012.754600.
- SAS Institute Inc. 2013. SAS/IML® 9.4 User’s Guide. Cary, NC: SAS Institute Inc.
- Schweikert A, Chinowsky P, Espinet X, Tarbert M, Climate Change and Infrastructure Impacts: Comparing the Impact on Roads in ten Countries through 2100, Procedia Engineering, Volume 78, 2014, Pages 306-316, ISSN 1877-7058, https://doi.org/10.1016/j.proeng.2014.07.072.
- Shafiee, M., Maadani, O., & Egorov, I. (2021). Climate Change Challenges for Flexible Pavement in Canada: An Overview. Journal of Cold Regions Engineering, 35(4), 03121002.
- Shi Dong, Jian Zhong, Peiwen Hao, Wenjin Zhang, Jun Chen, Yong Lei, Adam Schneider, (2018), Mining multiple association rules in LTPP database: An analysis of asphalt pavement thermal cracking distress, Construction and Building Materials, Volume 191, Pages 837-852, ISSN 0950-0618, https://doi.org/10.1016/j.conbuildmat.2018.09.162.

- Stocker, T.F., D. Qin, G.-K. Plattner, M. Tignor, S.K. Allen, J. Boschung, A. Nauels, Y. Xia, V. Bex and P.M. Midgley (eds.), IPCC, 2013: Climate Change 2013: The Physical Science Basis. Contribution of Working Group I to the Fifth Assessment Report of the Intergovernmental Panel on Climate Change. Cambridge University Press, Cambridge, United Kingdom and New York, NY, USA, 1535 pp.
- Stoner, A., Daniel, J., Jacobs, J., Hayhoe, K., & Scott-Fleming, I. (2019). Quantifying the impact of climate change on flexible pavement performance and lifetime in the United States. Transportation Research Record: Journal of the Transportation Research Board, 2673(1), 110–122. https://doi.org/10.1177/0361198118821877.
- Surya T. Swarna, Kamal Hossain, (2020), Changes in Asphalt Binder Grade Due to Climate Change in Canada, TAC Conference & Exhibition. https://www.tac-atc.ca/sites/default/files/conf_papers/swarnasuryateja-changes_in_asphalt_binder_grade_due_to_climate_change.pdf
- Swarna ST, Hossain K, Pandya H, Mehta YA. Assessing Climate Change Impact on Asphalt Binder Grade Selection and its Implications. Transportation Research Record. 2021;2675(10):786-799. doi:10.1177/03611981211013026
- Transportation Association of Canada, TAC (1997), "Pavement Design and Management Guide", Ottawa, Ontario
- The ABCs of PGAC, Issue 2.0, 1999, http://www.onasphalt.org/files/Publications/ABCs%20of%20PGAC.pdf. (Last accessed: Dec 2021).

- Underwood, B. S., Guido, Z., Gudipudi, P., and Feinberg, Y., Increased costs to US pavement infrastructure from future temperature rise, Nature Climate Change, vol. 7, no. 10, pp. 704–707, 2017. doi:10.1038/nclimate3390.
- Van Deusen, D., C. Schrader, D. Bullock, and B. Worel. 1998. Springtime Thaw Weakening and Load Restrictions in Minnesota. Paper No. 98-0621. Transportation Research Record: Journal of the Transportation Research Board, No. 1615, pp. 21–28.
- Vincent, L. A., X. L. Wang, E. J. Milewska, H. Wan, F. Yang, and V. Swail (2012), A second generation ofhomogenized Canadian monthly surface air temperature for climate trend analysis,J. Geophys. Res.,117, D18110, DOI:10.1029/2012JD017859.
- Watson, D. K., and Rajapakse, R. (2000). "Seasonal variation in material properties of a flexible pavement." Can. J. Civ. Eng., 27(1), 44–54.
- World Meteorological Organization (WMO) Report (2020). https://public.wmo.int/en/our-mandate/climate/wmo-statement-state-of-global-climate
- Xuebin Zhang, Lucie A. Vincent, W.D. Hogg & Ain Niitsoo (2000) Temperature and precipitation trends in Canada during the 20th century, Atmosphere-Ocean, 38:3, 395-429, DOI: 10.1080/07055900.2000.9649654
- Y. Li et al., Temperature predictions for asphalt pavement with thick asphalt layer, Constr. Build. Mater, (2018), https://doi.org/10.1016/j.conbuildmat.2017.12.145
- Yaning Qiao, Andrew R. Dawson, Tony Parry, Gerardo W. Flintsch, (2015), Evaluating the effects of climate change on road maintenance intervention strategies and Life-Cycle Costs, Transportation Research Part D: Transport and Environment, Volume 41, Pages 492-503, ISSN 1361-9209, https://doi.org/10.1016/j.trd.2015.09.019.

- Yi Li, Liping Liu, Feipeng Xiao, Lijun Sun, (2017), Effective temperature for predicting permanent deformation of asphalt pavement, Construction and Building Materials, Volume 156, Pages 871-879, ISSN 0950-0618, https://doi.org/10.1016/j.conbuildmat.2017.08.118.
- Zhiqi Sun, Huining Xu, Yiqiu Tan, Huijie Lv, Ogoubi Cyriaque Assogba, (2019), Low-temperature performance of asphalt mixture based on statistical analysis of winter temperature extremes: A case study of Harbin China, Construction and Building Materials, Volume 208, Pages 258-268, ISSN 0950-0618, https://doi.org/10.1016/j.conbuildmat.2019.02.131.

Appendices

Appendix A: Temperature Profiles for SLA Stations

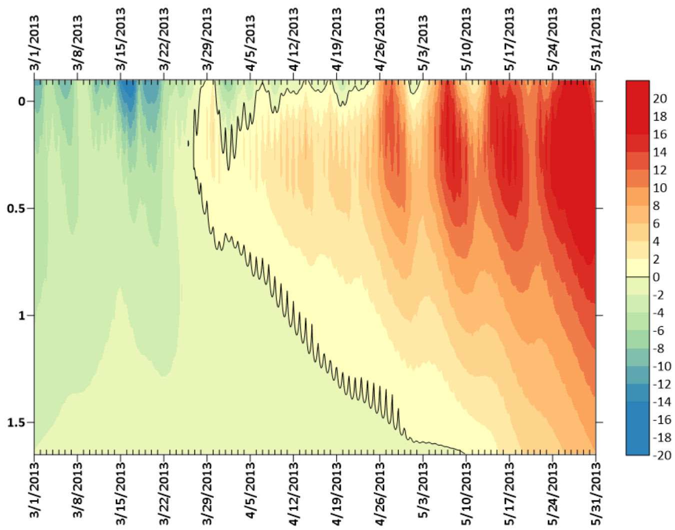

Figure A1: Temperature Contours at Different Depths from March to May 2013 using SLA 671 Temperature Data

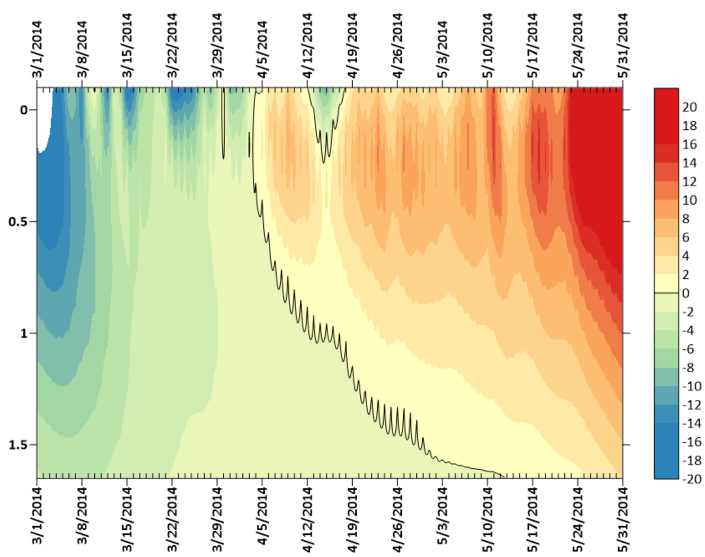

Figure A2: Temperature Contours at Different Depths from March to May 2014 using SLA 671 Temperature Data

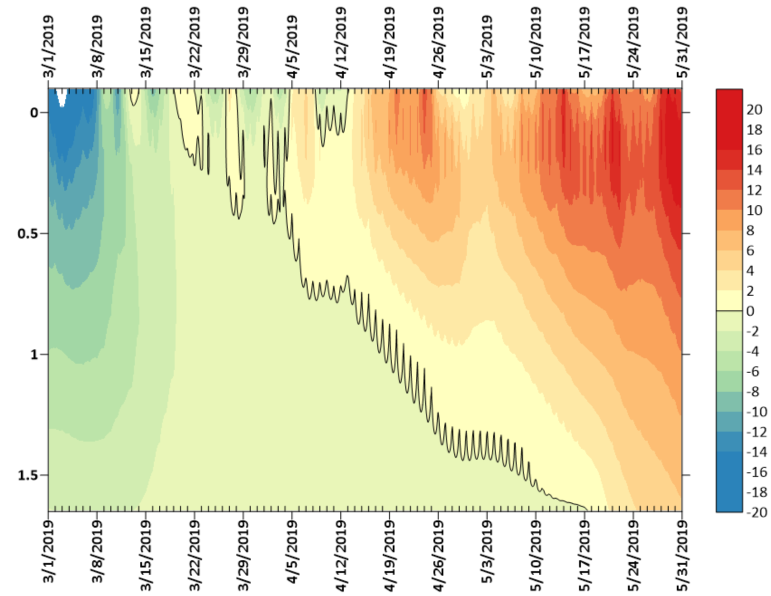

Figure A3: Temperature Contours at Different Depths from March to May 2019 using SLA 671 Temperature Data

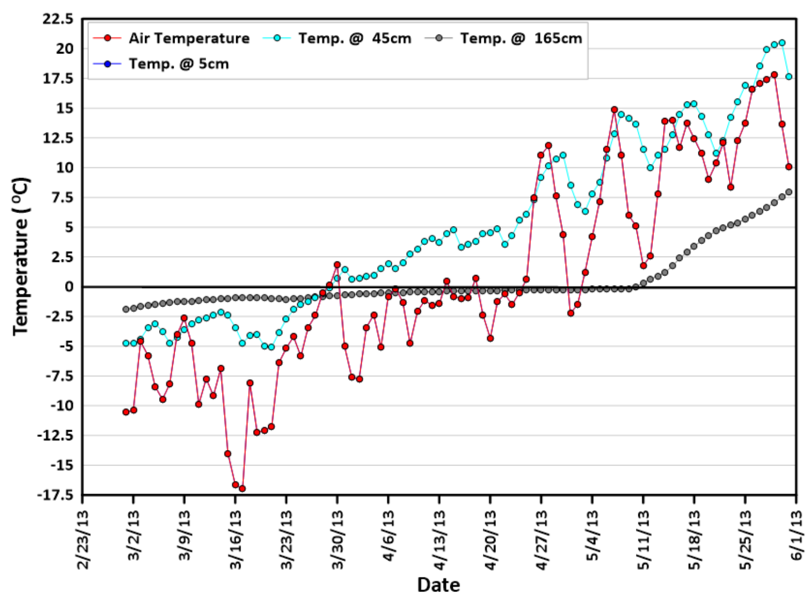

Figure A4: Air Temperatures and Soil Temperatures at Different Depths from March to May 2013 using SLA 671 Temperature Data

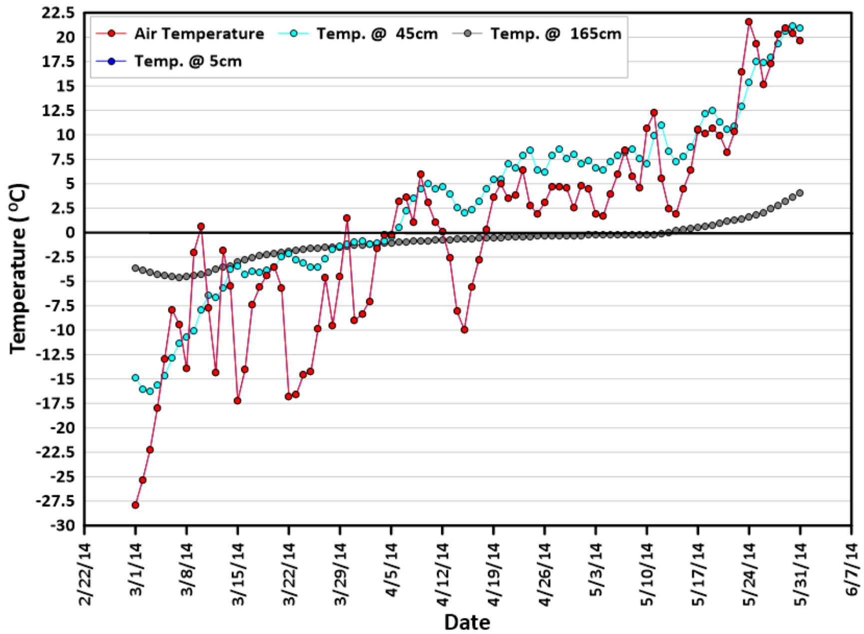

Figure A5: Air Temperatures and Soil Temperatures at Different Depths from March to May 2014 using SLA 671 Temperature Data

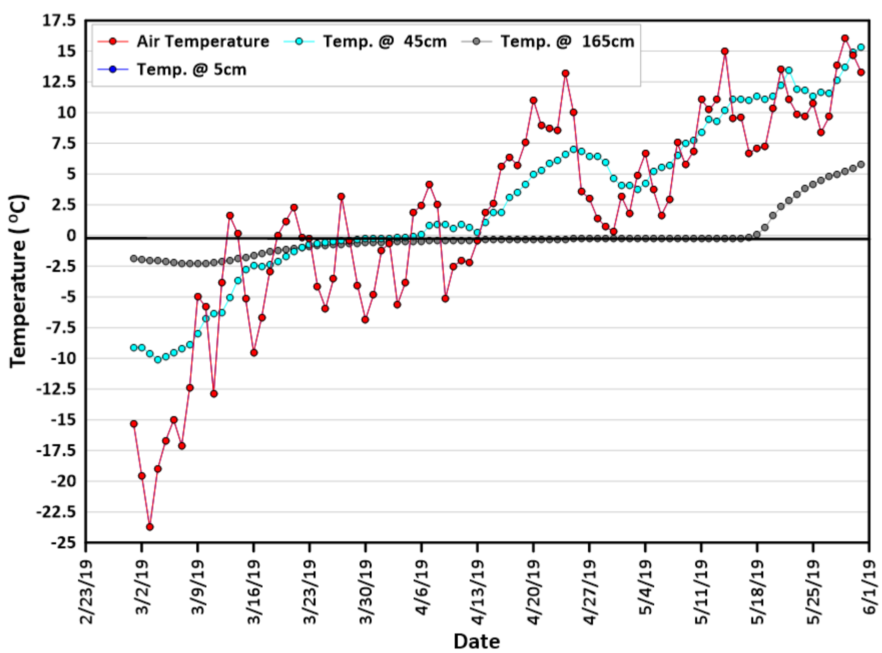

Figure A6: Air Temperatures and Soil Temperatures at Different Depths from March to May 2019 using SLA 671 Temperature Data

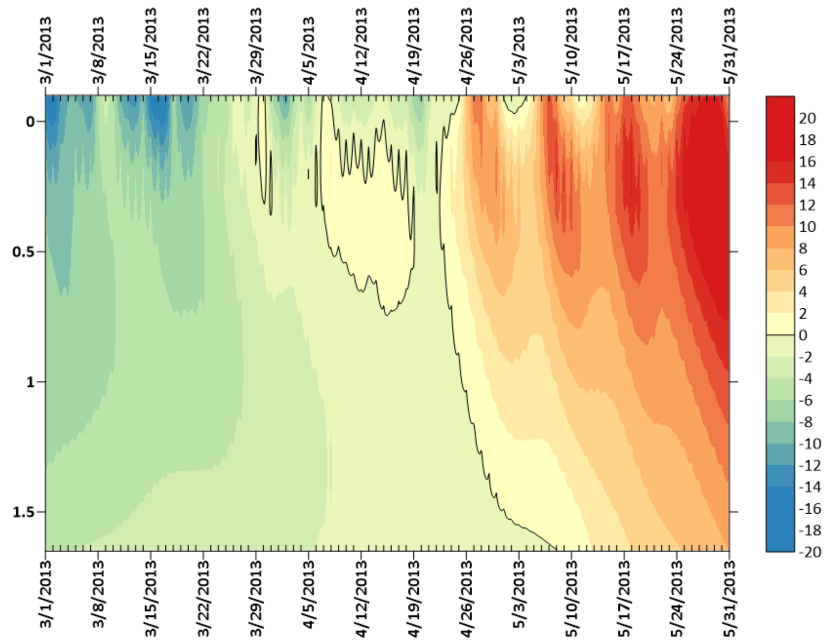

Figure A7: Temperature Contours at Different Depths from March to May 2013 using SLA 599 Temperature Data

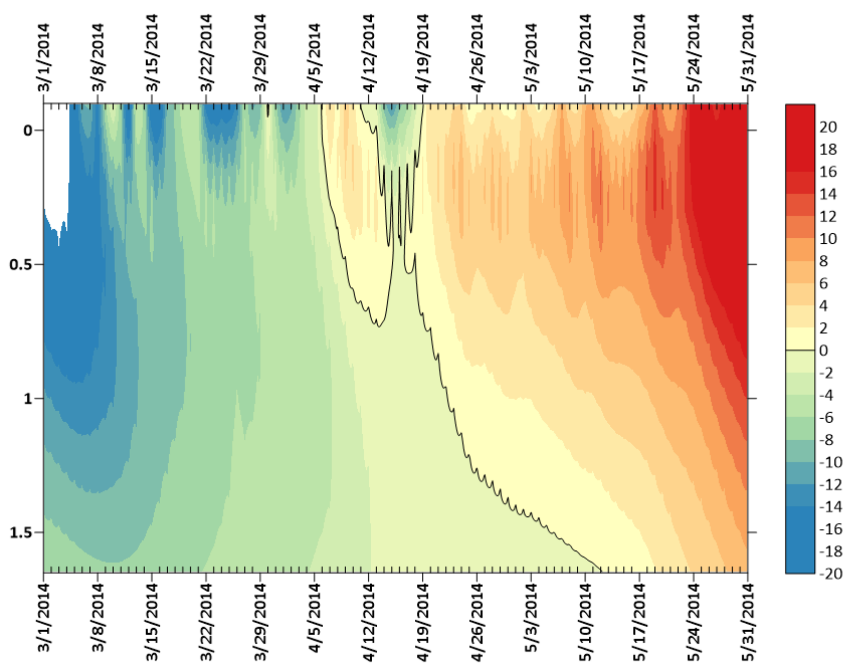

Figure A8: Temperature Contours at Different Depths from March to May 2014 using SLA 599 Temperature Data

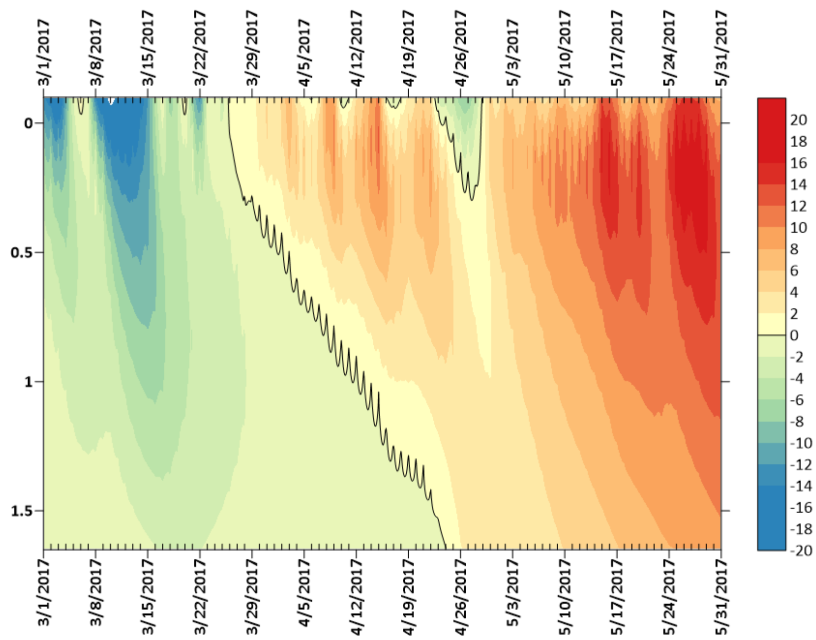

Figure A9: Temperature Contours at Different Depths from March to May 2017 using SLA 599 Temperature Data

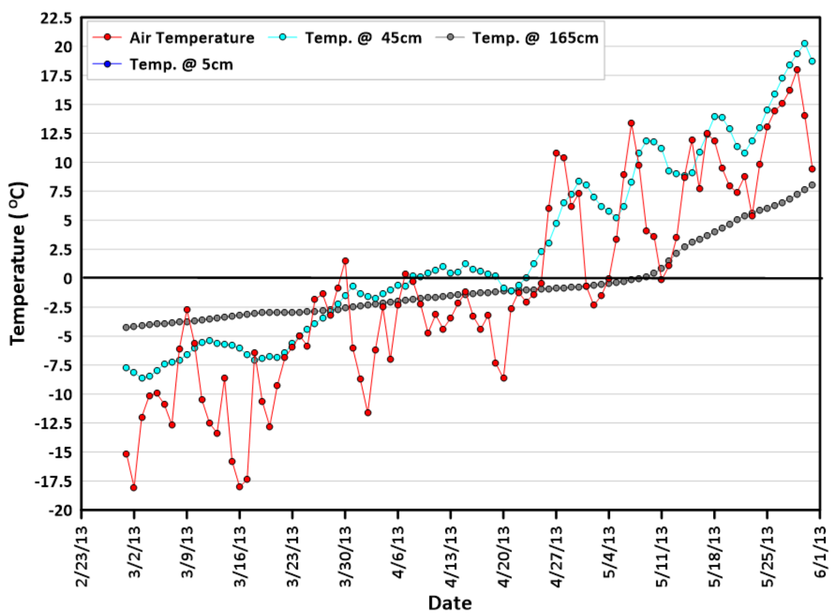

Figure A10: Air Temperatures and Soil Temperatures at Different Depths from March to May 2013 using SLA 599 Temperature Data

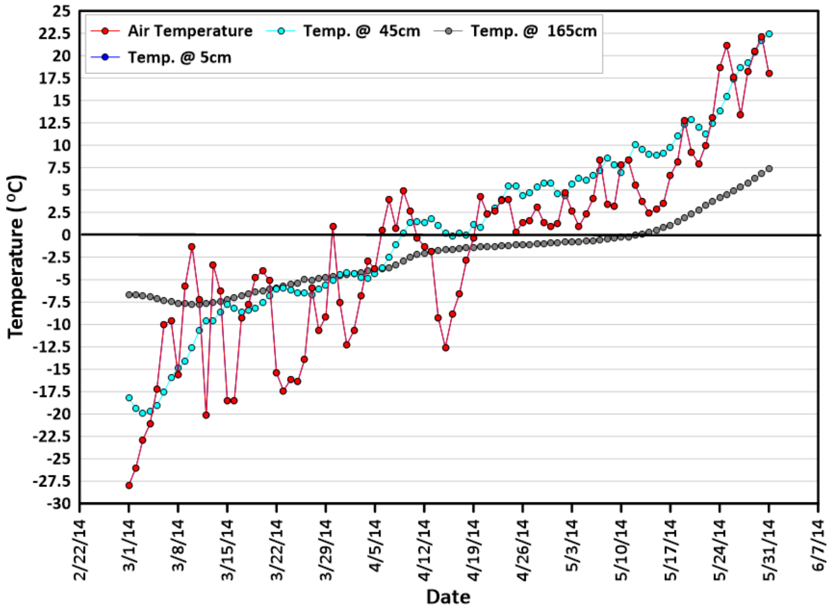

Figure A11: Air Temperatures and Soil Temperatures at Different Depths from March to May 2014 using SLA 599 Temperature Data

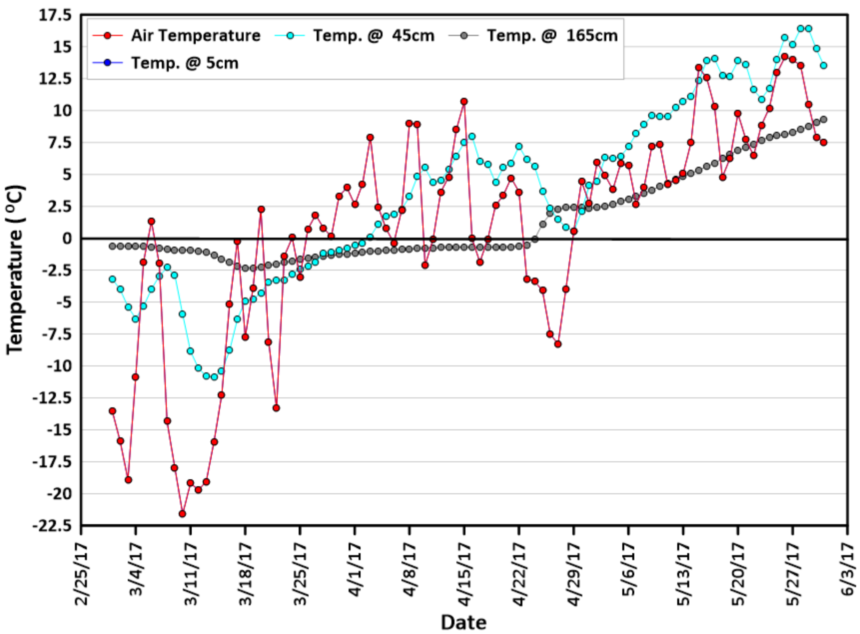

Figure A12: Air Temperatures and Soil Temperatures at Different Depths from March to May 2017 using SLA 599 Temperature Data

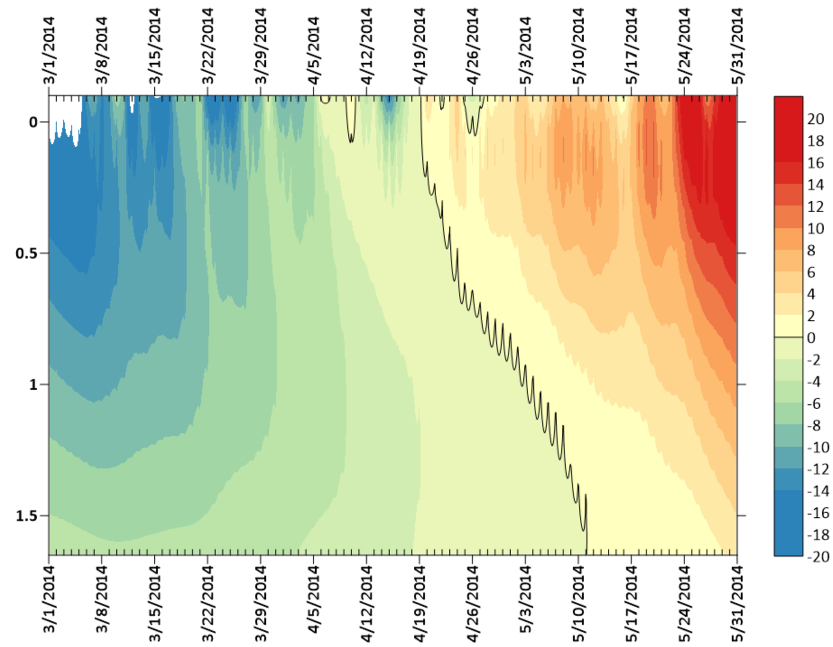

Figure A13: Air Temperatures and Soil Temperatures at Different Depths from March to May 2014 using SLA 643 Temperature Data

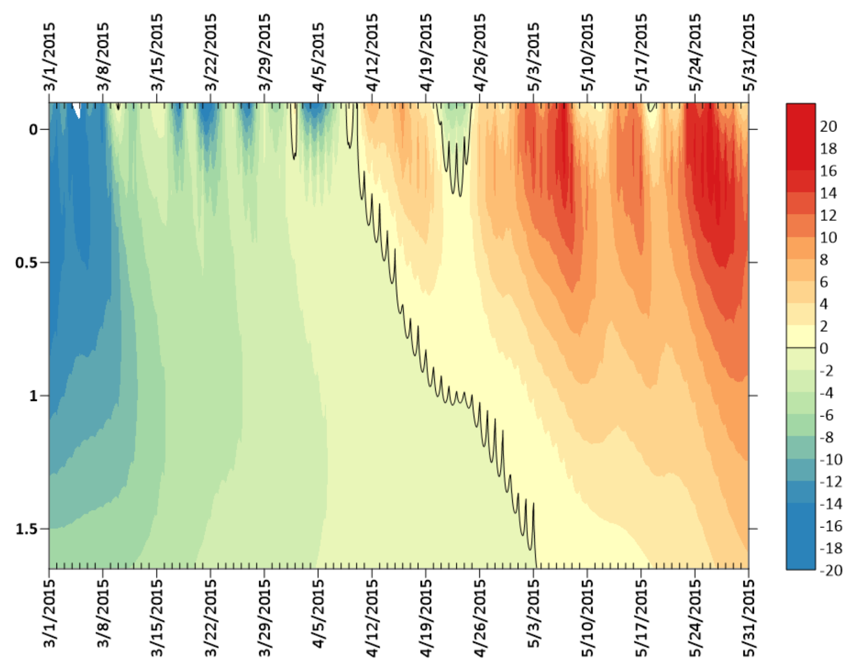

Figure A14: Air Temperatures and Soil Temperatures at Different Depths from March to May 2015 using SLA 643 Temperature Data

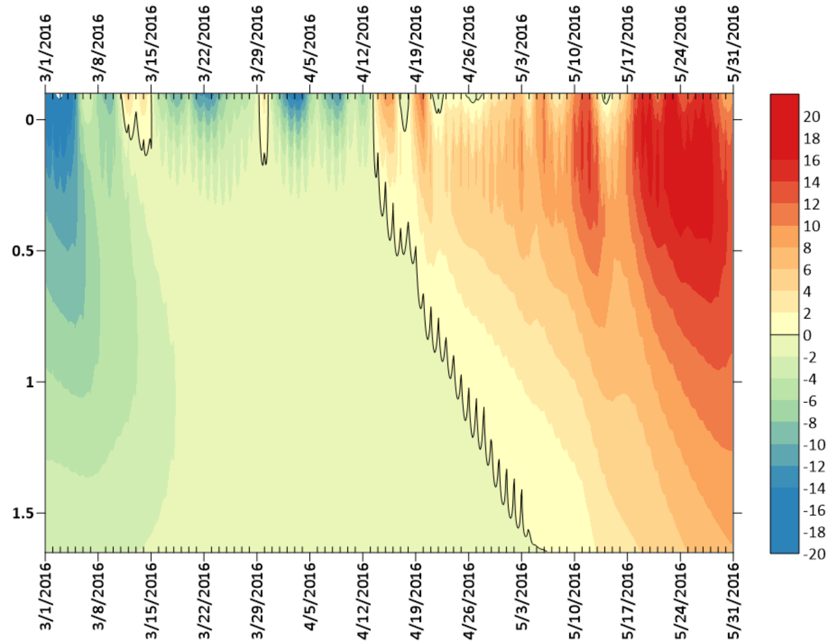

Figure A15: Air Temperatures and Soil Temperatures at Different Depths from March to May 2016 using SLA 643 Temperature Data

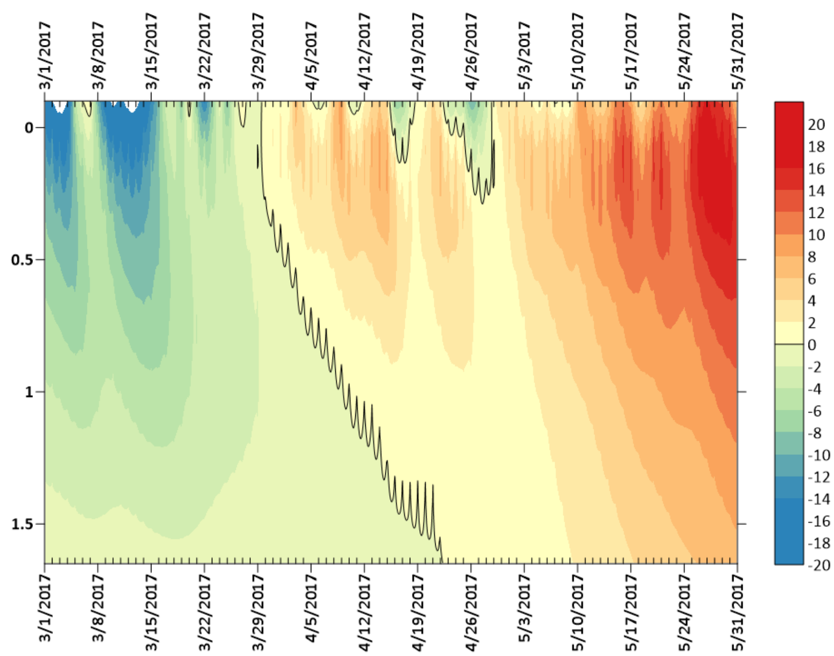

Figure A16: Air Temperatures and Soil Temperatures at Different Depths from March to May 2017 using SLA 643 Temperature Data

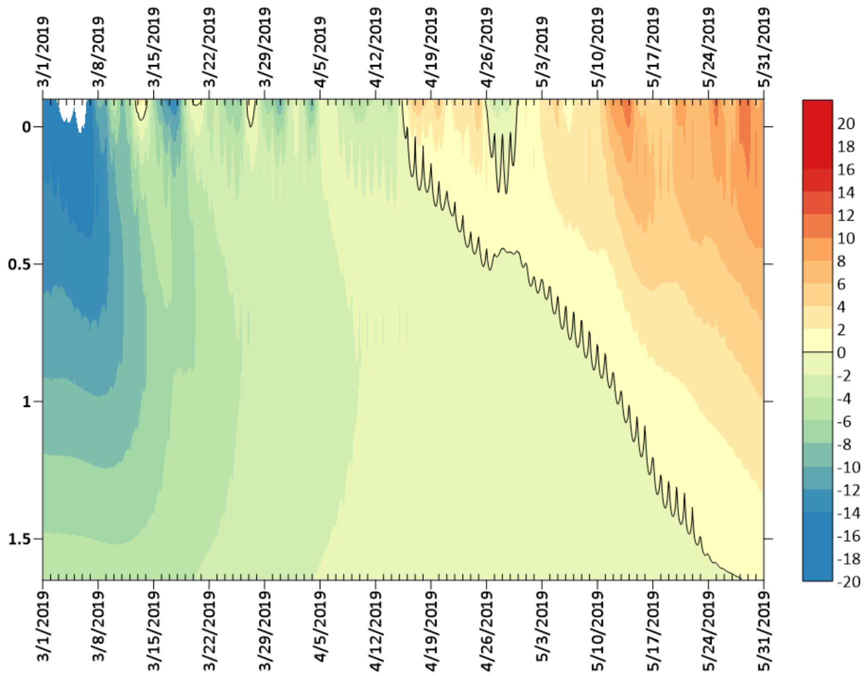

Figure A17: Air Temperatures and Soil Temperatures at Different Depths from March to May 2019 using SLA 643 Temperature Data

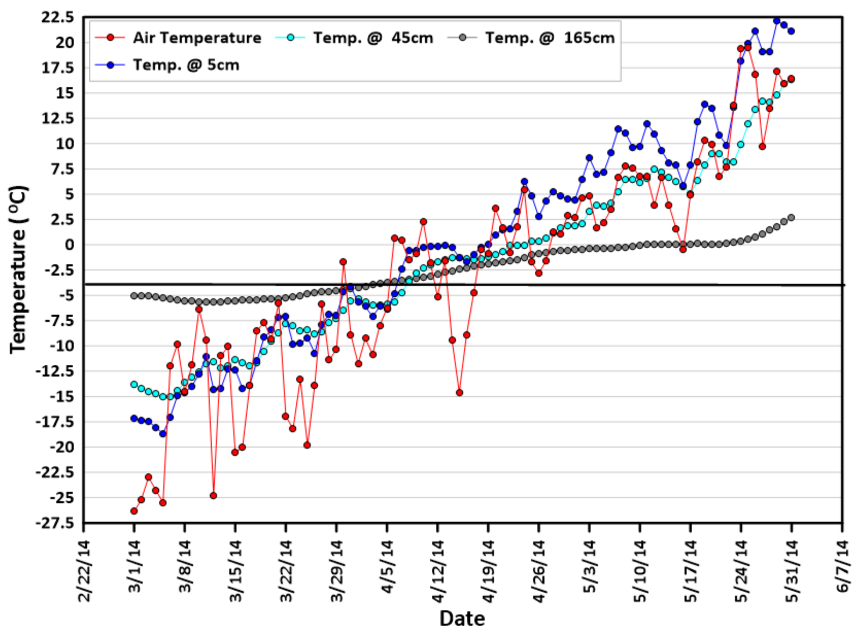

Figure A18: Air Temperatures and Soil Temperatures at Different Depths from March to May 2014 using SLA 643 Temperature Data

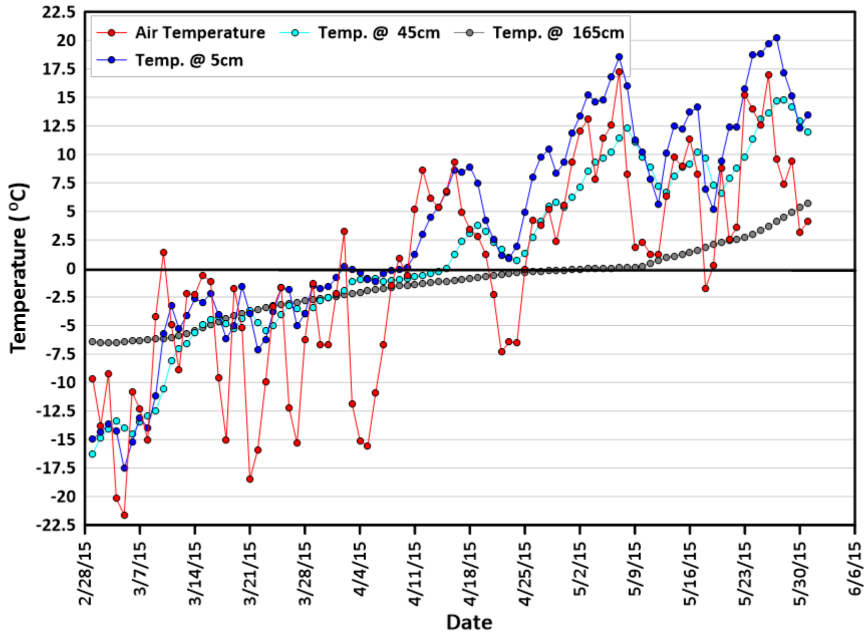

Figure A19: Air Temperatures and Soil Temperatures at Different Depths from March to May 2015 using SLA 643 Temperature Data

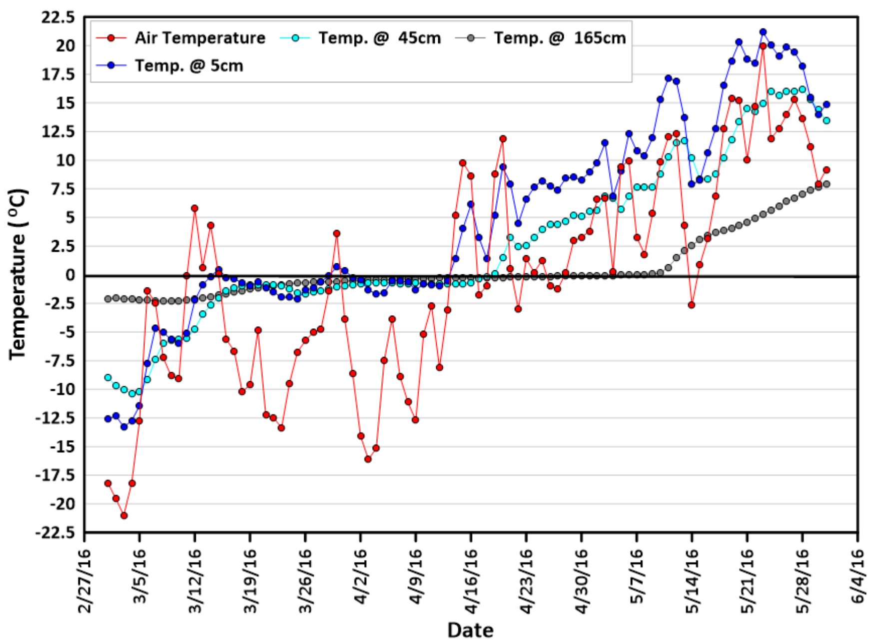

Figure A20: Air Temperatures and Soil Temperatures at Different Depths from March to May 2016 using SLA 643 Temperature Data

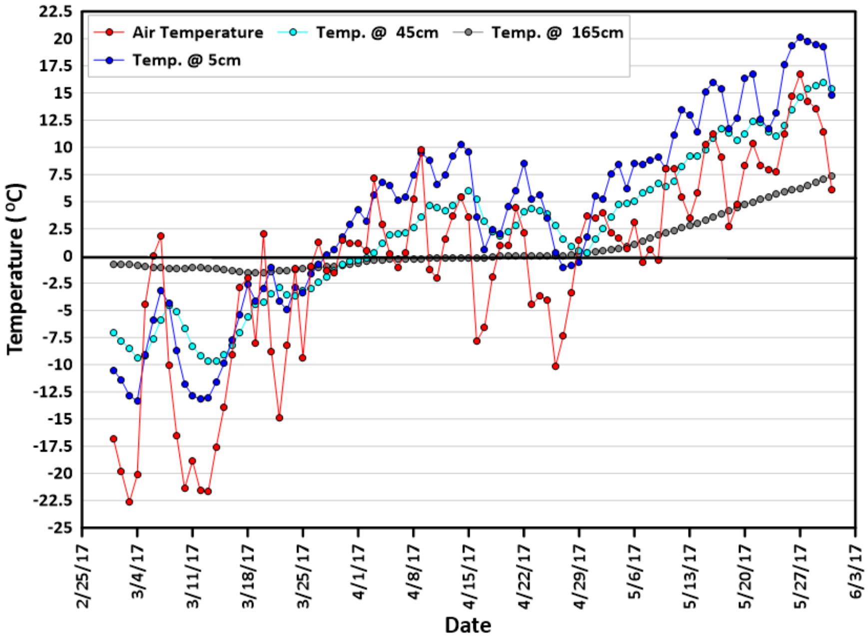

Figure A21: Air Temperatures and Soil Temperatures at Different Depths from March to May 2017 using SLA 643 Temperature Data

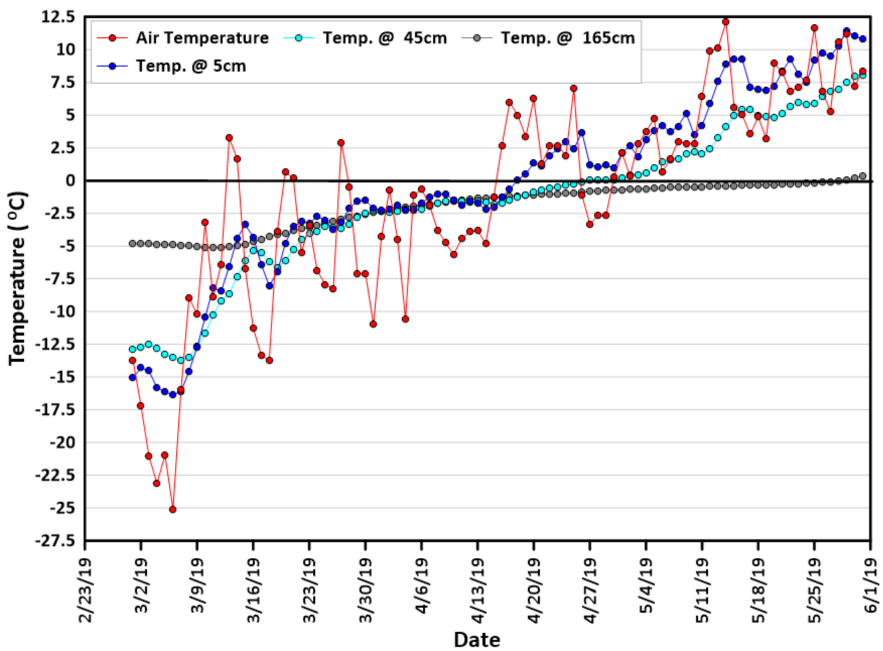

Figure A21: Air Temperatures and Soil Temperatures at Different Depths from March to May 2019 using SLA 643 Temperature Data

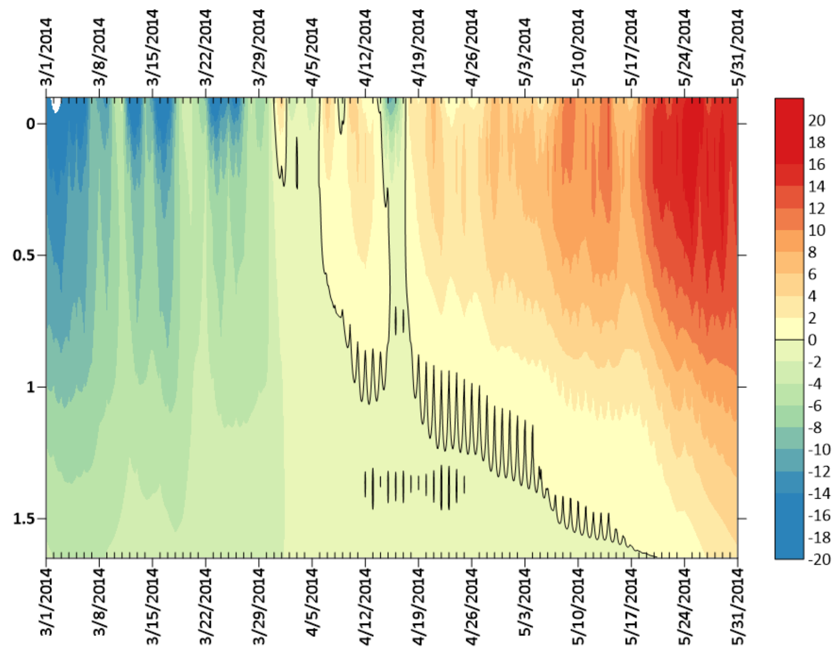

Figure A22: Temperature Contours at Different Depths from March to May 2014 using SLA 624 Temperature Data

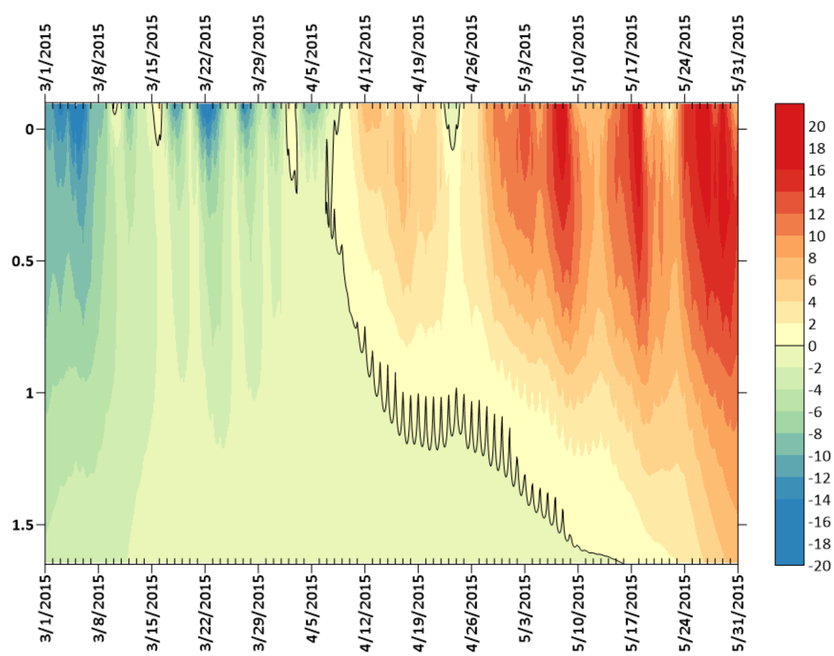

Figure A23: Temperature Contours at Different Depths from March to May 2015 using SLA 624 Temperature Data

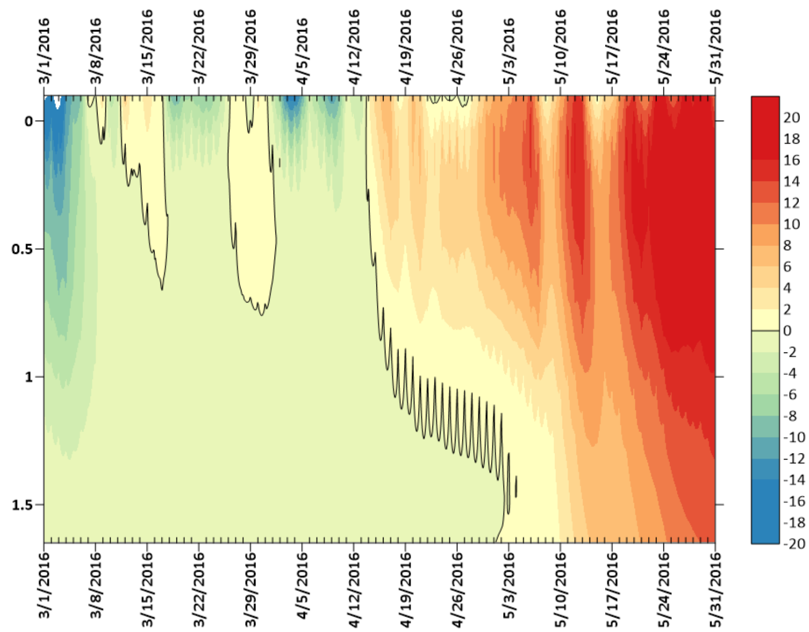

Figure A24: Temperature Contours at Different Depths from March to May 2016 using SLA 624 Temperature Data

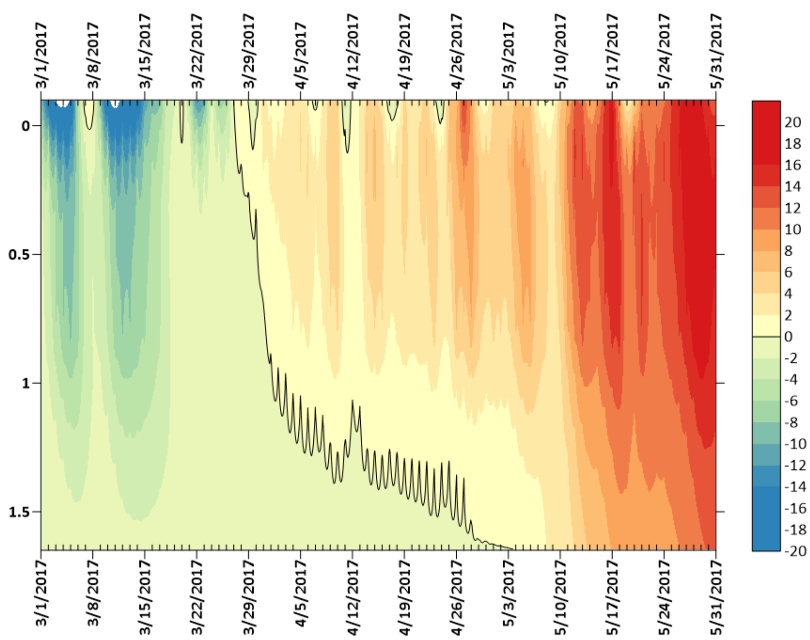

Figure A25: Temperature Contours at Different Depths from March to May 2017 using SLA 624 Temperature Data

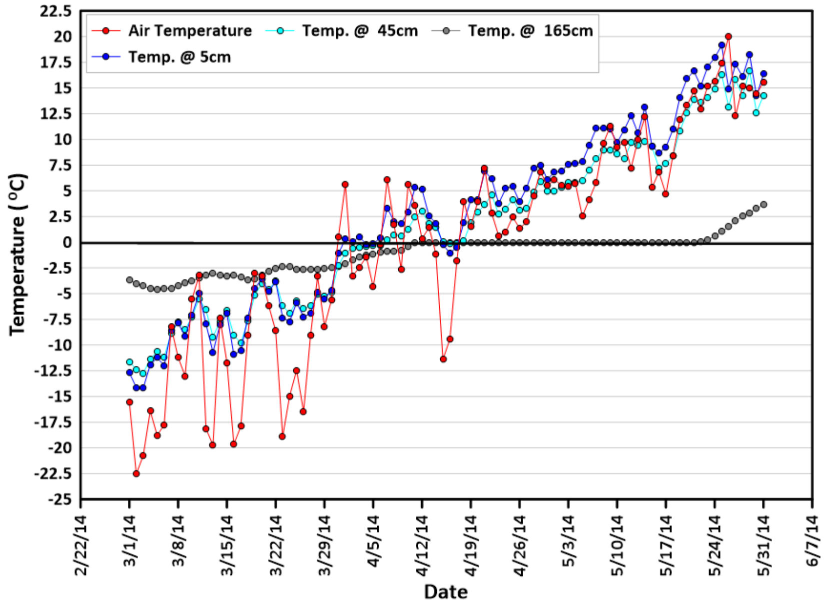

Figure A26: Air Temperatures and Soil Temperatures at Different Depths from March to May 2014 using SLA 624 Temperature Data

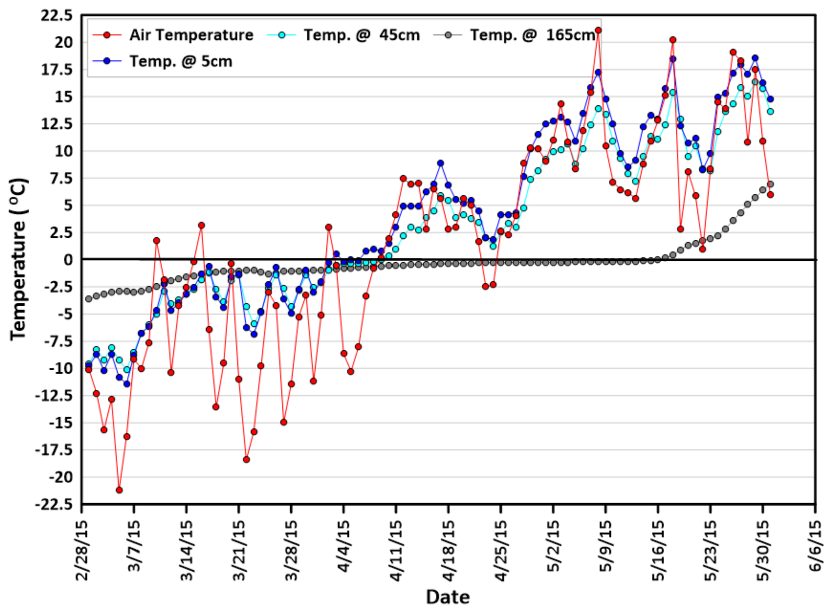

Figure A27: Air Temperatures and Soil Temperatures at Different Depths from March to May 2015 using SLA 624 Temperature Data

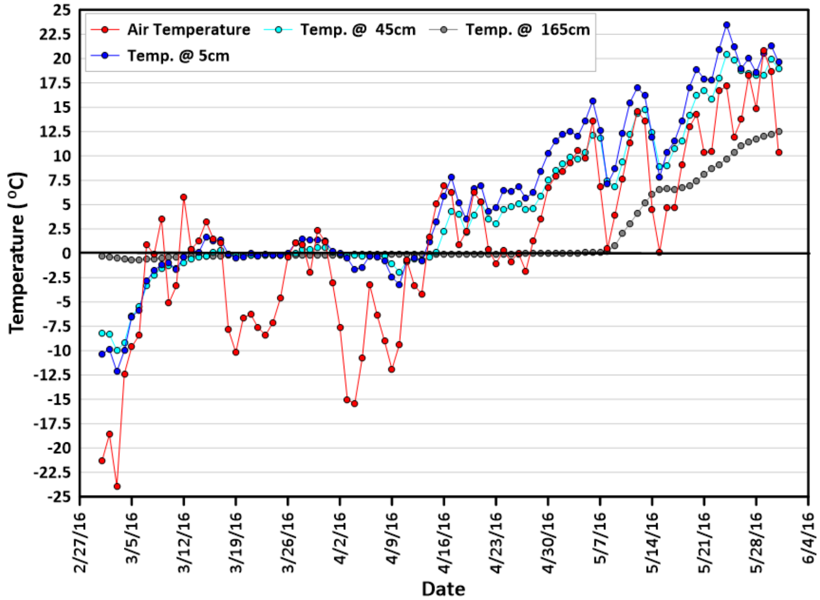

Figure A28: Air Temperatures and Soil Temperatures at Different Depths from March to May 2016 using SLA 624 Temperature Data

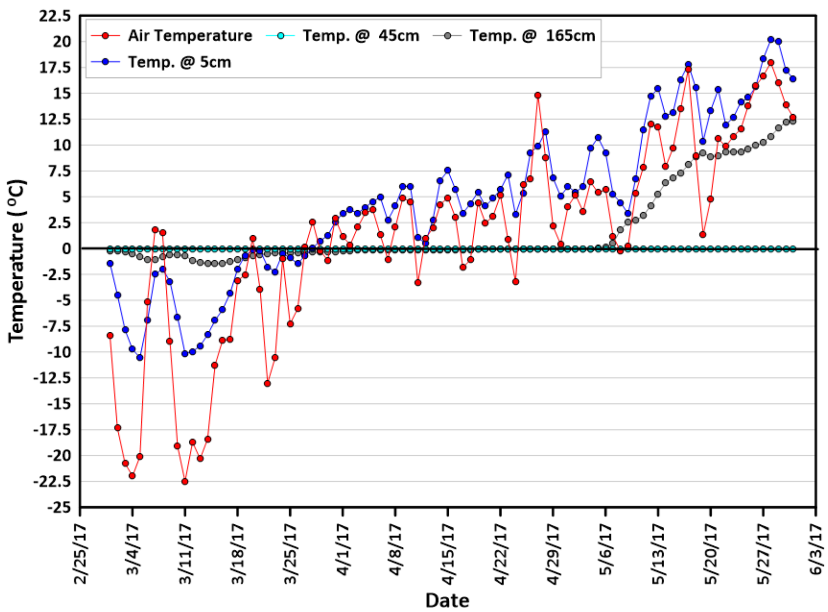

Figure A29: Air Temperatures and Soil Temperatures at Different Depths from March to May 2017 using SLA 624 Temperature Data